Supplementary Materials for

Double *PIK3CA* mutations in cis increase oncogenicity and sensitivity to PI3Kα inhibitors

Neil Vasan, Pedram Razavi*, Jared L. Johnson*, Hong Shao*, Hardik Shah, Alesia Antoine, Erik Ladewig, Alexander Gorelick, Ting-Yu Lin, Eneda Toska, Guotai Xu, Abiha Kazmi, Matthew T. Chang, Barry S. Taylor, Maura N. Dickler, Komal Jhaveri, Sarat Chandarlapaty, Raul Rabadan, Ed Reznik, Melissa L. Smith, Robert Sebra, Frauke Schimmoller, Timothy R. Wilson, Lori S. Friedman, Lewis C. Cantley, Maurizio Scaltriti†, José Baselga†

*These authors contributed equally to this work.
†Corresponding author. Email: scaltrim@mskcc.org (M.S.); jose.baselga@astrazeneca.com (J.B.)

Published 8 November 2019, *Science* **366**, 714 (2019)
DOI: 10.1126/science.aaw9032

This PDF file includes:

Materials and Methods:

Mutational Data

All cases reported with *PIK3CA* mutation were downloaded from www.cbioportal.org on September 18, 2018. Ten breast cancer studies were analyzed within the Breast Cancer cohort. Those cases not found in METABRIC and TCGA were combined as Breast Cancers (others). Cell line and xenograft studies were removed in Breast and Pan Cancer cohorts.

The MSK-IMPACT dataset consisted of 28139 tumor samples from patients who were prospectively sequenced as part of their active care at Memorial Sloan Kettering Cancer Center (MSKCC) between January 2014 and September 2018, as part of an Institutional Review Board-approved research protocol (NCT01775072). All patients provided written informed consent, in compliance with ethical regulations. The details of patient consent, sample acquisition, sequencing and mutational analysis have been previously published (*19*, *61*). Briefly, matched tumor and blood specimens for each patient were sequenced using Memorial Sloan Kettering-integrated mutation profiling of actionable cancer targets (MSK-IMPACT)—an FDA-authorized hybridization capture-based next-generation sequencing assay, which analyzes all protein-coding exons and selected intronic and regulatory regions of 341 to 468 cancer-associated genes (*19*). All samples were sequenced with 1 of 3 incrementally larger versions of the IMPACT assay, including 341, 410, and 468 cancer-associated genes, respectively. All the versions of the MSK-IMPACT assay included all exonic regions of *PIK3CA*. Somatic mutations, DNA copy number alterations, and structural rearrangements were identified as previously described (*19*) and all mutations were manually reviewed. The tumors were categorized as containing single, double, or multiple *PIK3CA* mutations.

Codon enrichment analysis

PIK3CA single and double mutant tumors were combined in the indicated cohorts. Tumors were analyzed for the frequency of a particular amino acid site mutation across the whole p110α protein in double mutant tumors versus single mutant tumors, compared to chance, as assessed by Fisher's exact test. Resulting p values were corrected for multiple hypothesis testing with Benjamini and Hochberg method. We rejected the null hypotheses with a two-sided $\alpha = 0.05$.

Mutational phasing

To determine the allelic configuration of multiple somatic mutations in the same gene and tumor, we implemented a computational framework for read-backed phasing. To this end, we exploited the fact that if two mutations were near enough in genomic position to be spanned by the same sequencing reads, then the identification of individual sequencing reads calling both variants at once unambiguously indicated that the different variants arose on the same DNA fragment, and therefore were in *cis* in the tumor genome. Conversely, if a large proportion of the reads spanning both mutations' loci called either mutation, but none called them both, and the two mutations were clonal enough to have arisen in the same cells, then this implied that the two mutations arose in *trans*. Briefly, when two or more mutations in the same gene were found in a sample in the tumor sequencing dataset, the tumor's raw sequencing data in BAM format was algorithmically queried using Samtools (version 1.3.1) (*62*) for the reads mapping to the loci of each mutation in that gene. The unique barcodes for the individual read-pairs calling each mutant allele were then obtained using the sam2tsv function from jvarkit (Lindenbaum P. (2015) JVarkit: java-based utilities for bioinformatics. *FigShare*, doi:10.6084/m9.figshare.1425030). By inspecting the barcodes calling the different mutant alleles in a gene, we called two mutations in *cis* if both mutations were called

by the same read-pair (in at least two distinct read-pairs, to mitigate false positives due to sequencing error). Conversely, we called two mutations in *trans* if their loci were spanned by at least 10 reads, but less than two called them both at once, and their cancer cell fractions (as estimated by the FACETS algorithm (version 0.3.9)) (*27*) summed to at least 100%, indicating that they likely arose in the same cancer cells.

Clonality analysis

Clonality analyses was performed on the MSKCC cohort (*9*). Genome-wide total and allele-specific DNA copy numbers were determined using the FACETS algorithm (*27*) for tumors that underwent MSK-IMPACT tumor sequencing assay. Purity, average ploidy, and allele-specific integer-copy number for each segment were then determined by maximum likelihood. To determine the clonality of each mutation, we used allele-specific copy number inference from FACETS to calculate the fraction of mutated cancer cells (cancer cell fraction, CCF) as previously described (*63*). Clonal mutations were those with a CCF (assuming the number of mutant copies was equal to the number of copies of the more frequent allele) greater than 0.8 or with the upper bound of the CCF confidence interval > 0.85. Mutations with CCFs not meeting these conditions were defined as subclonal. Clonality assessment was adequate on 86 of the 99 double mutant patients, and final analysis was restricted to the cases with both major (i.e. E542K, E545K or H1047R) and minor mutations (i.e. E453X, E726X, or M1043X) (n=62). The binomial exact confidence intervals were calculated for the fraction of tumors in each category and the difference between fraction of samples in each major and minor clone clonality category was assessed using Fisher's exact test. The statistical hypothesis tests were two-sided with $\alpha = 0.05$.

Clinicopathologic and survival analyses

For clinicopathologic analyses, METABRIC 2019 (*64*) and MSKCC cohorts (*9*) were analyzed. For METABRIC 2019 (n=1981), breast carcinoma cases (n=1964) were analyzed for *PIK3CA* mutational status: WT (n=1169), single mutant (n=681), and multiple mutant (n=114). For the MSKCC cohort (n=1918), cases were analyzed for *PIK3CA* mutational status: WT (n=1193), single mutant (n=626), and multiple mutant (n=99). Final analyses included the single and multiple mutant patients. p values were calculated by t-test (age) and chi square or Fisher's exact test, when appropriate.

For survival analyses, analysis was restricted to HR+/HER2- patients. Invasive disease-free survival, as defined by locoregional recurrence or distant recurrence whichever was first (*65*), was analyzed from the METABRIC 2019 cohort (*64*). Overall survival, as defined by time of metastatic recurrence until death or last follow up, was analyzed from the MSKCC cohort (*9*). For univariate analysis, p values were calculated using the log-rank test. For multivariate analyses, Cox proportional hazard models were utilized and adjusted for age, menopausal status, histology, stage at diagnosis, and receipt of chemotherapy, hormonal therapy, and radiotherapy. For the overall survival analysis, we further adjusted all the models for the late entry by left truncation. Late entry was defined as performing tumor sequencing to assess *PIK3CA* status after the metastatic recurrence. Therefore, for the time period between the metastatic diagnosis and tumor sequencing, the late entry patients are considered immortal. Adjusted for late entry bias was performed using left truncation method described in (*66*). We used the R package "survival" Kaplan-Meier survival function surv (t_1, t_2, event), where t_1 is time interval between metastatic recurrence and tumor sequencing and t_2 is time interval between metastatic recurrence and death or last follow-up.

Fresh frozen tumor acquisition

Double *PIK3CA* mutant tumors were obtained on MSKCC IRB# 17-364. Patients were initially identified as having double *PIK3CA* mutant tumors by MSK-IMPACT on FFPE samples, then were consented to #17-364 for collection of fresh tumor biopsies.

RNA extraction and cDNA generation

RNA was extracted from cell pellets (1 x 10^7 cells) using the RNeasy Mini Kit (Qiagen), as specified by the manufacturer. Briefly, cells were homogenized in 350 µL lysis buffer (buffer RLT) by needle shearing, passing the resuspended pellet through a 20-gauge needle attached to a 5 mL syringe 10 times until a homogenous lysate was achieved. RNA extract from the lysate was then mixed with 70% ethanol and applied to the RNeasy spin column. Following the designated binding and wash steps, total RNA was eluted from the column twice using 30 µL RNase free water for each elution, resulting in 60 µL extracted RNA per sample. Upon extraction, total RNA was aliquoted and stored at -80 °C for later use. Total cDNA for SMRT-seq was generated using the SuperScript IV First Strand Synthesis System for RT-PCR (part no. 18091050; Thermo Fisher Scientific) using 5 µL total RNA input and the provided oligo (dT) to prime first-strand synthesis, according to the manufacturer's protocol. Aliquots of cDNA were stored at -20 °C until needed for custom-primer, targeted *PIK3CA* amplification to achieve full-length molecules to phase variants of interest for diagnostic purposes. Total cDNA for Sanger sequencing was generated using the iScript cDNA Synthesis Kit (Bio-Rad).

Sanger sequencing

BT20, CAL148, HCC202, and MDA-MB-361 cells were purchased from ATCC. Fresh frozen tumors were acquired from MSKCC IRB #17-364, and samples were homogenized in RIPA buffer

supplemented with protease and phosphatase inhibitors (Roche). Full length *PIK3CA* cDNA was amplified using Taq polymerase to generate 3' A-tailed fragments and purified using a Qiaquick Gel Extraction kit (Qiagen). Full length *PIK3CA* cDNA was ligated into pGEM-T (Promega), transformed into *E. coli*, and plated on LB plates containing ampicillin, IPTG, and X-Gal for blue and white colony selection. White colonies were selected, miniprep plasmid DNA was isolated (Qiagen), and were submitted for Sanger sequencing.

PIK3CA amplification for SMRT-seq

Targeted *PIK3CA* amplification was performed using polymerase chain reaction (PCR) with High Performance Liquid Chromatography (HPLC)-purified SMRT-seq primers. SMRT-seq primers were:

Forward: TGGGACCCGATGCGGTTA
Reverse: AATCGGTCTTTGCCTGCTGA

The primers were synthesized at Integrated DNA Technologies, purified, and diluted to 10 μM in 0.1X TE buffer before use. Each reaction totaled 50 μL and consisted of 5 μL total cDNA, 5 μL 10X LA PCR Buffer II (Mg^{2+} plus), 8 μL of 2.5 mM dNTP mix, 2 μL each of PIK3CA-F and PIK3CA-R, 27.5 μL of nuclease free water, and 0.5 μL of LA-Taq polymerase (part no. RR02C, Takara Bio). Reactions were heated to 98 °C for 3 minutes and then subjected to 32 cycles of PCR using the following parameters: 25-sec denaturation at 98 °C, followed by 15-sec annealing at 55 °C, followed by 8-min extension at 68 °C. After the 32nd cycle, the reactions were incubated for 15 min at 68 °C and then held at 4 °C. *PIK3CA* amplicons were purified from PCR reactions using 1X AMPure PB beads, as described by the manufacturer (part no. 100-265-900, Pacific Biosciences). *PIK3CA* amplicons were visualized and quantified using the 2100 Bioanalyzer System with the DNA 12000 kit (Agilent Biosciences).

SMRTbell library preparation and sequencing

SMRTbell template libraries of the ~3.3-kb *PIK3CA* amplicon insert size were prepared according to the manufacturer's instructions using the SMRTbell Template Prep Kit 1.0 (part no. 100-259-100; Pacific Biosciences). A total of 250 ng of purified *PIK3CA* amplicon was added directly into the DNA damage repair step of the Amplicon Template Preparation and Sequencing protocol. Library quality and quantity were assessed using the DNA 12000 Kit and the 2100 Bioanalyzer System (Agilent), as well as the Qubit dsDNA Broad Range Assay kit and Qubit Fluorometer (Thermo Fisher). Sequencing primer annealing and P6 polymerase binding were performed using the recommended 20:1 primer:template ratio and 10:1 polymerase:template ratio, respectively. SMRT sequencing was performed on the PacBio RS II using the C4 sequencing kit with magnetic bead loading and one-cell-per-well protocol and 240-minute movies.

SMRT-seq haplotype generation and variant calling

To generate haplotypes and identify variants, data were processed by the Minor Variants Analysis Tool as part of the SMRTLink 5.1 bioinformatics suite (Pacific Biosciences) using NM_006218.3, the NCBI Reference Sequence for *PIK3CA*. Briefly, circular consensus sequence (CCS) reads were generated and filtered on reads that were ≥ 99.9% (Q30) accurate as input for haplotype and variant analysis. A conservative 5% variant frequency threshold was also applied, such that the phased haplotypes were generated using variants called with very high confidence. Phased haplotypes indicated those variants that were present in *cis*- or *trans*- within each selected sample.

Mutagenesis and cloning

We cloned *PIK3CA* without affinity tags, as N-terminal tags artificially increase kinase activity and C-terminal tags may interfere with membrane binding (*42, 67*). pBabe puro HA PIK3CA was a gift from Jean Zhao (Addgene plasmid #12522). pcDNA 3.4-PIK3CA untagged WT vector was obtained as a gift from Lewis Cantley (Weill Cornell Medical Center). For pBabe puro HA PIK3CA and pcDNA 3.4-PIK3CA, the SNP coding for I143V was mutated back to the WT isoleucine by site-directed mutagenesis. For pBabe puro HA PIK3CA, the N-terminal HA tag was deleted by site-directed mutagenesis. pDONR223_PIK3CA_WT was a gift from Jesse Boehm & William Hahn & David Root (Addgene plasmid # 81736). For pDONR223_PIK3CA_WT, a C-terminal stop codon was inserted by site-directed mutagenesis. In total, these modifications resulted in untagged WT *PIK3CA* in the various plasmids. Onto these WT backbones, E545K and H1047R mutants were cloned. After this first round of mutagenesis, E453Q, E726K, and M1043L were cloned into the E545K and H1047R plasmids to create double *cis* mutants. pLX302 was a gift from David Root (Addgene plasmid # 25896). pDONR plasmids were recombined with the pLX-302 acceptor plasmid using Gateway LR Clonase II Enzyme mix (Thermo Fisher). Plasmid backbone mutagenesis primers were:

PIK3CA WT C-terminal stop codon (pDONR223)
Forward: CATGCATTGAACTGATTGCCAACTTTC
Reverse: GAAAGTTGGCAATCAGTTCAATGCATG

PIK3CA V143I to WT isoleucine
Forward: GACTTCCGAAGAAATATTCTGAACGTTTGTAAA
Reverse: TTTACAAACGTTCAGAATATTTCTTCGGAAGTC

PIK3CA N-terminal HA tag removal (pBabe puro Myr HA PIK3CA)
Forward: GATCCAAGCTTCACCATGCCTCCAAGACCATCATCA
Reverse: TGATGATGGTCTTGGAGGCATGGTGAAGCTTGGATC

PIK3CA mutagenesis primers were:

E545K
Forward: CCTCTCTCTGAAATCACTAAGCAGGAGAAAGATTTTC
Reverse: GAAAATCTTTCTCCTGCTTAGTGATTTCAGAGAGAGG’

H1047R
Forward: CAAATGAATGATGCACGTCATGGTGGCTGGAC
Reverse: GTCCAGCCACCATGACGTGCATCATTCATTTG'

E453Q
Forward: CCAGTACCTCATGGATTACAGGATTTGCTGAACCCTATTG
Reverse: CAATAGGGTTCAGCAAATCCTGTAATCCATGAGGTACTGG

E726K
Forward: GAGAAGAAGGATAAAACACAAAAGGTAC
Reverse: GTACCTTTTGTGTTTTATCCTTCTTCTC

M1043L
Forward: GTATTTCATGAAACAACTGAATGATGCACATCATGGTGGCTGGAC
Reverse: GTCCAGCCACCATGATGTGCATCATTCAGTTGTTTCATGAAATAC

Cell lines, retroviral, and lentiviral production, and drugs

All cell lines were purchased from ATCC except for MCF7 [*PIK3CA* WT] cells which were obtained as a gift from Josh Lauring (Johns Hopkins University). NIH-3T3 cells were maintained in DMEM media supplemented with 10% FCS and 1% Pen/Strep. MCF-10A cells were maintained in DF-12 media supplemented with 5% filtered horse serum (Invitrogen), EGF (20 ng/μL) (Sigma), hydrocortisone (0.5 mg/mL) (Sigma), cholera toxin (100 mg/mL) (Sigma), insulin (10 μg/mL) (Sigma), and 1% penicillin/streptomycin. MCF7 cells and 293T cells were maintained in DMEM media supplemented with 10% FBS and 1% Pen/Strep. Cells were used at low passages and were incubated at 37°C in 5% CO2.

For retroviral and lentiviral production, 7 x 10^6 293T cells were seeded in 10-cm plates and transfected with the plasmid of interest, pCMV-VSVG, and pCMV-dR8.2 (for lentivirus) using Jetprime (Polyplus Transfection). Viruses were harvested 48 hours after transfection and were filtered through a 0.45 μm filter (Millipore). Target cells were infected using fresh viral

supernatants and were selected using puromycin (2 μg/mL) to obtain stable clones. For *trans* mutants, a 1:1 ratio of viruses was infected. Cell lines were genotyped to confirm the presence of the *PIK3CA* cDNA sequence. Alpelisib and everolimus were purchased (Selleck). GDC-0077 was obtained on MTA from Genentech.

Cell proliferation assays

MCF10A cell lines were seeded in serum starved media (MCF10A media without EGF or insulin), at 10000 cells/mL in 12 well plates. Cells were grown, and time points were collected daily from 0-4 days and fixed in formalin. Formalin fixed cells were developed using crystal violet and pictures were taken for day 4 growth. Acetic acid was added and OD_{595} was obtained. OD values were normalized to day 0 for each cell lines and plotted.

Western blotting

MCF10A, NIH-3T3 cells, and MCF7 cells were seeded in normal growth medium, either 4 million cells in 10 cm dishes or 400000 cells in 6 cm plates. 24 hours later, cells were washed twice with PBS then refreshed with serum starved media. Serum starved media for MCF10A cells used MCF10A media with 5% horse serum and without EGF or insulin. Serum starved media for NIH-3T3 and MCF7 cells used 0.1% FCS and 0.1% FBS, respectively. For growth factor stimulation experiments, PDGF-BB (20 ng/mL) was added for 30 minutes, and IGF-1 (10 nM) was added for 10 minutes, after serum starvation. For drugging experiments cells were washed twice with PBS then refreshed with serum starved media with DMSO or 1μM alpelisib or 62.5 nM GDC-0077 (the IC_{50} [GDC-0077] of MCF10A E545K cells per Fig. 4d) for the indicated time points. Cells were washed with PBS twice, and lysed in RIPA buffer supplemented with protease and phosphatase

inhibitors (Roche). Allograft tumor samples were also lysed in RIPA buffer supplemented with protease and phosphatase inhibitors. Protein extracts were quantified and normalized (NuPage), separated using SDS-PAGE gels, and transferred to PVDF membranes. All primary antibodies were diluted 1:1000 and anti-rabbit IgG secondary antibody (GE Healthcare) (1:4000) was used. Membranes were probed using specific antibodies. p110α (#4249), pAKT (S473) (#4060), pAKT (T308) (#13038), total AKT (#4691), pPRAS40 (T246) (#13175), pS6 (S240/244) (#5364), pS6 (S235/236) (#4858), total S6 (#2217), pERK1/2 (T202/Y204) (#4370), total ERK (#4695), and vinculin (#13901) were purchased from Cell Signaling Technology (CST). All primary antibodies were diluted 1:1000 and anti-rabbit IgG secondary antibody (GE Healthcare) (1:4000) was used. For quantification, densitometry was performed using ImageJ (*68*).

Mouse allografts

Animals were maintained and treated in accordance with Institutional Guidelines of Memorial Sloan Kettering Cancer Center (Protocol number 12-10-019). 5 x 10^6 NIH-3T3 cells in 1:1 PBS/Matrigel (Corning) were injected subcutaneously into six-week-old female athymic nude mice. When tumors reached a volume of ~150mm^3, mice measured twice a week during a month. 4 tumors per group were used in these studies. For statistical analysis, outliers were removed using Grubbs' test ($\alpha = 0.05$). Tumors were harvested at the end of the experiment, fixed in 4% formaldehyde in PBS, and paraffin-embedded. IHC was performed on a BOND RX processor platform (Leica) using standard protocols with BOND Epitope Retrieval Solution 2 (Leica). Primary staining with pAKT (S473) (D9E) (#4060), 1:100 (CST) for 30 minutes was followed by staining with a Bond Polymer Refine Detection kit (Leica) for 60 minutes. Studies were performed in compliance with MSKCC institutional guidelines under an IACUC approved protocol. The

animals were immediately euthanized as soon as investigators were notified that the tumors reached the IACUC set limitations.

Structural mapping

PI3K structural mapping was performed on PDB 2RD0, 3HHM, and 4OVU using PyMOL (*69*).

Protein expression and purification

EXPI-293F cells (Thermo Fisher) were incubated at 37 °C in 8% CO2, in spinner flasks on an orbital shaker at 125 rpm in Expi293 Expression Medium (Thermo Fisher). pcDNA 3.4-FLAG-His_6-TEV-PIK3R1 plasmid was obtained as a gift from the laboratory of Lewis Cantley (Weill Cornell Medical Center). 300 μg of pcDNA 3.4-PIK3CA and 200 μg pcDNA 3.4-PIK3R1 were combined and diluted in Opti-MEM I Reduced Serum Medium (Thermo Fisher). ExpiFectamine 293 Reagent (Thermo Fisher) was diluted with Opti-MEM separately then combined with diluted plasmid DNA for 10 minutes at room temperature. The mixture was then transferred slowly to 500 mL EXPI-293F cells (3 x 10^6 cells/mL) and incubated. 24 hours later, ExpiFectamine 293 Transfection Enhancer 1 and Enhancer 2 (Thermo Fisher) were added. Cells were harvested 3 days after transfection and centrifuged at 4000 rpm for 30 minutes and frozen at -20°C.

All steps of protein purification were performed at 4°C. Cell pellets were solubilized in lysis buffer (50 mM Tris pH 8.0, 400 mM NaCl, 2 mM $MgCl_2$, 5% glycerol, 1% Triton X-100, 5 mM β-mercaptoethanol, 20 mM imidazole) supplemented with EDTA-free protease inhibitor (Sigma) and lysed using a Dounce homogenizer for 20 strokes. Lysates were centrifuged at 14000 rpm for 60 minutes and clarified lysates were affinity purified on Ni-NTA resin (Qiagen) by batch binding

for 1 hour. Resin was washed with 10 column volumes of lysis buffer (50 mM Tris pH 8.0, 500 mM NaCl, 2 mM $MgCl_2$, 2% glycerol, 20 mM imidazole) and eluted in 10 column volumes of elution buffer (50 mM Tris pH 8.0, 100 mM NaCl, 2 mM $MgCl_2$, 2% glycerol, 1mM TCEP, 250 mM imidazole). Eluted protein was buffer exchanged with elution buffer without imidazole, concentrated using 100 kDa Ultra Centrifugal Filter Units (Amicon), and flash frozen in liquid nitrogen with 20% glycerol. Concentrations of PI3K complexes used in all biochemistry experiments were normalized by Western blotting for p110α as compared to 1 μg WT PI3K complex.

Thermal shift assays

1 μg of PI3K complex was added to 10 μL 5x Assay Buffer I (SignalChem), 2 μL ATP (1 mM), and 1 μL BSA (2 mg/mL) and distilled water to a total volume of 50 μL into each tube of a MicroAmp Optical 8-Cap strip (Thermo Fisher) at room temperature. For each experiment, one 8-cap strip was prepared per PI3K construct. Tubes were placed in a C1000 Touch Thermocycler (BioRad). Samples were cycled at 46 °C for 30 seconds, then on a temperature gradient from 46 °C – 61.7 °C for 3 minutes, then 25 °C for 3 minutes. Samples were spun in a Minispin centrifuge for 30 seconds and 40 μL of the supernatant was transferred to separate Eppendorf tubes. Tubes were centrifuged at 15000 rpm for 20 minutes at 4 °C. 30 μL of the supernatant was transferred to separate Eppendorf tubes with SDS buffer. Samples were loaded and soluble p110α was probed by Western blotting across the temperature gradient with anti-p110α antibody to determine the temperature at which p110α becomes insoluble. For quantification, densitometry was performed using ImageJ (*68*). Western blot densitometry measurements were normalized to the densitometry

of the lowest temperature point (46 °C), curves were fit to a Boltzmann sigmoid function, and melting temperatures (T_m (50%)) were determined.

Liposome preparation and liposome sedimentation assays

PS, PE, and PI were purchased (Avanti) and cholesterol was purchased (Nu Chek Prep). Anionic lipid stocks were prepared at 10 mg/mL in HPLC-grade chloroform from using molar percentages of 35% PE, 25% PS, 5% PI, and 35% cholesterol. PIP_2 lipid stocks were prepared at 35% PE, 25% PS, 4.9% PI, 0.1% PIP_2, and 35% cholesterol. A gentle stream of argon gas was applied for 15 seconds and tubes were frozen and stored at -20 °C. Prior to experiments, the lipid stocks were vortexed and 100 µL of chloroform (HPLC-grade) was transferred to a clean glass vial. Argon gas was immediately applied to the stock tube, capped, and stored at -20 °C. Argon gas was applied the 100 µL aliquot leaving a translucent lipid film. 2 mL of 1x filter-sterilized TBSM buffer (50 mM Tris pH 8.0, 50 mM NaCl, 5 mM $MgCl_2$) was added and lipids were hydrated at room temperature for 1 hour. Liposomes were extruded 15 times through a 0.8 µm membrane using a Mini-Extruder kit (Avanti). Liposomes were transferred to a clean Eppendorf tube and centrifuged at 15000 rpm for 8 minutes. Supernatant was discarded, and the lipid pellet was resuspended in 100 µL TBSM buffer vigorously until resuspended. 900 µL of TBSM was added for a final volume of 1 mL. Differential light scattering was performed to assess size of the liposome population. 1 µg of PI3K complex in PBS was added to 70 µL liposomes (10 mg/mL) in a total volume of 100 µL. Binding reactions proceeded for 30 minutes at room temperature. Solutions were centrifuged at 15000 rpm for 15 minutes and supernatant was removed by aspiration. Lipid pellets were mixed with 50 µL SDS buffer, and the amount of bound p110α was probed by Western blotting. For

quantification, densitometry was performed using ImageJ (*68*) and measurements were normalized to the densitometry of WT PI3K.

Lipid kinase assays

For triplicate kinase reactions, radioactive ATP buffer, protein, and PIP_2 master mixes were assembled. The radioactive ATP buffer master mix contained 1100 µL 5x Assay Buffer I (SignalChem), 55 µL ATP (10 mM), 55 µL BSA (2 mg/mL), 55 µL ^{32}P-labeled ATP (0.01 mCi/µL), and 2805 µL distilled water. The protein master mix contained 4 µg PI3K complex in 16 µL total volume. The PIP_2 master mix contained 50 µL PIP_2 (Avanti) and 450 µL distilled water. For each construct, 296 µL buffer master mix was combined with 14 µL protein master mix (buffer + protein master mix) and was mixed well by pipetting. 90 µL of the buffer + protein master mix was aliquoted in triplicate, corresponding to a total amount of 1.016 µg PI3K complex per reaction. To this was added 10 µL of PIP_2 master mix (100 uL total volume per reaction) and the solution was mixed well by pipetting to start the reaction. Kinase reactions proceeded at 30°C for 10 minutes. 50 µL of HCl (4N) was added to quench the reaction followed by 100 µL of 1:1 methanol-chloroform. Tubes were vortexed for 30 seconds each and centrifuged at 15000 rpm for 10 minutes. Using gel loading pipet tips pipetted with chloroform in and out, 20 µL of the bottom hydrophobic phase was removed and spotted onto a TLC plate (EMD Millipore, M1164870001). Plates were placed in a sealed chamber with 65:35 1-propanol and 2M acetic acid and TLC was run overnight. Plates were exposed to a phosphor screen for 4 hours and imaged on a Typhoon FLA 7000.

IC_{50} determination of recombinant PI3K

We used the Transcreener ADP^2 fluorescence intensity assay (Bellbrook Labs) to determine IC_{50} values for PI3Kα inhibitors with recombinant PI3Kα. A standard curve was prepared with varied concentrations of ATP and ADP (100 μM total of nucleotide). Enzyme titrations were performed, and enzyme concentrations were chosen within the EC_{50}-EC_{80} range for fluorescence intensity. Kinase reactions were prepared in triplicate in 384 well low volume black round bottom polystyrene NBS microplates (Corning #5414). 10 μL kinase reactions were prepared by combining PI3K with 1 uL alpelisib for 30 minutes at room temperature then adding ATP and diC8-PIP_2 (Avanti) in kinase buffer at 30 ºC for 1 hour. Final concentrations of reagents were 0-10 μM alpelisib, 100 μM ATP, 50 μM diC8-PIP_2, and in the kinase buffer, 50 mM HEPES (pH 7.5), 4 mM $MgCl_2$, 1% DMSO, and 0.01% Brij-35. Reactions were quenched by adding 10 μL of a mixture containing ADP^2 antibody mixture and Alexa Fluor 594 Tracer. Detection of ADP fluorescence intensity was measured with a Phera Star plate reader (BMG Labtech) at excitation 584 nM, emission 620 nM, and gain adjustment of 2500. IC_{50} values were calculated using a log curve fitting to a non-linear regression model. Data were analyzed by the GraphPad Prism software.

Cell viability assays.

1000 MCF10A cells were seeded in 100 μL of MCF10A media (containing 2% horse serum) lacking EGF or insulin, per well, in a 96-well plate. 24 hours later, serial concentrations of alpelisib or GDC-0077 were added in 100 μL of MCF10A media (containing 2% horse serum) lacking EGF or insulin. Cells were incubated for 4 days and then developed with CellTiter-Glo (Promega). Fraction of cell viability was calculated relative to cell growth condition without drug.

Analysis of patient response to endocrine therapy

Retrospective PFS analysis was performed on tumors from a large breast cancer dataset (n=1918) sequenced by MSK-IMPACT (*9*). Tumors were included in analysis if both pre- and post-endocrine therapy (aromatase inhibitor or fulvestrant) biopsies confirmed WT, single *PIK3CA* mutation, or multiple *PIK3CA* mutations. Kaplan-Meier curves were generated for PFS after firstline aromatase inhibitor or firstline fulvestrant therapy. p values were calculated using the log-rank test.

Analysis of patient response to PI3K inhibitor therapy

PFS analysis was performed on patients enrolled in NCT01870505, a phase 1 clinical trial (n=51) of alpelisib plus letrozole or exemestane for patients with hormone-receptor positive locally-advanced unresectable or metastatic breast cancer. Patients separately provided written informed consent to MSKCC IRB #12-245 (NCT01775072) for tumor sequencing. Five patients had indeterminate *PIK3CA* mutational status by NGS and were excluded from analysis. Cases were analyzed for *PIK3CA* mutational status: WT (n=6), single mutant (n=31), and multiple mutant (n=9). Progression free-survival was defined as time interval between enrollment in the clinical trial to disease progression or death (whichever was first). Survival analysis was performed using Kaplan-Meier methods and Statistical significance was determined by log-rank. We rejected the null hypotheses with a two-sided $\alpha = 0.05$.

For analysis of the SANDPIPER clinical trial (*12*) patient ctDNA samples (n=631), 508 patient samples met quality control parameters and were analyzed by Foundation Medicine Foundation One Liquid test (*70*) which sequences half the exons of *PIK3CA* and can detect mutations at amino

acid positions 545, 1047, 453, 726, and 1043 (Fig. S10). 339 samples were identified with *PIK3CA* mutations, of which 66 contained two or more *PIK3CA* mutations. Patients with measurable disease from the ctDNA *PIK3CA* mutant cohort, on the taselisib arm, were analyzed based on the percentage change in the sum of longest diameter (SLD) of target lesion from baseline and were tabulated by waterfall plot. Patients with both measurable and nonmeasurable disease from the ctDNA *PIK3CA* mutant cohort were assessed on the placebo and taselisib arms for objective response rate (ORR) defined by RECIST v1.1 criteria (*50*). 95% CI for rates were constructed using the Blyth-Still-Casella method. The CI for the difference in ORRs between the two treatment arms were determined using the normal approximation to the binomial distribution. Response rates in the treatment arms were compared (p-value) using the stratified Cochran-Mantel-Haenszel test.

Statistical analysis

All statistical analyses are shown in the appropriate method and figure legend. Investigators were unblinded when assessing the outcome of the *in vivo* experiments. All cellular and biochemical experiments were repeated at least three times unless otherwise indicated.

Supplementary Text

Postulated biochemical mechanisms of *PIK3CA* mutations

E545K and E453Q are located in the binding interfaces between p110α and p85α (*38, 39*) and are predicted to be disrupters. E545K, located in the helical domain, disrupts binding to the p85α nSH2 domain and has a similar biochemical effect as phosphotyrosine peptide binding to p85α (Fig. 3A and B), and E453Q impairs p110α C2 domain binding to the p85α iSH2 domain (Fig. 3A and B). The orientations of p110α C2 to p85α iSH2 are similar in the WT, WT + PIP_2, and H1047R structures, with root mean square deviation (RMSD) values < 1 Å (Fig. S7A); however, there are subtle changes in the C2 loop regions interacting with p85α iSH2 including the orientation of E453 which may be functionally relevant (Fig. S7A, S7B) (*35, 38, 39*). H1047R and M1043L are located along the C-terminal tail (*38*), which forms part of the membrane-docking surface and are therefore predicted to be binders (Fig. 3A and B). Structurally, H1047R is postulated to increase membrane binding through interactions of the mutated arginine as well as reorganization of a C-terminal loop that also interacts with membrane (*38*). E726K is in the kinase domain and has been reported to be activating (*29*), but its mechanism is unknown. In crystal structures (*35, 38, 39*), E726 is located in the membrane binding interface (Fig. S7C) and is oriented outwards, directed towards the membrane (Fig. S7D). Therefore, we hypothesized that E726K is also a binder, as the mutant lysine would increase positive charge and promote binding to the negatively charged phospholipids at the plasma membrane (Fig. 2B, S7D).

Rationale for recombinant protein purification strategy

Recombinant full-length human PI3Kα complexes were purified from suspension EXPI293 human embryonic kidney cells (Fig. S8A). Fusing affinity tags to the termini of *PIK3CA* alters its basal

catalytic activity (*67*). Structurally, the N-terminus sits along its binding interface with p85α and the C-terminus is located near its catalytic site. To generate recombinant p110α in its most native form, we developed a purification scheme that utilizes a polyhistidine tag on the N-terminus p85α to purify untagged p110α, as a heterodimeric complex.

A

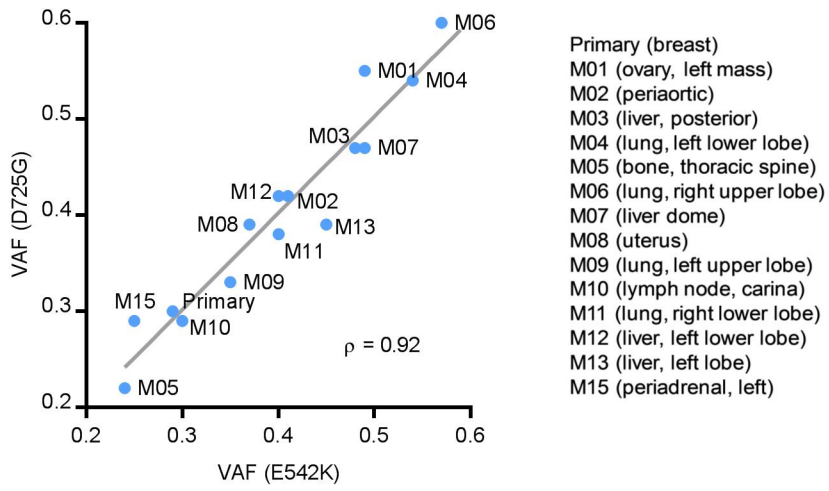

Primary (breast)
M01 (ovary, left mass)
M02 (periaortic)
M03 (liver, posterior)
M04 (lung, left lower lobe)
M05 (bone, thoracic spine)
M06 (lung, right upper lobe)
M07 (liver dome)
M08 (uterus)
M09 (lung, left upper lobe)
M10 (lymph node, carina)
M11 (lung, right lower lobe)
M12 (liver, left lower lobe)
M13 (liver, left lobe)
M15 (periadrenal, left)

B

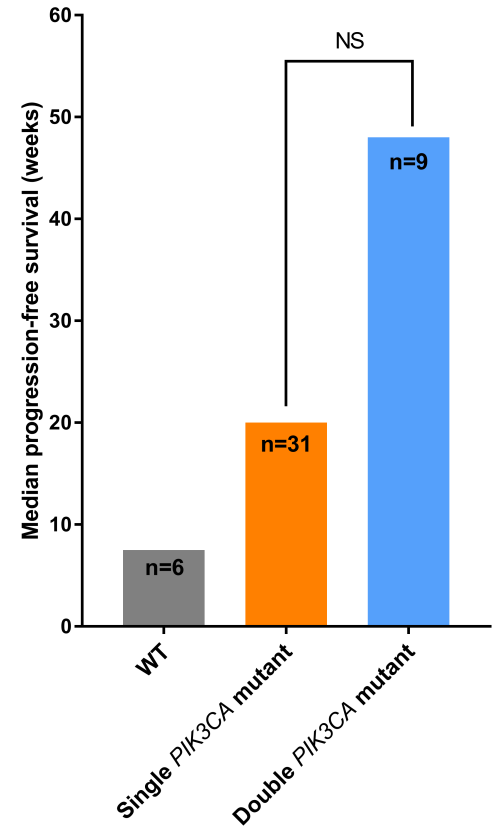

C

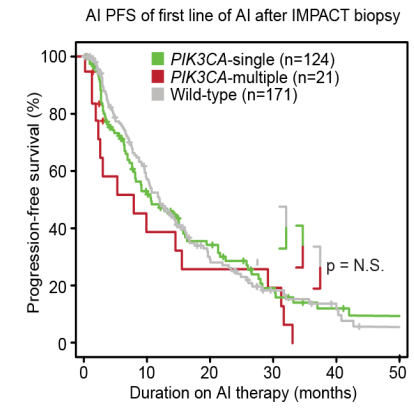

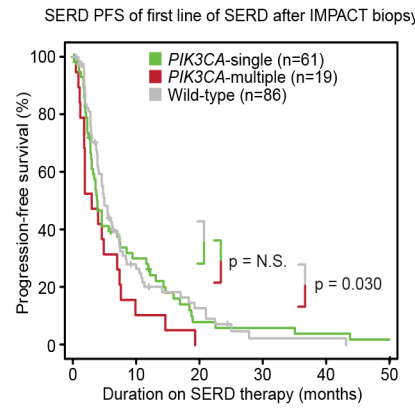

Fig. S1

Fig. S1: Signals of improved clinical response to PI3K inhibition in some breast cancer patients with double *PIK3CA* mutations. (A) Variant allele frequencies of the primary tumor and 14 metastases of an exceptional responder patient to alpelisib monotherapy (*18*). The plot was fitted to a 1:1 distribution, with ρ correlation coefficient indicated. (**B**) Bar graphs of progression free survival of ER+ metastatic breast cancer patients with WT, single, and double *PIK3CA* mutant tumors on a phase 1 clinical trial (NCT01870505) of alpelisib and an aromatase inhibitor (7.5 weeks [95% CI 5 weeks – not reached] vs 20 weeks [95% CI 10 weeks – not reached] vs 48 weeks [95% CI 13 weeks – 49 weeks]). NS = not significant. (**C**) Retrospective analysis of PFS of patients with double *PIK3CA* mutant, single *PIK3CA* mutant, and WT *PIK3CA* breast cancers on aromatase inhibitor (top) or fulvestrant (bottom) therapy from the MSKCC cohort (*9*). p values were calculated using the logrank test.

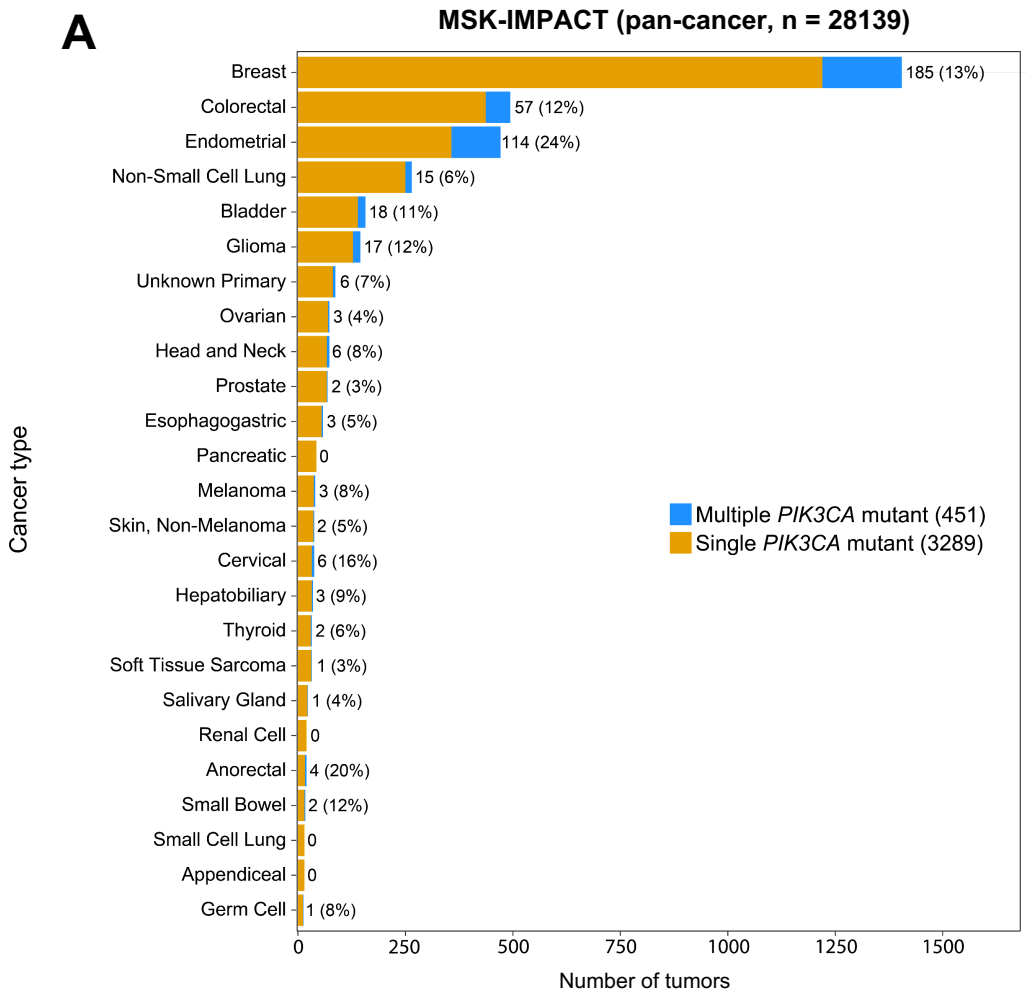
A
MSK-IMPACT (pan-cancer, n = 28139)
Cancer type
Breast
Colorectal
Endometrial
Non-Small Cell Lung
Bladder
Glioma
Unknown Primary
Ovarian
Head and Neck
Prostate
Esophagogastric
Pancreatic
Melanoma
Skin, Non-Melanoma
Cervical
Hepatobiliary
Thyroid
Soft Tissue Sarcoma
Salivary Gland
Renal Cell
Anorectal
Small Bowel
Small Cell Lung
Appendiceal
Germ Cell
185 (13%)
57 (12%)
114 (24%)
15 (6%)
18 (11%)
17 (12%)
6 (7%)
3 (4%)
6 (8%)
2 (3%)
3 (5%)
0
3 (8%)
2 (5%)
6 (16%)
3 (9%)
2 (6%)
1 (3%)
1 (4%)
0
4 (20%)
2 (12%)
0
0
1 (8%)
Multiple PIK3CA mutant (451)
Single PIK3CA mutant (3289)
0
250
500
750
1000
1250
1500
Number of tumors

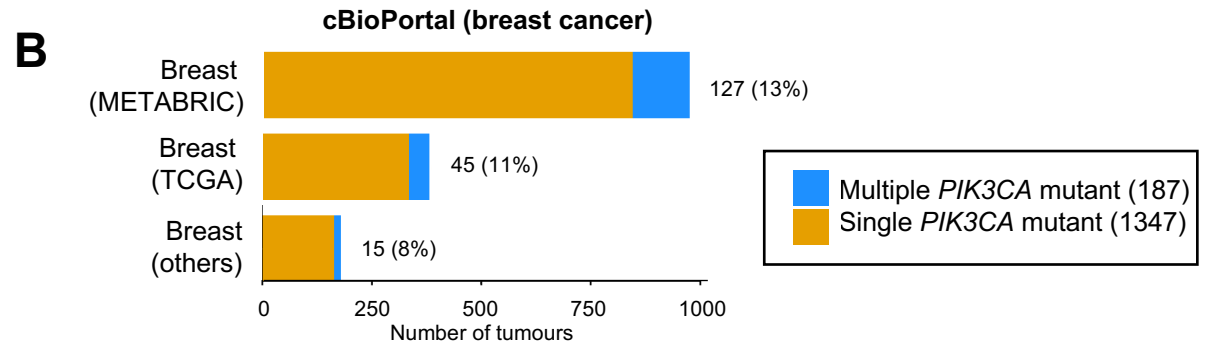
B
cBioPortal (breast cancer)
Breast (METABRIC)
Breast (TCGA)
Breast (others)
127 (13%)
45 (11%)
15 (8%)
Multiple PIK3CA mutant (187)
Single PIK3CA mutant (1347)
0
250
500
750
1000
Number of tumours

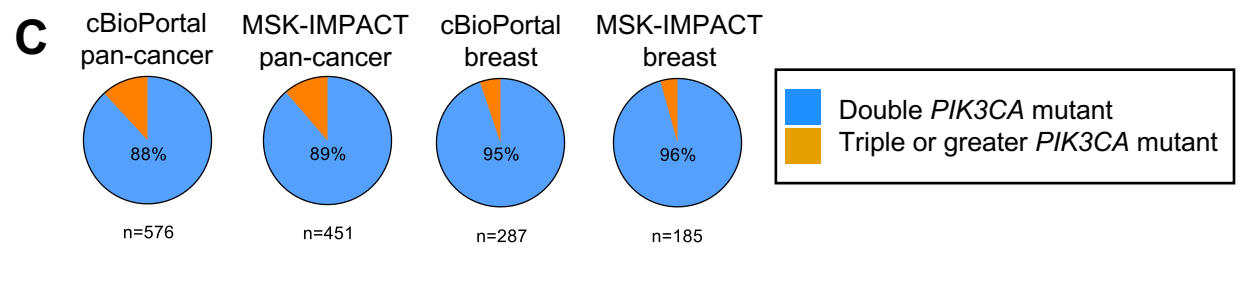
C
cBioPortal pan-cancer
MSK-IMPACT pan-cancer
cBioPortal breast
MSK-IMPACT breast
88%
89%
95%
96%
n=576
n=451
n=287
n=185
Double PIK3CA mutant
Triple or greater PIK3CA mutant

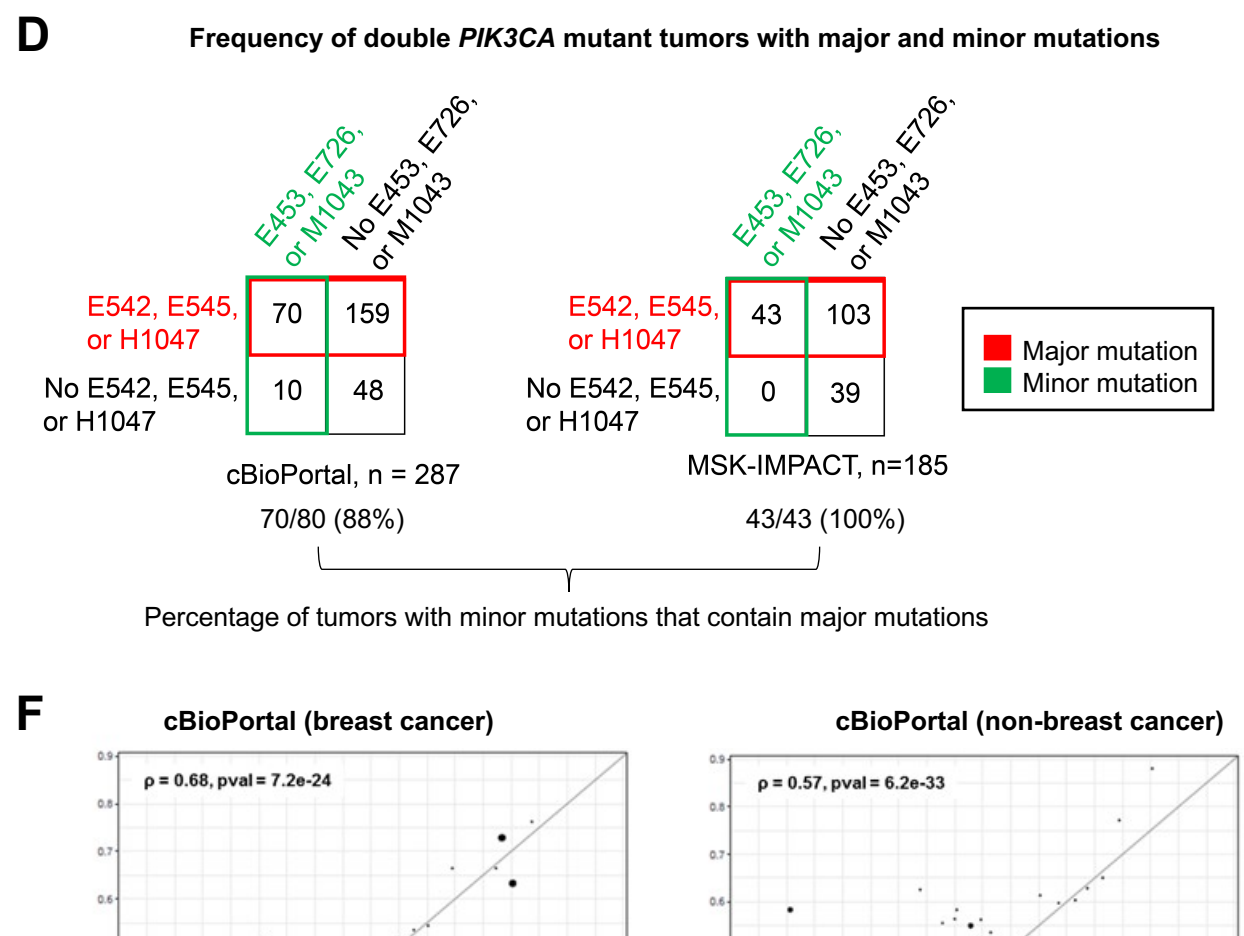
D
Frequency of double PIK3CA mutant tumors with major and minor mutations
E453, E726, or M1043
No E453, E726, or M1043
E542, E545, or H1047
No E542, E545, or H1047
70
159
10
48
43
103
0
39
Major mutation
Minor mutation
cBioPortal, n = 287
70/80 (88%)
MSK-IMPACT, n=185
43/43 (100%)
Percentage of tumors with minor mutations that contain major mutations

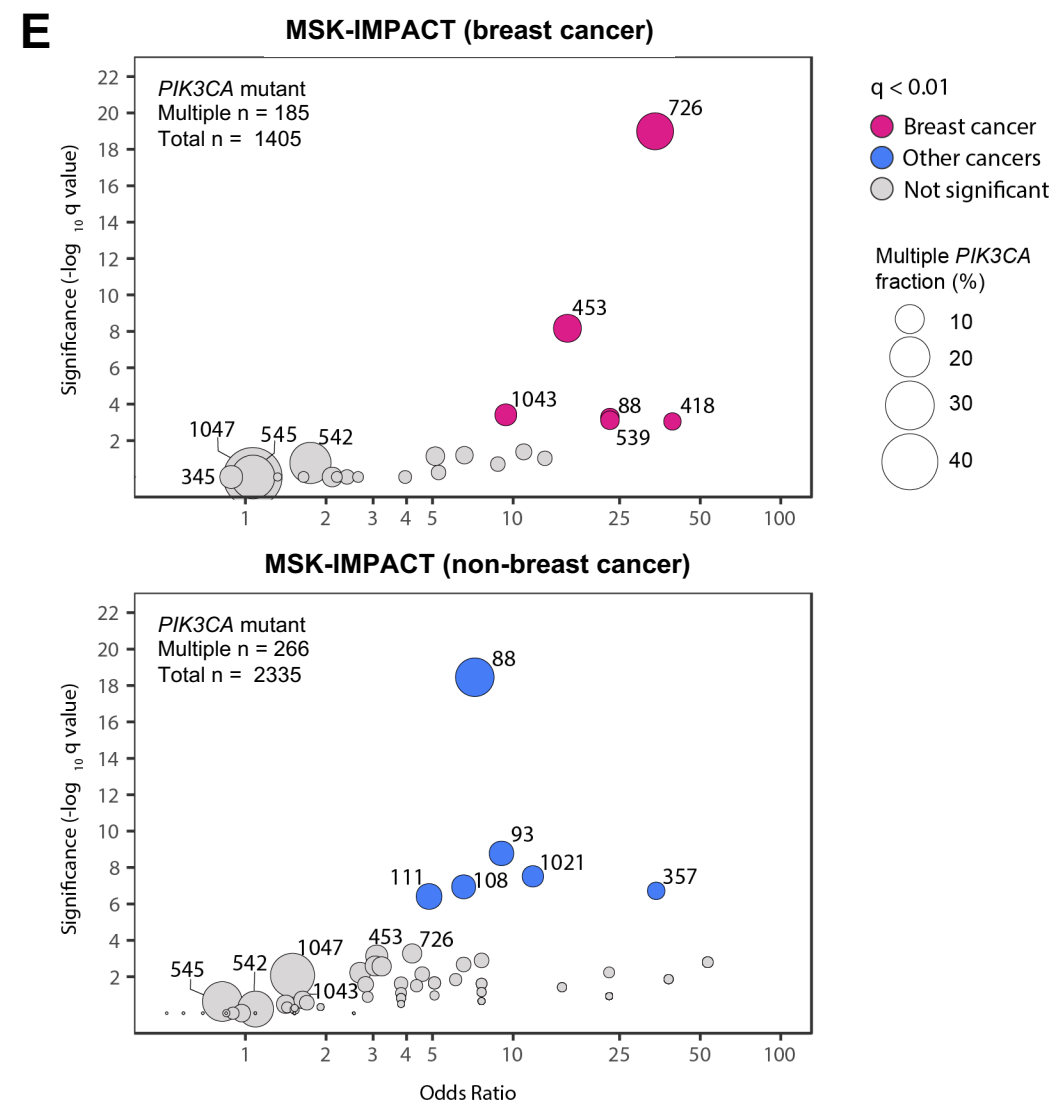
E
MSK-IMPACT (breast cancer)
PIK3CA mutant
Multiple n = 185
Total n = 1405
Significance (-log 10 q value)
726
453
1043
88
539
418
1047
545
542
345
q < 0.01
Breast cancer
Other cancers
Not significant
Multiple PIK3CA fraction (%)
10
20
30
40
1
2
3
4
5
10
25
50
100
MSK-IMPACT (non-breast cancer)
PIK3CA mutant
Multiple n = 266
Total n = 2335
88
93
1021
111
108
357
1047
453
726
545
542
1043
Odds Ratio

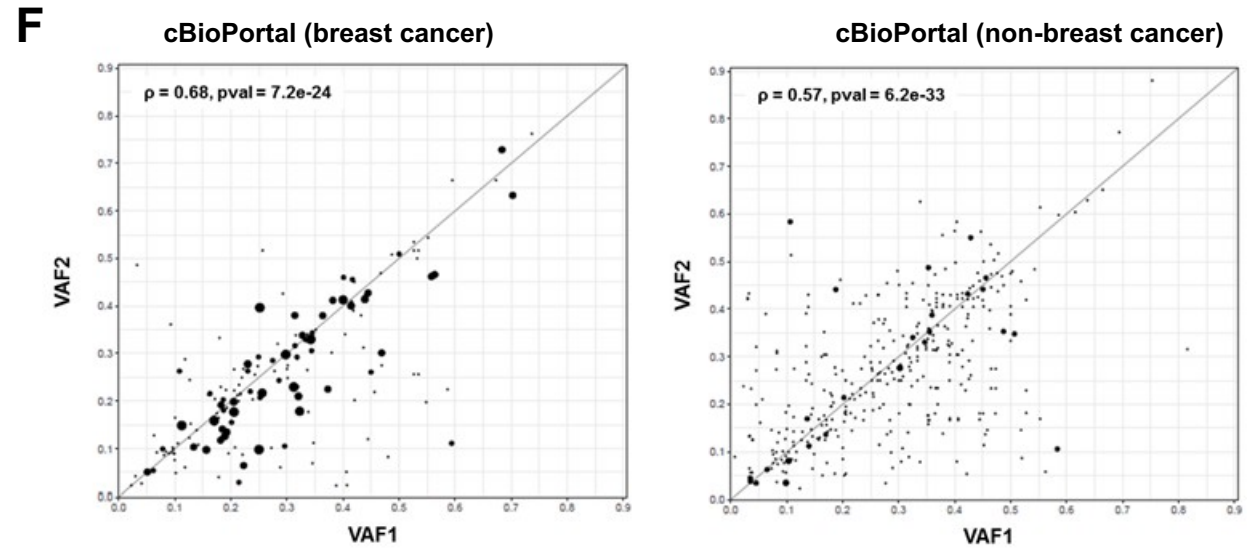
F
cBioPortal (breast cancer)
ρ = 0.68, pval = 7.2e-24
cBioPortal (non-breast cancer)
ρ = 0.57, pval = 6.2e-33
VAF2
VAF1

Fig. S2

Fig. S2: Double *PIK3CA* mutations are frequent across all cancers including breast cancer. (**A, B**) Bar plot showing number and frequency of multiple *PIK3CA* mutant tumors among all *PIK3CA* mutant tumors across different histologies (MSK-IMPACT) (**A**) and among *PIK3CA* mutant breast tumors (cBioPortal) (**B**). (**C**) Pie charts showing frequency of double *PIK3CA* mutated tumors among multiple *PIK3CA* mutated tumors across datasets. (**D**) 2 x 2 tables showing frequency of double *PIK3CA* mutant breast tumors from cBioPortal and MSK-IMPACT with major mutations E542, E545, or H1047 (boxed in red) and with minor mutations E453, E726, or M1043. Tumors containing major and minor mutations are boxed in red and green, respectively. (**E**) Codon enrichment analysis of amino acid positions most recurrently found in multiple *PIK3CA* mutated breast tumors (top) and non-breast tumors (bottom) as compared to single *PIK3CA* mutant tumors (MSK-IMPACT). Samples containing the same double mutant are depicted as a circle, sized according to the number of samples. Samples colored in pink or blue are those with an FDR corrected pvalue (qval) < 0.01. Statistics were calculated independently using two-sided Fisher's exact tests. (**F**) Variant allele frequencies in double *PIK3CA* mutant breast (left) and non-breast (right) tumors (cBioPortal). Plots were fitted to a 1:1 distribution, with ρ correlation coefficient and p-value indicated.

METABRIC 2019

***PIK3CA* mutational status**	**Multiple**	**Single**	**p**
n	114	681	
Age at diagnosis = mean (SD)	62.50 (12.76)	62.31 (12.22)	0.881
Inferred menopausal state = pre (%)	21 (18.4)	121 (17.8)	0.971
Stage (%)			0.071
1	35 (39.3)	164 (32.9)	
2	51 (57.3)	290 (58.1)	
3	2 (2.2)	43 (8.6)	
4	1 (1.1)	2 (0.4)	
Lymph nodes (%)			0.194
1-3	33 (28.9)	210 (30.8)	
4+	12 (10.5)	111 (16.3)	
None	69 (60.5)	360 (52.9)	
Grade (%)			0.165
1	16 (14.4)	98 (15.0)	
2	59 (53.2)	287 (43.8)	
3	36 (32.4)	270 (41.2)	
Receptor status (%)			0.001
HR+/HER2-	109 (95.6)	568 (83.4)	
HR+/HER2+	1 (0.9)	35 (5.1)	
HR-/HER2+	0 (0.0)	42 (6.2)	
HR-/HER2-	4 (3.5)	36 (5.3)	
ER expression = + (%)	106 (93.0)	583 (85.6)	0.046
PR expression = + (%)	79 (69.3)	443 (65.1)	0.437
HER2 expression = + (%)	1 (0.9)	77 (11.3)	<0.001
Histology (%)			0.078
IDC	87 (76.3)	583 (85.7)	
ILC	16 (14.0)	53 (7.8)	
Mixed IDC/ILC	9 (7.9)	36 (5.3)	
Other	2 (1.8)	8 (1.2)	
Received (neo)adjuvant chemotherapy (%)	14 (12.3)	105 (15.4)	0.467
Received adjuvant hormonal therapy (%)	71 (62.3)	432 (63.4)	0.895
Received adjuvant radiotherapy (%)	62 (54.4)	375 (55.1)	0.973
PAM50 subtype (%)			0.155
Basal	3 (2.7)	45 (6.6)	
HER2	10 (8.8)	86 (12.7)	
Luminal A	62 (54.9)	334 (49.2)	
Luminal B	21 (18.6)	145 (21.4)	
Normal	17 (15.0)	69 (10.2)	
Nottingham Prognostic Index (mean (SD))	3.69 (0.99)	3.87 (1.17)	0.116

MSKCC cohort

***PIK3CA* mutational status**	**Multiple**	**Single**	**p**
n	99	626	
Age at diagnosis = mean (SD)	53.27 (11.51)	53.58 (11.98)	0.811
Menopausal state (%)			0.769
Pre/perimenopausal	52 (52.5)	304 (48.6)	
Postmenopausal	47 (47.5)	317 (50.6)	
Male or Unknown	0 (0.0)	5 (0.8)	
Stage (%)			0.341
1	27 (27.3)	200 (31.9)	
2	26 (26.3)	191 (30.5)	
3	25 (25.3)	108 (17.3)	
4	21 (21.2)	122 (19.5)	
Undefined	0 (0.0)	5 (0.8)	
Grade (%)			0.131
1	7 (7.1)	45 (7.2)	
2	37 (37.4)	171 (27.3)	
3	43 (43.4)	346 (55.3)	
Unknown	12 (12.1)	64 (10.2)	
Receptor status (%)			0.041
HR+/HER2-	93 (93.9)	521 (83.2)	
HR+/HER2+	3 (3.0)	66 (10.5)	
HR-/HER2+	1 (1.0)	18 (2.9)	
HR-/HER2-	2 (2.0)	21 (3.4)	
ER status (%)			0.621
Positive	88 (88.9)	533 (85.1)	
Negative	8 (8.1)	73 (11.7)	
Unknown/not defined	3 (3.0)	20 (3.2)	
PR status (%)			0.907
Positive	63 (63.6)	406 (64.9)	
Negative	31 (31.3)	193 (30.8)	
Unknown/not defined	5 (5.1)	27 (4.3)	
HER2 status (%)			0.003
Positive	1 (1.0)	64 (10.2)	
Negative	93 (93.9)	533 (85.1)	
Unknown/not defined	5 (5.1)	29 (4.6)	
Histology (%)			0.132
IDC	63 (63.6)	442 (70.6)	
ILC	28 (28.3)	125 (20.0)	
Mixed IDC/ILC	7 (7.1)	35 (5.6)	
Other	1 (1.0)	24 (3.8)	
Received chemotherapy (%)	47 (47.5)	305 (48.7)	0.902
Received hormonal therapy (%)	30 (30.3)	250 (39.9)	0.086

Fig. S3

Fig. S3: Clinicogenomic analysis of *PIK3CA* mutant breast cancers. METABRIC 2019 (*64*) and MSKCC cohorts (*9*) were analyzed. p values were calculated by t-test (age) and chi square or Fisher's exact test, when appropriate.

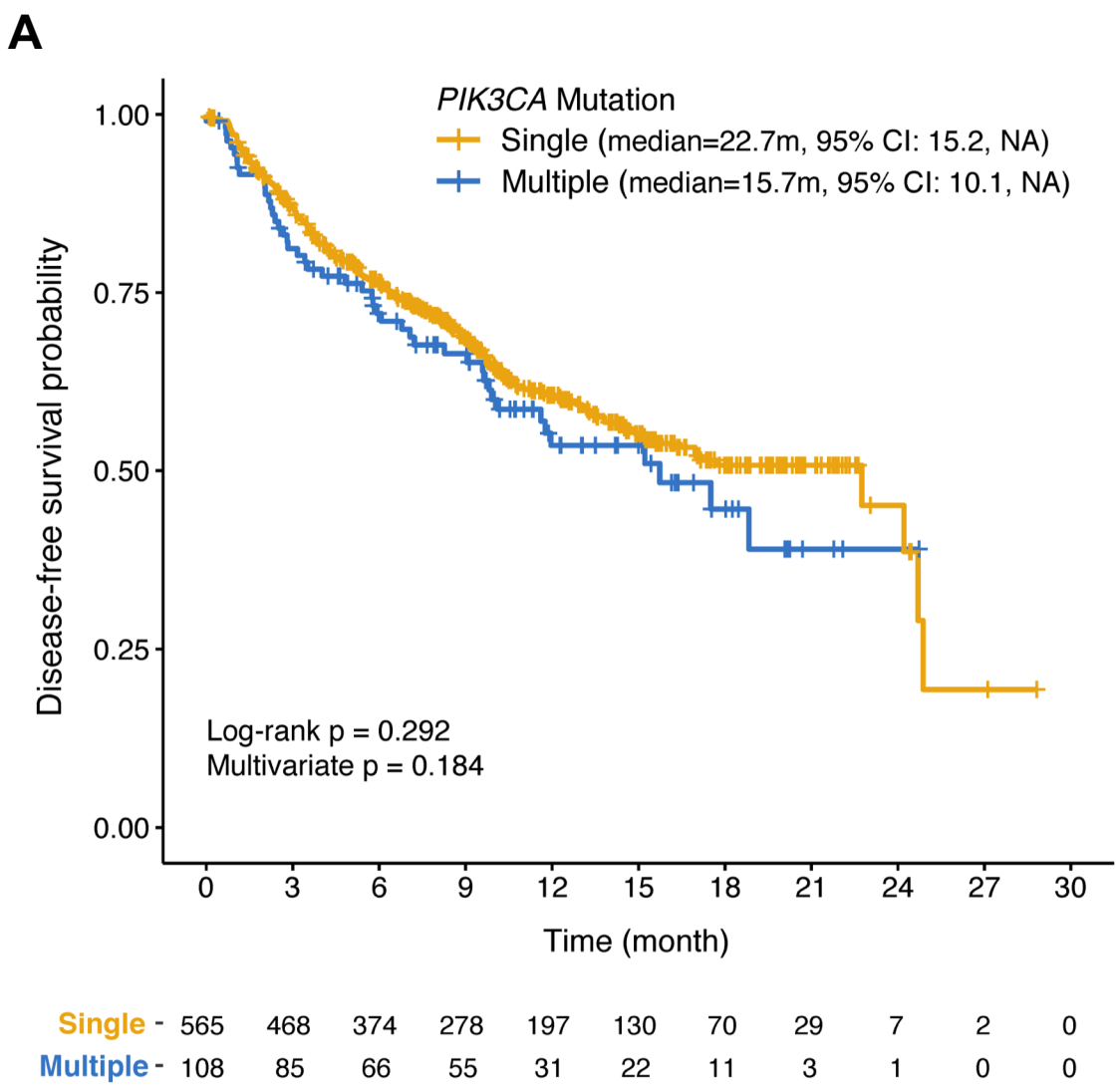
A
PIK3CA Mutation
Single (median=22.7m, 95% CI: 15.2, NA)
Multiple (median=15.7m, 95% CI: 10.1, NA)
Disease-free survival probability
1.00
0.75
0.50
0.25
0.00
Log-rank p = 0.292
Multivariate p = 0.184
0 3 6 9 12 15 18 21 24 27 30
Time (month)
Single - 565 468 374 278 197 130 70 29 7 2 0
Multiple - 108 85 66 55 31 22 11 3 1 0 0

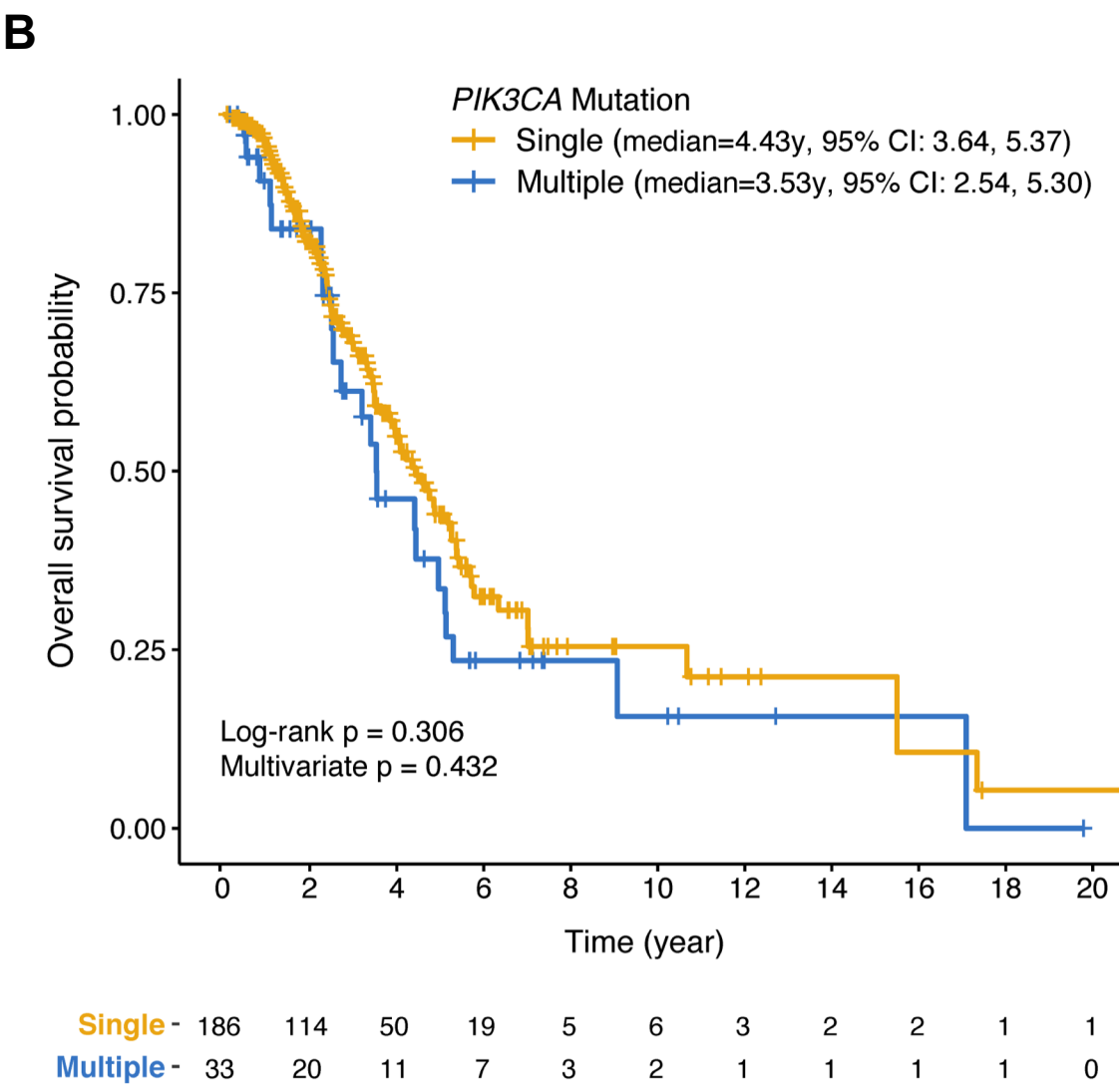
B
PIK3CA Mutation
Single (median=4.43y, 95% CI: 3.64, 5.37)
Multiple (median=3.53y, 95% CI: 2.54, 5.30)
Overall survival probability
1.00
0.75
0.50
0.25
0.00
Log-rank p = 0.306
Multivariate p = 0.432
0 2 4 6 8 10 12 14 16 18 20
Time (year)
Single - 186 114 50 19 5 6 3 2 2 1 1
Multiple - 33 20 11 7 3 2 1 1 1 1 0

Fig. S4

Fig. S4: Survival analysis of *PIK3CA* mutant HR+/HER2- breast cancer patients. (**A**) Invasive disease-free survival analysis of METABRIC 2019 cohort (*64*). (**B**) Overall survival analysis of MSKCC cohort (*9*). For multivariate analyses, Cox proportional hazard models were utilized and adjusted for age, menopausal status, histology, stage at diagnosis, and receipt of chemotherapy, hormonal therapy, and radiotherapy. For the overall survival analysis, all models were further adjusted for the late entry by left truncation. For univariate analysis, p values were calculated using the log-rank test. For multivariate analysis, p values were calculated using the Cox proportional hazard model.

A

Double *PIK3CA* mutants	FFPE archival tumor sample: gDNA distance	FFPE archival tumor sample: Resolvable by NGS	Fresh tumor sample: cDNA distance	Fresh tumor sample: Resolvable by NGS	Fresh tumor sample: Resolvable by Sanger-seq	Fresh tumor sample: Resolvable by SMRT-seq
E542K + E453Q/K	8.00 kb	No	0.27 kb	Yes	Yes	**Yes**
E542K + E726K	2.85 kb	No	0.56 kb	No	Yes	**Yes**
E542K + M1043L/I	16.00 kb	No	1.51 kb	No	No	**Yes**
E545K + E453Q/K	8.01 kb	No	0.28 kb	Yes	Yes	**Yes**
E545K + E726K	2.84 kb	No	0.55 kb	No	Yes	**Yes**
E545K + M1043L/I	15.98 kb	No	1.50 kb	No	No	**Yes**
H1047R + E453Q/K	24.01 kb	No	1.79 kb	No	No	**Yes**
H1047R + E726K	13.15 kb	No	0.97 kb	No	No	**Yes**

Major mutation
Minor mutation

B

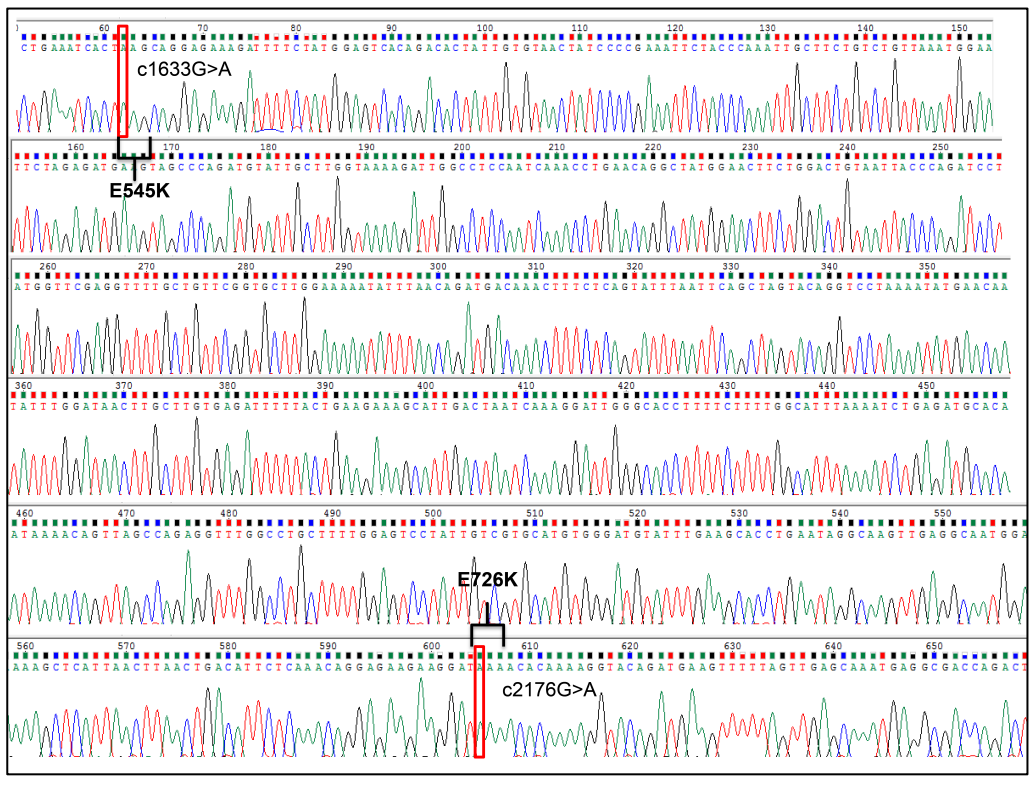

Sanger sequencing of double *PIK3CA* mutant breast tumor cDNA

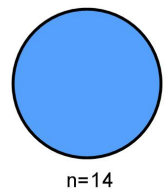

E545K/E726K

n=14

C

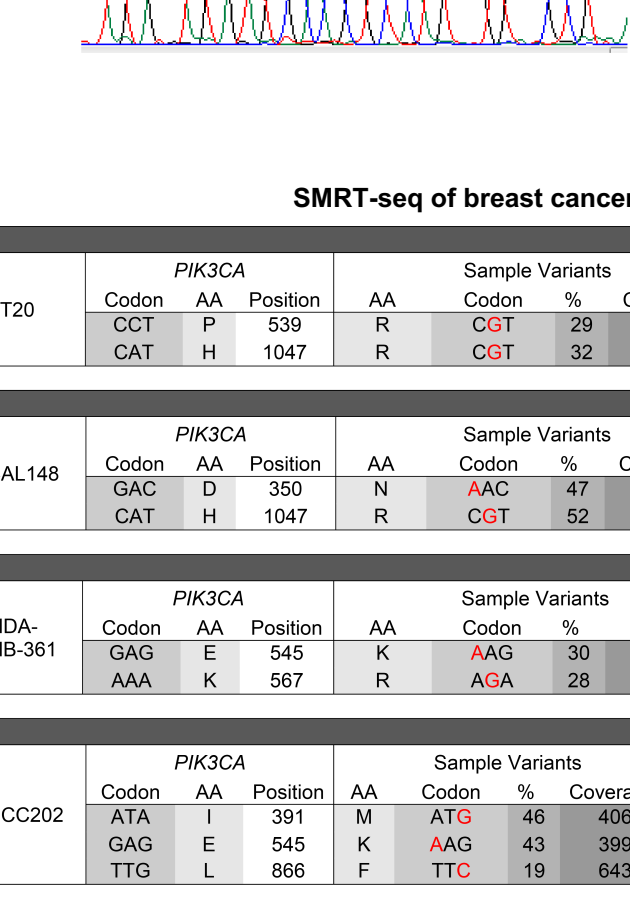

Sanger sequencing of double *PIK3CA* mutant BT20 breast cancer cell line cDNA

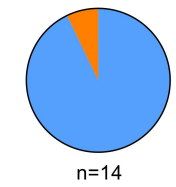

P539/H1047R
H1047R

n=14

D

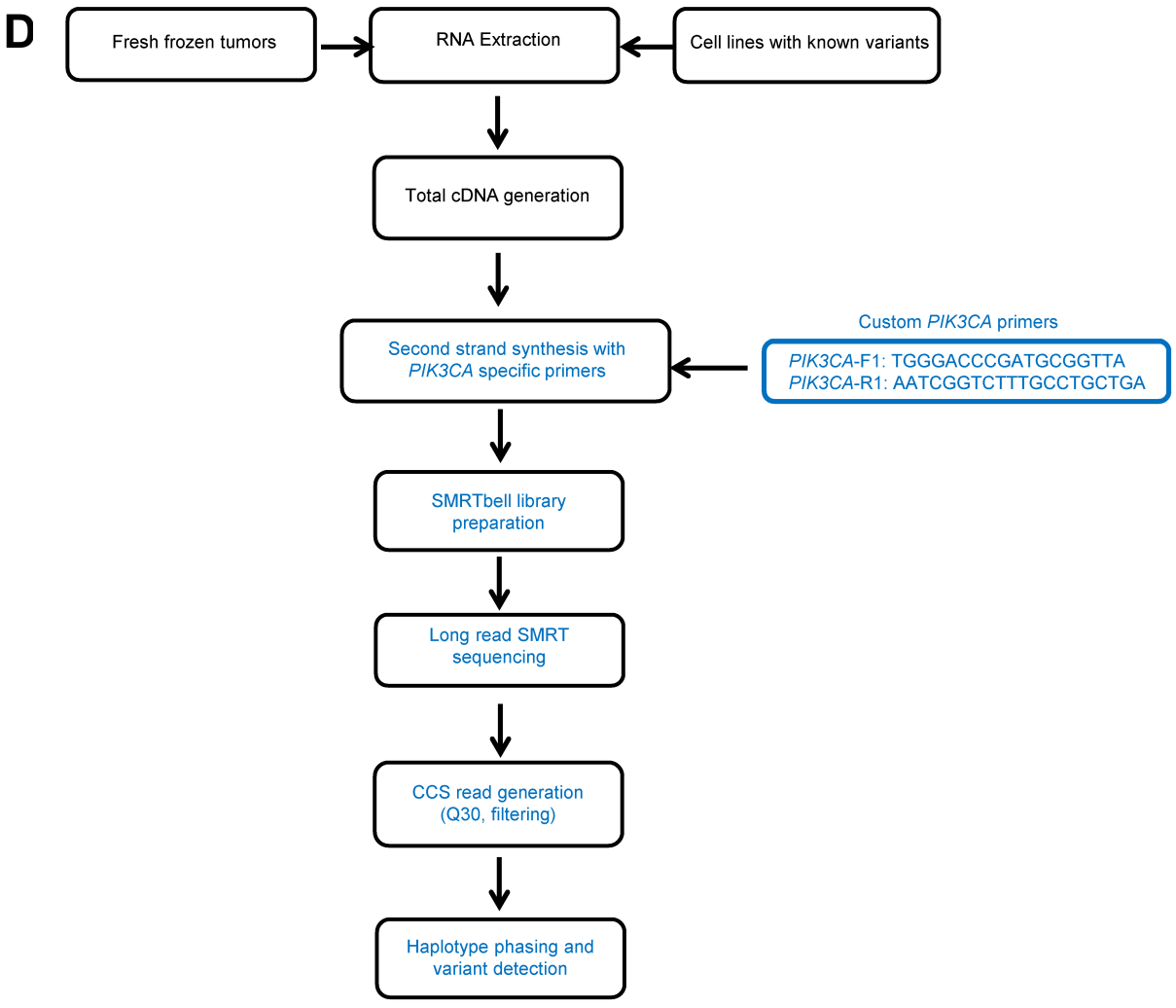

E

SMRT-seq of breast cancer cell lines

	PIK3CA Codon	*PIK3CA* AA	*PIK3CA* Position	Sample Variants AA	Sample Variants Codon	Sample Variants %	Sample Variants Coverage	Haplotype % A	B	C	D
BT20	CCT	P	539	R	CGT	29	3710	66.9	21.6	6.1	5.4
	CAT	H	1047	R	CGT	32	7573				

	PIK3CA Codon	*PIK3CA* AA	*PIK3CA* Position	Sample Variants AA	Sample Variants Codon	Sample Variants %	Sample Variants Coverage	Haplotype % A	B	C	D
CAL148	GAC	D	350	N	AAC	47	1788	43.8	43.8	7	5.4
	CAT	H	1047	R	CGT	52	4704				

	PIK3CA Codon	*PIK3CA* AA	*PIK3CA* Position	Sample Variants AA	Sample Variants Codon	Sample Variants %	Sample Variants Coverage	Haplotype % A	B	C
MDA-MB-361	GAG	E	545	K	AAG	30	3774	40.6	30.5	28.9
	AAA	K	567	R	AGA	28	3308			

	PIK3CA Codon	*PIK3CA* AA	*PIK3CA* Position	Sample Variants AA	Sample Variants Codon	Sample Variants %	Sample Variants Coverage	Haplotype % A	B	C	D	E
HCC202	ATA	I	391	M	ATG	46	4063	48.4	28	22.7	0.6	0.4
	GAG	E	545	K	AAG	43	3990					
	TTG	L	866	F	TTC	19	6436					

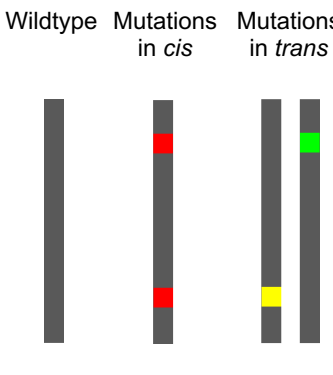

Fig. S5

Fig. S5: Double *PIK3CA* mutations are in *cis* on the same allele. (**A**) Table showing recurrent double *PIK3CA* mutations, distances in genomic DNA (gDNA) and complementary DNA (cDNA), and resolution abilities by different sequencing techniques from FFPE archival and fresh tumors. Double mutants resolvable by SMRT-seq are bolded. (**B**) Sanger sequencing of cDNA from double *PIK3CA* mutant breast tumor (E545K/E726K) with representative tracing (n=14 colonies). (**C**) Sanger sequencing of cDNA from double *PIK3CA* mutant breast cancer cell line BT20 (P539/H1047R), with representative tracings from two separate priming reactions from cDNA from the same single colony (n=14 colonies). (**D**) Workflow for SMRT sequencing from fresh frozen tumors. (**E**) SMRT-seq phasing of allelic configuration of four double *PIK3CA* mutant breast cancer cell lines (BT20 [P539R/H1047R], CAL148 [D350N/H1047R], MDA-MB-361 [E545K/K567R], HCC202 [E545K/L866F]). *Cis* mutations are shown as red vertical squares, *trans* mutations as single yellow or green squares, and WT sequences as grey vertical squares, as in legend, in order of amplicon frequency.

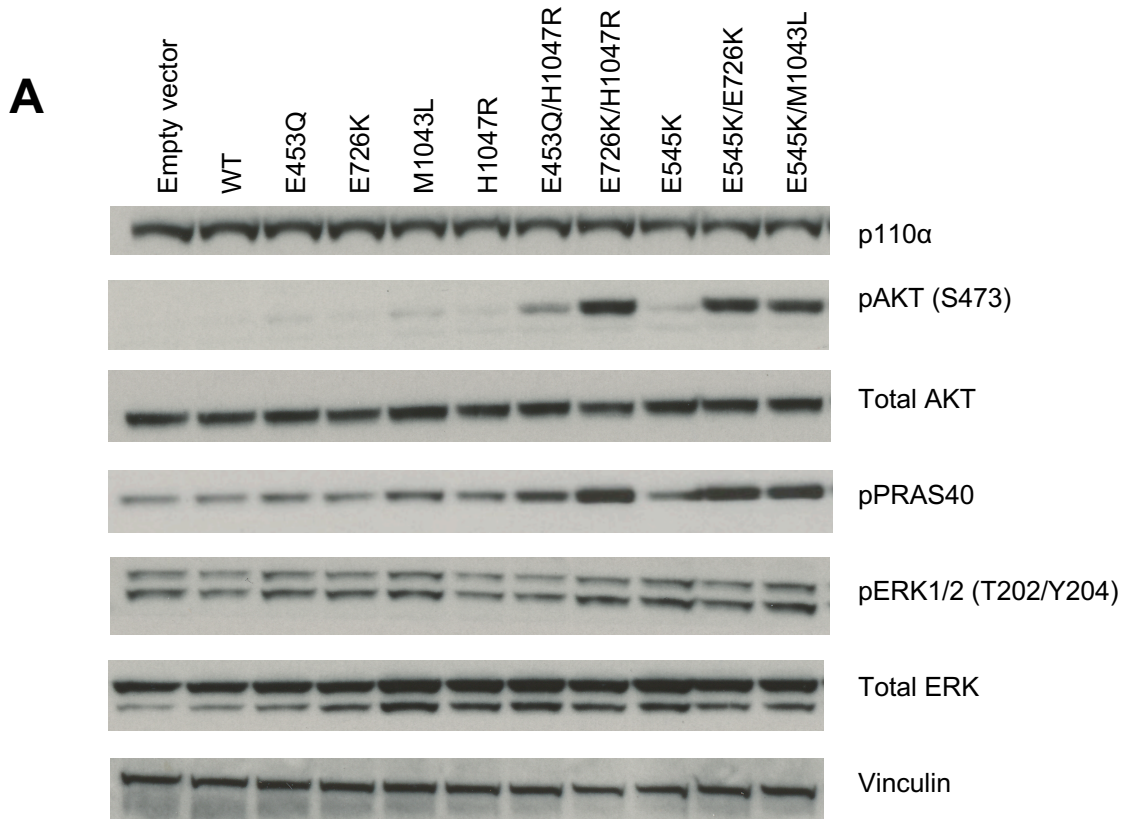
A
Empty vector
WT
E453Q
E726K
M1043L
H1047R
E453Q/H1047R
E726K/H1047R
E545K
E545K/E726K
E545K/M1043L
p110α
pAKT (S473)
Total AKT
pPRAS40
pERK1/2 (T202/Y204)
Total ERK
Vinculin
MCF7 (PIK3CA WT background), serum starved

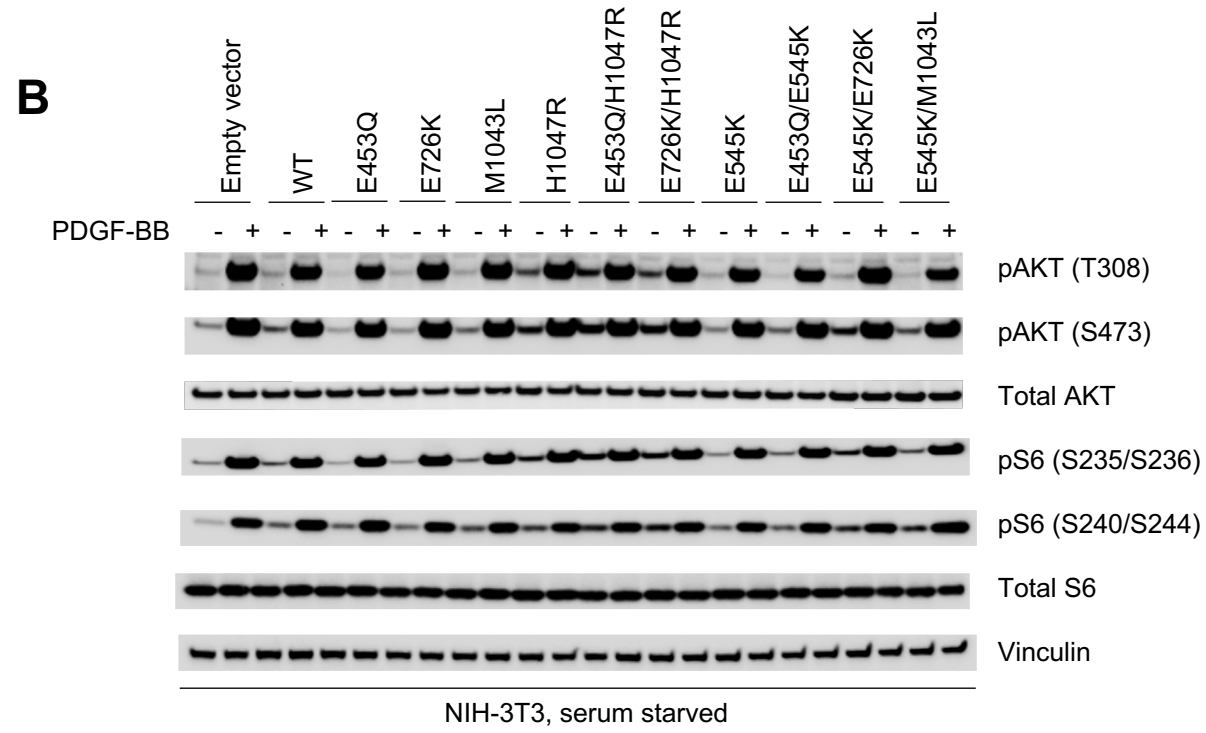
B
Empty vector
WT
E453Q
E726K
M1043L
H1047R
E453Q/H1047R
E726K/H1047R
E545K
E453Q/E545K
E545K/E726K
E545K/M1043L
PDGF-BB
- + - + - + - + - + - + - + - + - + - + - + - +
pAKT (T308)
pAKT (S473)
Total AKT
pS6 (S235/S236)
pS6 (S240/S244)
Total S6
Vinculin
NIH-3T3, serum starved

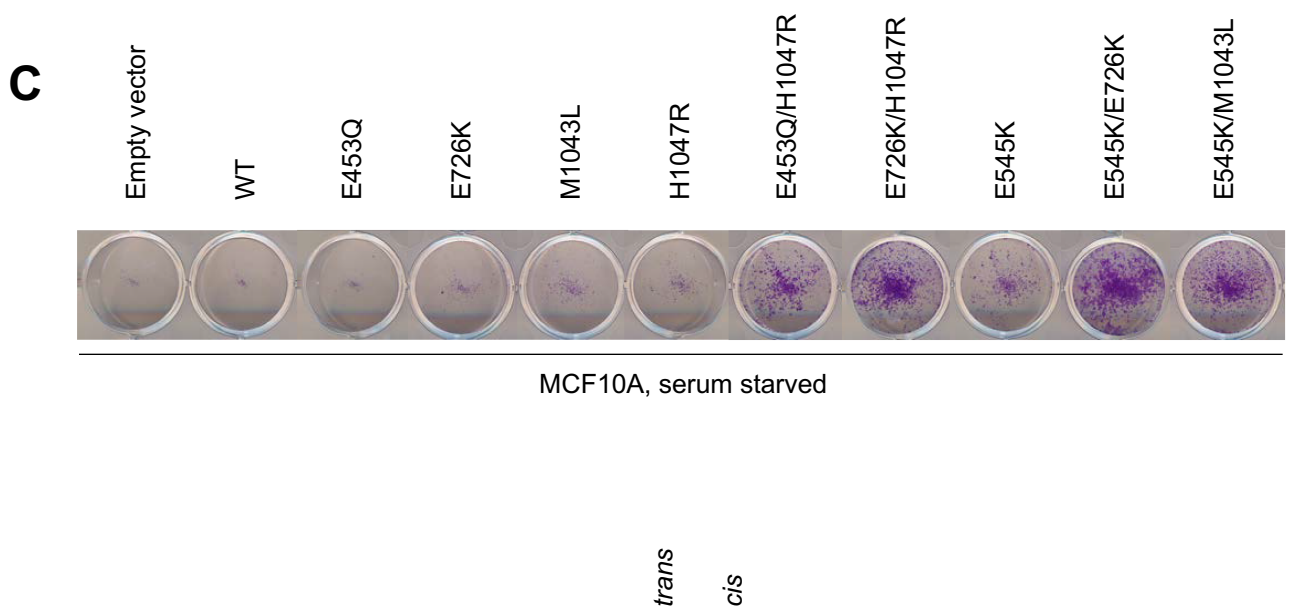
C
Empty vector
WT
E453Q
E726K
M1043L
H1047R
E453Q/H1047R
E726K/H1047R
E545K
E545K/E726K
E545K/M1043L
MCF10A, serum starved

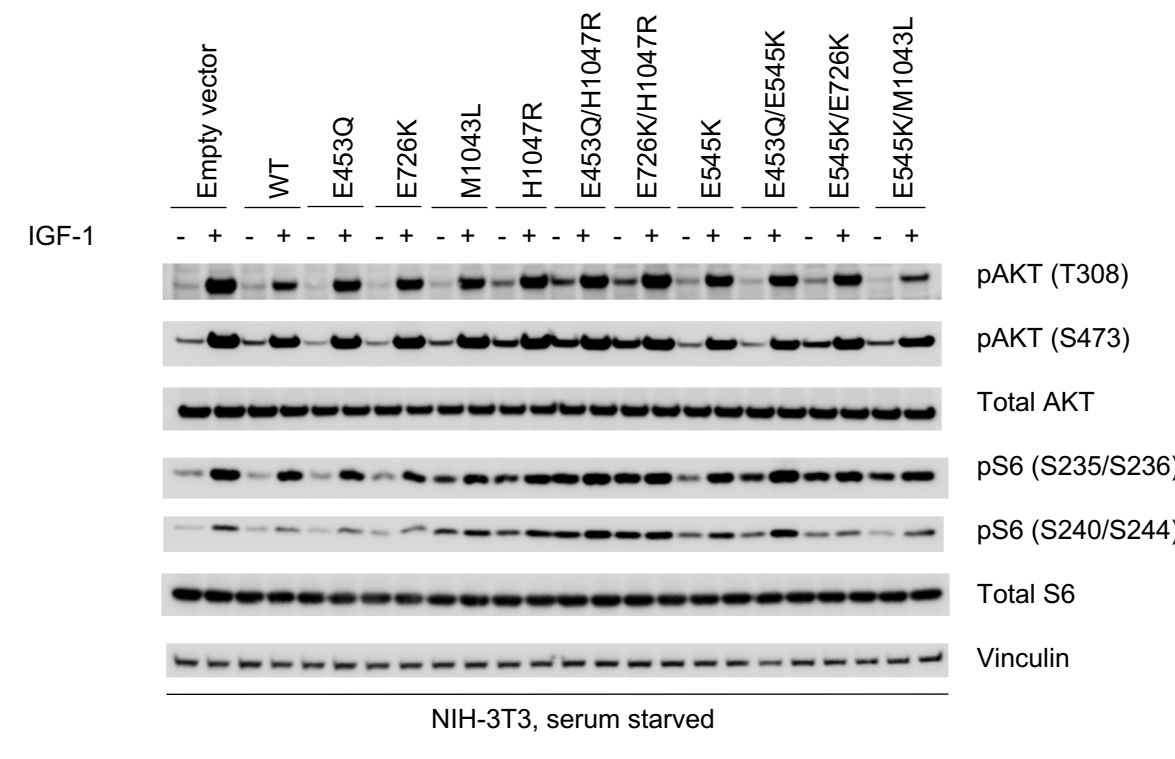
Empty vector
WT
E453Q
E726K
M1043L
H1047R
E453Q/H1047R
E726K/H1047R
E545K
E453Q/E545K
E545K/E726K
E545K/M1043L
IGF-1
- + - + - + - + - + - + - + - + - + - + - + - +
pAKT (T308)
pAKT (S473)
Total AKT
pS6 (S235/S236)
pS6 (S240/S244)
Total S6
Vinculin
NIH-3T3, serum starved

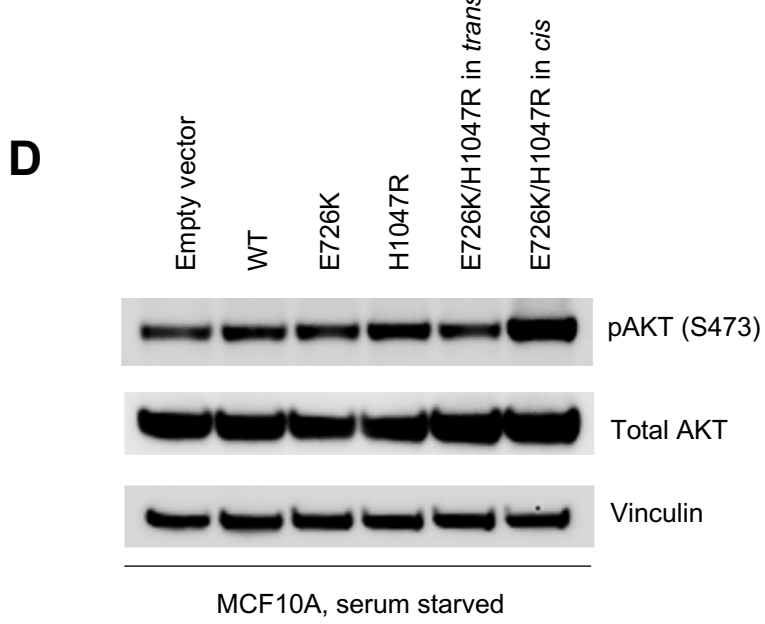
D
Empty vector
WT
E726K
H1047R
E726K/H1047R in trans
E726K/H1047R in cis
pAKT (S473)
Total AKT
Vinculin
MCF10A, serum starved

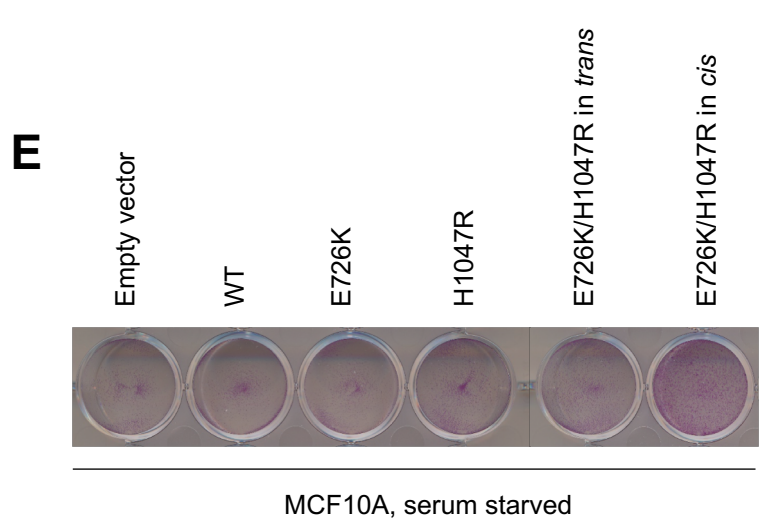
E
Empty vector
WT
E726K
H1047R
E726K/H1047R in trans
E726K/H1047R in cis
MCF10A, serum starved

Fig. S6

Fig. S6: Cellular assays of *PIK3CA* mutations in *cis* and *trans*. (**A**) Western blotting of PI3K effectors of *PIK3CA* mutant stably transduced MCF7 cells (in a *PIK3CA* WT background) under serum starvation for 1 day. (**B**) Western blotting of PI3K effectors of *PIK3CA* mutant stably transduced NIH-3T3 cells, serum starved for 1 day, then stimulated with (top) PDGF-BB (20 ng/mL, 30 minutes) or (bottom) IGF-1 (10 nM, 10 minutes). (**C**) Crystal violet assay of *PIK3CA* mutant stably transduced MCF10A cells under serum starvation for 4 days (representative sample shown, n=3). (**D**) Western blotting of PI3K effectors of E726K/H1047R in *cis*, in *trans*, and single *PIK3CA* mutant MCF10A cells serum starved for 1 day. (**E**) Crystal violet assay of *PIK3CA* mutant MCF10A cells under serum starvation for 4 days (representative sample shown, n=3).

A

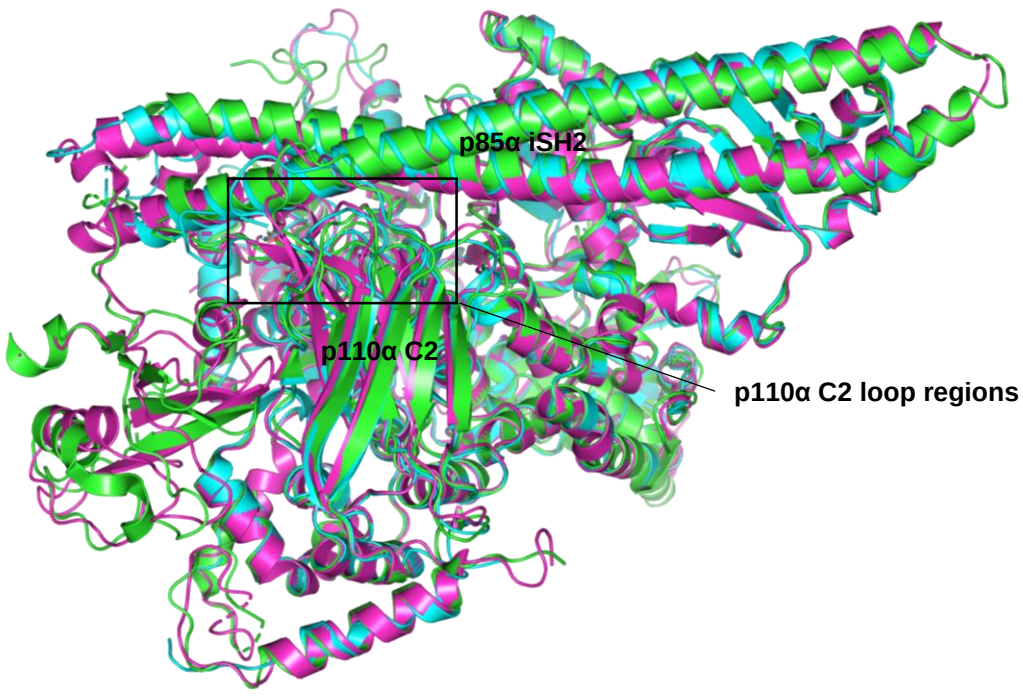

B

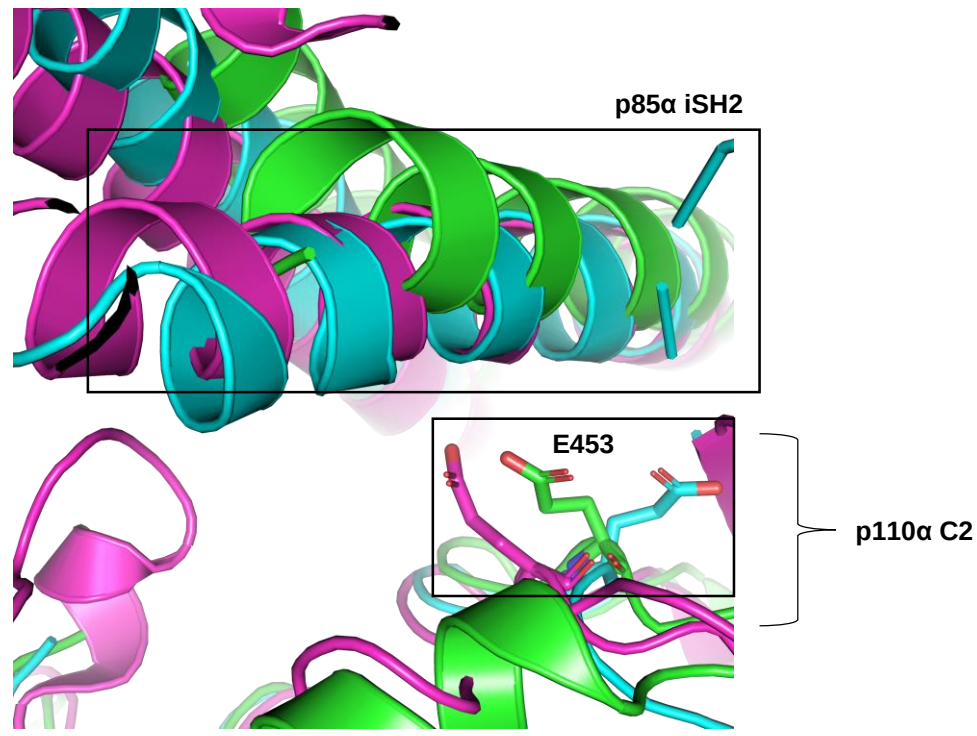

RMSD comparisons

PI3K WT (PDB 2RD0)	2RD0:4OVU	RMSD = 0.624
PI3K WT + PIP_2 (PDB 4OVU)	2RD0:3HHM	RMSD = 0.715
PI3K H1047R (PDB 3HHM)	4OVU:3HHM	RMSD = 0.852

C

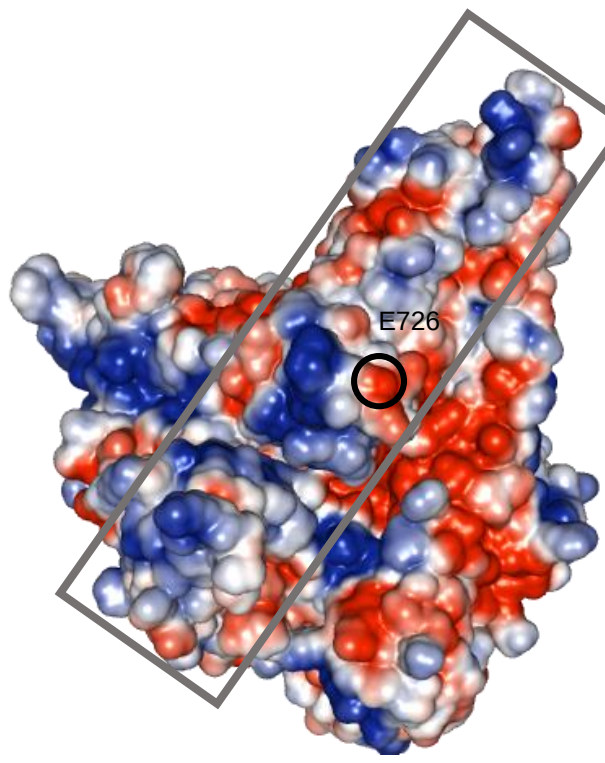

Positively charged surfaces
Negatively charged surfaces
Putative membrane binding surface of PI3Kα

D

PI3K WT (PDB 2RD0)
PI3K WT + PIP_2 (PDB 4OVU)
PI3K H1047R (PDB 3HHM)

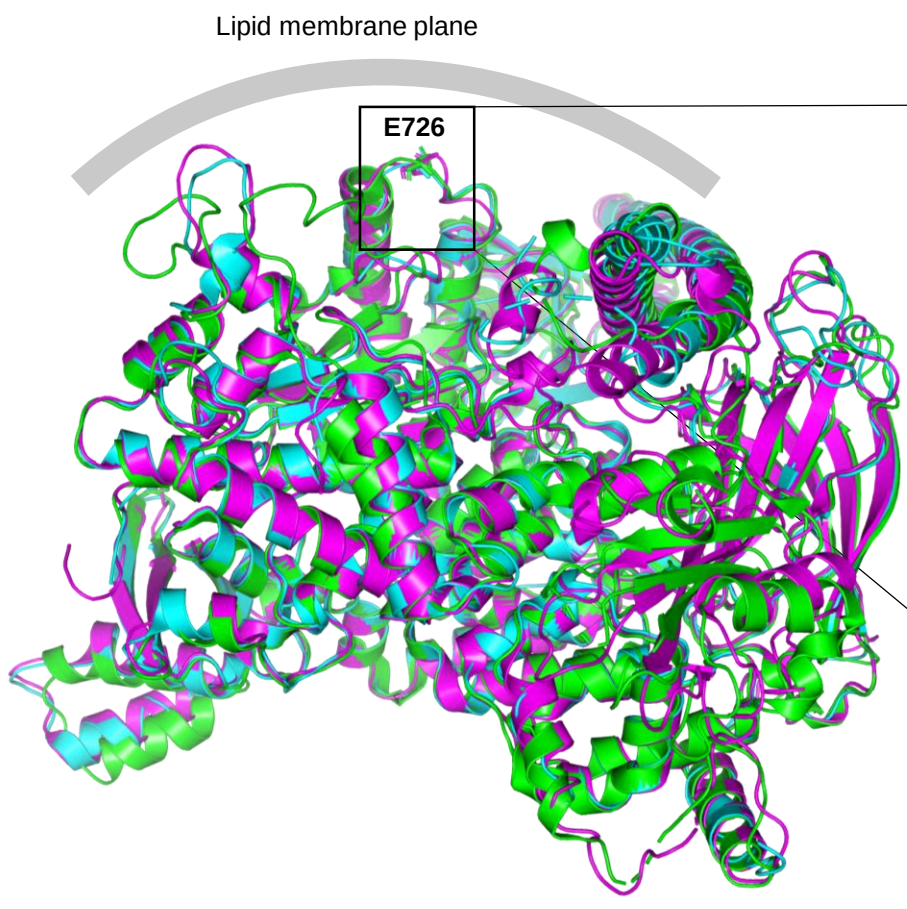

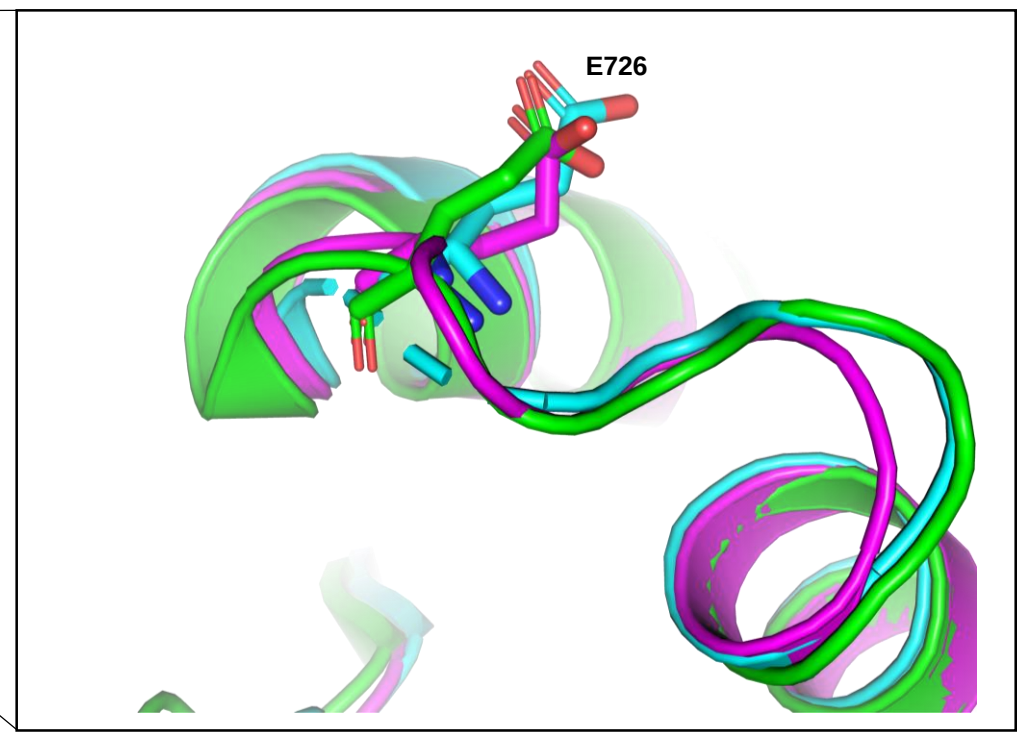

Fig. S7

Fig. S7: Structural mapping of p110α E453 and E726 residues in PI3Kα. (**A**) Structural alignments of PDB 2RD0, 4OVU, and 3HHM PI3Kα crystal structures. RMSD comparisons are shown in box. (**B**) p110α-C2:p85α-iSH2 interface is magnified with E453 shown as sticks. (**C**) (Top) Electrostatic surface diagram of solvent-accessible area of PI3Kα, based on PDB 4OVU. Negatively and positively charged surfaces are colored in red and blue, respectively. The putative membrane binding surface (*35*) is shown in gray box with E726 shown. (**D**) On left, structural alignments of PDB 2RD0, 4OVU, and 3HHM PI3Kα crystal structures in the putative membrane binding mode (as in (**C**)), with E726 shown as sticks and magnified on right.

A

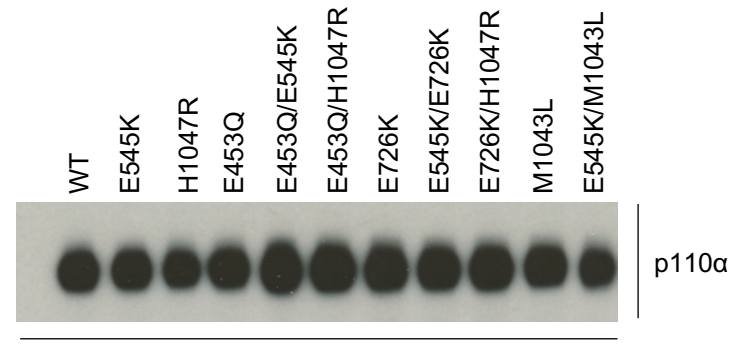

B

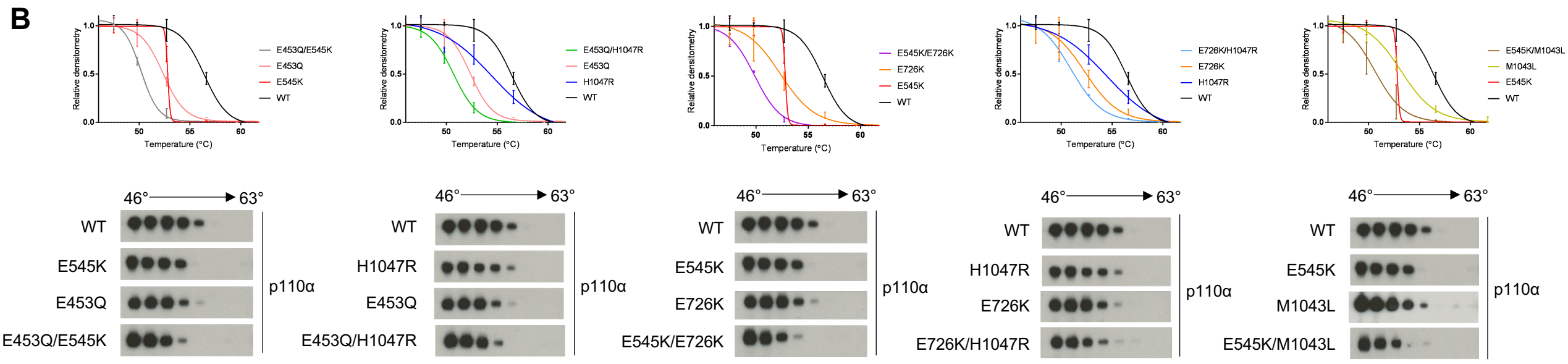

C

	IC_{50} [alpelisib] (nM)	IC_{50} [GDC-0077] (nM)
WT	2.28	0.52
E545K	5.01	0.35
H1047R	1.52	0.17
E453Q	2.05	0.45
E453Q/E545K	6.22	0.15
E453Q/H1047R	1.35	0.15
E726K	3.12	0.40
E545K/E726K	5.06	0.40
E726K/H1047R	4.94	0.26
M1043L	3.88	0.57
E545K/M1043L	2.90	0.32

Fig. S8

Fig. S8: Biochemistry of recombinant *cis* mutant PI3Kα. (**A**) Input control of normalized amounts of *cis* and single mutant recombinant full length PI3K complexes, blotted for p110α. (**B**) Thermal shift assays of recombinant PI3K (as in Fig. 3C), shown for clarity for each individual *cis* mutant and constitutent single mutant, with corresponding Western blots (n=2). (**C**) IC_{50} values for recombinant single and *cis* PI3K mutant proteins for the PI3Kα inhibitors alpelisib and GDC-0077. Data are averages (n=3).

A

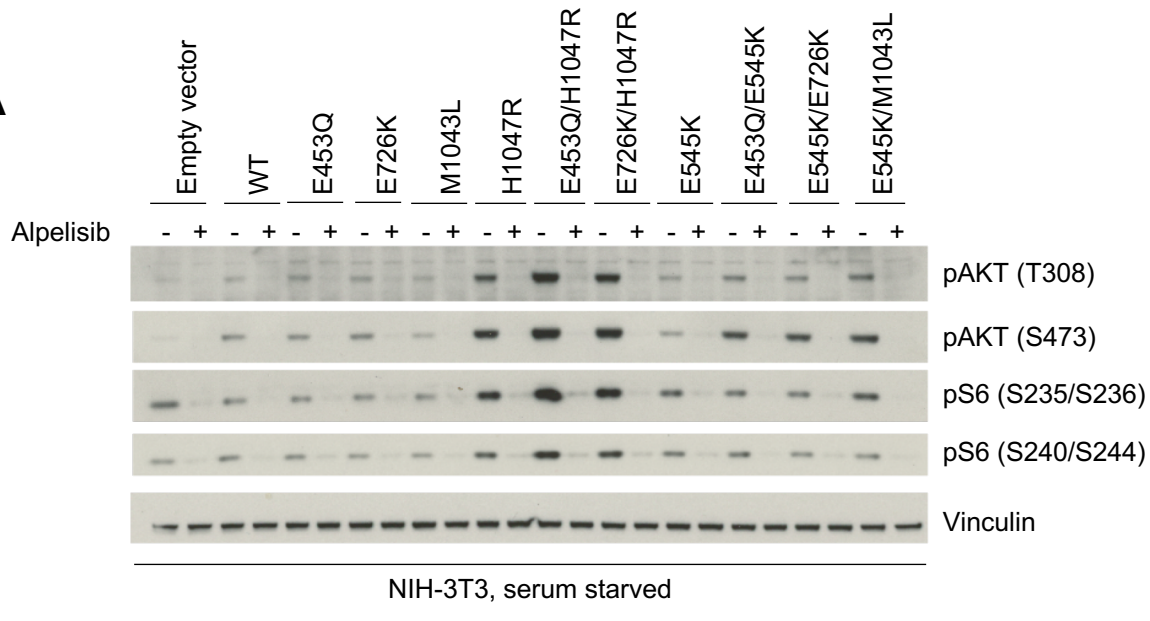

B

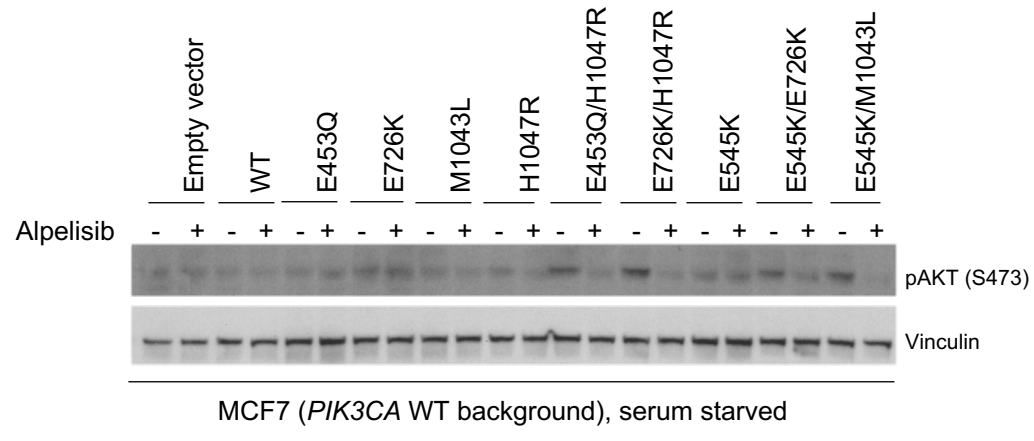

C

	IC_{50} [alpelisib] (μM)	E_{max} [alpelisib]	AUC [alpelisib]	IC_{50} [GDC-0077] (μM)	E_{max} [GDC-0077]	AUC [GDC-0077]
Empty vector	81.696	0.649	6.573	*Not reached*	0.695	6.936
WT	63.935	0.639	6.555	*Not reached*	0.648	6.698
E453Q	61.069	0.634	6.579	*Not reached*	0.712	7.12
E726K	60.406	0.586	6.162	*Not reached*	0.626	6.55
M1043L	48.064	0.591	6.18	*Not reached*	0.656	6.736
H1047R	3.770	0.482	5.129	0.371	0.488	5.394
E453Q/H1047R	0.136	0.209	3.281	0.011	0.207	3.461
E726K/H1047R	0.105	0.155	2.85	0.009	0.168	3.156
E545K	0.397	0.359	4.34	0.057	0.360	4.812
E545K/E726K	0.091	0.071	2.358	0.006	0.076	2.53
E545K/M1043L	0.124	0.220	3.23	0.011	0.239	3.574

D

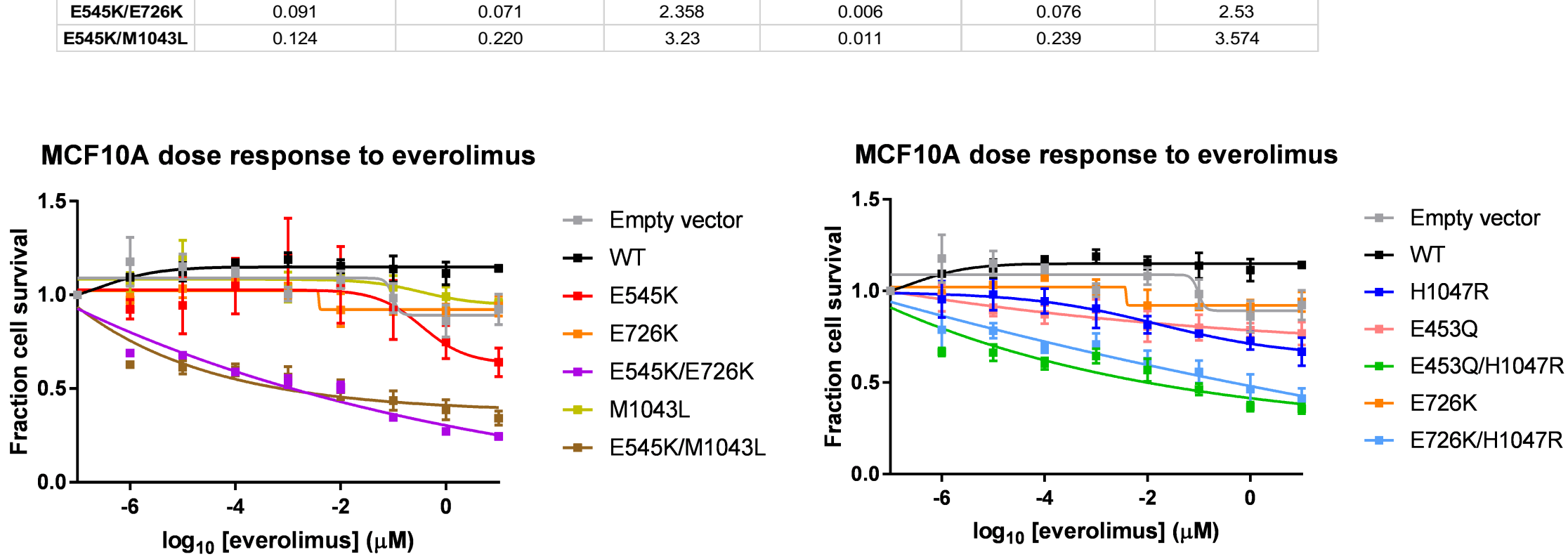

E

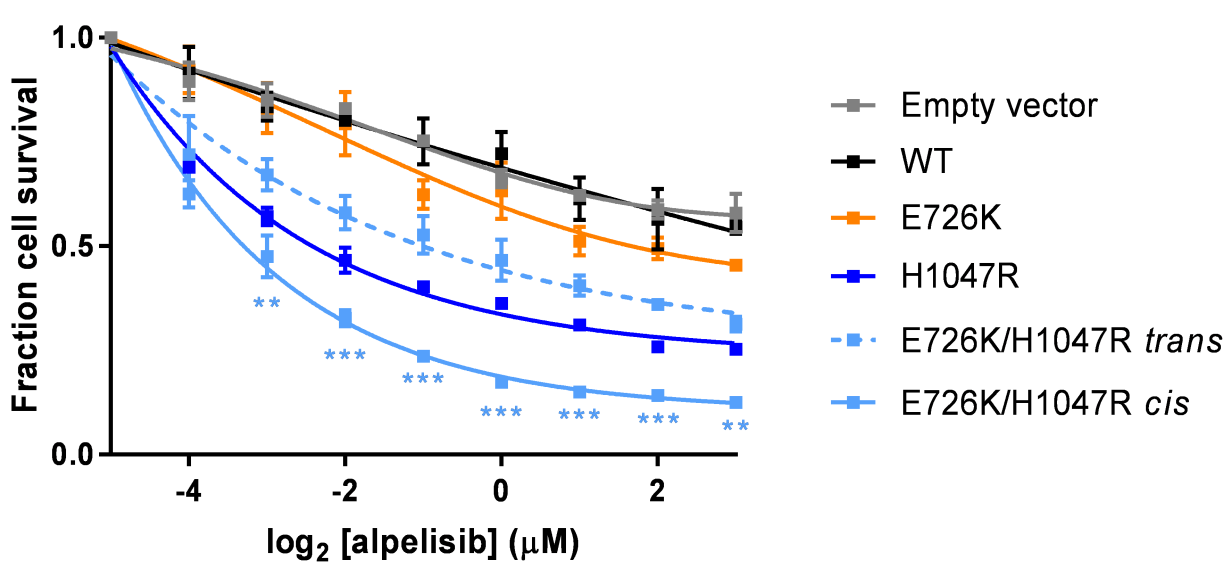

Fig. S9

Fig. S9: *PIK3CA* mutations in *cis* are inhibited by PI3K pathway inhibition more than single or *trans PIK3CA* mutants. (**A, B**) Western blotting of PI3K effectors of *PIK3CA* mutant stably transduced (**A**) NIH-3T3 cells and (**B**) MCF7 cells, serum starved for 1 day then exposed to DMSO (-) or alpelisib (1 μM) (+) for 1 hour. (**C**) IC_{50}, E_{max}, and AUC values for *PIK3CA* mutant MCF10A cells for alpelisib and GDC-0077. (**D**) Dose-response survival curves for MCF10A cell lines treated with everolimus under serum starvation for 4 days. E545K-containing *cis* mutants (left) and H1047R-containing *cis* mutants (right) are compared to single *PIK3CA* mutants. Data are mean ± s.e.m. (n=3) and were fit to asymmetric, five parameter sigmoidal curves. **** $p < 0.0001$, *** $p < 0.001$, ** $p < 0.01$, * $p < 0.05$, by two-way ANOVA corrected for multiple comparisons by Tukey's test, as compared to E545K [left] or H1047R [right]). (**E**) Dose-response survival curves for MCF10A cells treated with alpelisib under serum starvation for 4 days. Data are mean ± s.e.m. (n=3) and were fit to asymmetric, five parameter sigmoidal curves. For statistics, the *trans* mutant is compared to the *cis* mutant and to H1047R. **** $p < 0.001$, *** $p < 0.001$, ** $p < 0.01$, NS = not significant, by two-way ANOVA corrected for multiple comparisons by Tukey's test, as compared to E726/H1047R (*trans*).

Exon *(standard nomenclature)*	Exon *(RefSeq)*	Encoded amino acids	Mutations in this study
	1	Noncoding	
1	2	M1-G118	
2	3	G118-G188	
3	4	G188-K271	
4	5	Y272-K353	
5	6	I354-R382	
6	7	R382-E417	
7	8	E418-K468	E453Q
8	9	E469-L513	
9	10	S514-R555	E545K
10	11	R555-Q582	
11	12	M583-Q637	
12	13	V638-K672	
13	14	K672-K729	E726K
14	15	V730-R765	
15	16	R765-D806	
16	17	D806-R832	
17	18	R832-I889	
18	19	I889-Q928	
19	20	L929-R979	
20	21	R979-N1068	M1043L, H1047R

Fig. S10

Fig. S10: *PIK3CA* exon coverage by ctDNA testing. Exons are numbered based on historical nomenclature and RefSeq (*71*). Amino acids encoded by exons, and the mutations tested in this study are denoted. Exons sequenced by the Foundation Medicine Foundation One Liquid test are highlighted in blue.

Supplementary Tables:

Table S1: List of multiple *PIK3CA* mutant tumors (n=576) (cBioPortal).

Table S2: List of multiple *PIK3CA* mutant tumors (n=451) (MSK IMPACT).

Table S3: Double *PIK3CA* mutant breast tumors phased as *cis* or *trans* mutants, by NGS (MSK-IMPACT).

Table S4: Double *PIK3CA* mutant breast tumors phased as *cis* mutants, by RNA-sequencing (TCGA).

Table S1: List of multiple PIK3CA mutant tumours (n=576) (cBioPortal).

Sample ID	Cancer Type	Protein_Change_1	Protein_Change_2	Protein_Change_3	Protein_Change_4	Protein_Change_5	Protein_Change_6
AMPAC_2713	Ampullary Carcinoma	Y1021C	V146I				
P-0011521-T01-IM5	Anaplastic Astrocytoma	E542K	G106V				
P-0007319-T01-IM5	Basaloid Penile Squamous Cell Carcinoma	E545G	M1055I	R617W			
B52	Bladder combined	E726K	G451R				
B98	Bladder combined	E542K	E545Q				
BL033	Bladder combined	E545K	E542K				
DS-sig-003-P	Bladder combined	M1043I	D1017H	E1012Q			
P-0000043-T02-IM3	Bladder combined	E545K	V356A				
P-0000423-T01-IM3	Bladder combined	E545K	E453Q				
P-0002659-T01-IM3	Bladder combined	E545K	Q682H				
P-0004424-T01-IM5	Bladder combined	E542K	H1047R				
P-0009101-T01-IM5	Bladder combined	E545K	E542K				
P-0010921-T01-IM5	Bladder combined	E542K	E453Q	H1065Y			
TCGA-2F-A9KR-01	Bladder combined	E542K	E1012Q				
TCGA-4Z-AA7Y-01	Bladder combined	E545G	E545K				
TCGA-4Z-AA89-01	Bladder combined	N345K	R93Q				
TCGA-5N-A9KI-01	Bladder combined	E545K	R274K				
TCGA-FD-A5BX-01	Bladder combined	E365K	S66C				
TCGA-UY-A78P-01	Bladder combined	E418K	M1043I				
TCGA-XF-AAMG-01	Bladder combined	E542K	W552C				
TCGA-ZF-A9R2-01	Bladder combined	E726K	E710Q				
TCGA-ZF-A9RG-01	Bladder combined	E545K	E453K				
P-0004635-T01-IM5	Breast combined	H1047Y	C420R				
P-0000075-T01-IM3	Breast combined	H1047R	N142K				
P-0000107-T01-IM3	Breast combined	Y1021H	D1017E	I1019V			
P-0000138-T01-IM3	Breast combined	E542K	E453K				
P-0000138-T02-IM3	Breast combined	E542K	E453K				
P-0000155-T01-IM3	Breast combined	H1047R	D350N				
P-0000167-T01-IM3	Breast combined	K111E	E418K				
P-0000167-T02-IM3	Breast combined	E542K	K111E				
P-0000207-T01-IM3	Breast combined	K111E	N345K				
P-0000234-T01-IM3	Breast combined	E542K	M1043I				
P-0000234-T02-IM5	Breast combined	E542K	M1043I				
P-0000356-T01-IM3	Breast combined	H1047R	E453K				
P-0000381-T01-IM3	Breast combined	H1047R	E726K				
P-0000397-T01-IM3	Breast combined	E542K	E453K				
P-0000592-T01-IM3	Breast combined	E545K	M1043I				
P-0000607-T01-IM3	Breast combined	H1047L	E545Q				
P-0001043-T01-IM3	Breast combined	H1047R	R93L				
P-0001114-T02-IM3	Breast combined	E545K	E453Q	E978Q			
P-0001351-T01-IM3	Breast combined	E545K	E726K				
P-0001351-T02-IM5	Breast combined	E545K	E726K				
P-0001631-T01-IM3	Breast combined	E545K	M1043L				
P-0001631-T02-IM5	Breast combined	E545K	M1043L				
P-0001902-T01-IM3	Breast combined	E542K	E545D				
P-0001990-T01-IM3	Breast combined	H1047Y	N345K				
P-0002124-T01-IM3	Breast combined	H1047R	E365K				
P-0002562-T01-IM3	Breast combined	E545K	E453Q				
P-0002562-T02-IM5	Breast combined	E545K	E453Q				
P-0002657-T01-IM3	Breast combined	G118D	G364R				
P-0002667-T01-IM3	Breast combined	H1047R	N107I				
P-0002756-T02-IM5	Breast combined	E545K	E453Q				
P-0002841-T01-IM3	Breast combined	H1047R	K111N				
P-0002841-T02-IM6	Breast combined	H1047R	K111N				
P-0002922-T01-IM3	Breast combined	H1047R	E545Q				
P-0003224-T01-IM5	Breast combined	H1047R	G106V				
P-0003987-T01-IM5	Breast combined	E545K	H1047R				
P-0004187-T01-IM5	Breast combined	H1047R	E970K				
P-0004194-T01-IM5	Breast combined	E545K	D725G				
P-0004196-T01-IM5	Breast combined	H1047R	Q958K				
P-0004264-T01-IM5	Breast combined	H1047R	E726K				
P-0004433-T01-IM5	Breast combined	E545K	L252F				
P-0004913-T01-IM5	Breast combined	H1047R	E542A				
P-0005032-T01-IM5	Breast combined	L455Wfs*6	L452Qfs*5				
P-0005037-T01-IM5	Breast combined	N345K	R93Q				
P-0005120-T01-IM5	Breast combined	E542K	E726K				
P-0005154-T01-IM5	Breast combined	E542K	H1047R				
P-0005220-T01-IM5	Breast combined	H1047R	C407F				
P-0005242-T01-IM5	Breast combined	E545K	E726K				
P-0005314-T01-IM5	Breast combined	E542K	E726K				
P-0005611-T01-IM5	Breast combined	M1043I	E39K				
P-0005818-T01-IM5	Breast combined	H1047R	G118D				
P-0005968-T01-IM5	Breast combined	R88Q	H1047R				
P-0006161-T03-IM5	Breast combined	E542K	E453K				
P-0006166-T01-IM5	Breast combined	E542K	E726K				
P-0006335-T01-IM5	Breast combined	E545K	T1025A				
P-0006660-T01-IM5	Breast combined	R88Q	Q546H				
P-0006723-T01-IM5	Breast combined	H1047R	E81K				
P-0006780-T01-IM5	Breast combined	E726K	V344M				
P-0006787-T01-IM5	Breast combined	H1047R	E726K				
P-0007396-T01-IM5	Breast combined	N345K	E970K				
P-0008679-T01-IM5	Breast combined	H1047R	N345I				
P-0008679-T03-IM5	Breast combined	H1047R	N345I				
P-0008694-T01-IM5	Breast combined	E542K	E453K				
P-0008845-T01-IM5	Breast combined	K111E	G118D				
P-0009745-T02-IM6	Breast combined	C420R	E726K				
P-0010002-T01-IM5	Breast combined	G1049R	Q546P				
P-0010043-T01-IM5	Breast combined	H1047R	P539R				
P-0010703-T01-IM5	Breast combined	H1047L	E726K				
P-0010917-T01-IM5	Breast combined	E542K	E726K				
P-0011305-T01-IM5	Breast combined	E545K	E726K				
P-0011355-T01-IM5	Breast combined	H1047R	E81K				
P-0011420-T01-IM5	Breast combined	E545K	A1066V				
P-0012911-T01-IM5	Breast combined	C420R	R108H				
P-0013491-T01-IM5	Breast combined	G118D	E542Q				
P-0013771-T01-IM5	Breast combined	H1047R	E726K				

P-0013895-T01-IM5	Breast combined	E542K	E726K	
P-0014091-T01-IM5	Breast combined	H1047L	E81K	
P-0014136-T01-IM5	Breast combined	E542K	N457K	
P-0014278-T01-IM6	Breast combined	E542K	E726K	
P-0014479-T01-IM6	Breast combined	E545K	E542Q	
P-0014480-T01-IM6	Breast combined	E542K	E726K	
P-0014515-T01-IM6	Breast combined	Q546R	M1004I	
P-0014622-T01-IM6	Breast combined	H1047R	P104L	
P-0014737-T01-IM6	Breast combined	H1047L	P539R	
P-0014860-T01-IM6	Breast combined	H1047L	E545D	
P-0014940-T01-IM6	Breast combined	E542K	E726K	
P-0014943-T01-IM6	Breast combined	H1047R	E542G	
P-0015005-T01-IM6	Breast combined	E545K	Q546R	
P-0015097-T01-IM6	Breast combined	H1047R	E453K	
P-0015499-T01-IM6	Breast combined	H1047R	E418K	
P-0015633-T01-IM6	Breast combined	H1047L	I112F	
P-0015640-T01-IM6	Breast combined	N1044K	D350N	
P-0015944-T01-IM6	Breast combined	C420R	E726K	
P-0015964-T01-IM6	Breast combined	E545K	M1004I	
P-0016773-T01-IM6	Breast combined	G106V	Q546H	
P-0016786-T01-IM6	Breast combined	E545K	M1043I	
P-0016802-T01-IM6	Breast combined	H1047R	G118D	
P-0016840-T01-IM6	Breast combined	H1047R	V344M	
P-0017581-T01-IM5	Breast combined	E545G	T1025A	
P-0017818-T01-IM6	Breast combined	E545K	H1048R	
P-0018891-T01-IM6	Breast combined	H1047R	N107Y	
TCGA-D8-A1JS-01	Breast combined	H1047R	V344M	
TCGA-LD-A74U-01	Breast combined	E545K	C420R	
BR-M-150	Breast combined	E545G	E453K	
MB-0014	Breast combined	G1049R	Q546H	
MB-0162	Breast combined	L452Kfs*4	E453Dfs*7	
MB-0172	Breast combined	E545K	H1047R	
MB-0261	Breast combined	H1047R	E453K	
MB-0345	Breast combined	H1047R	R108H	
MB-0388	Breast combined	E545K	S509Y	
MB-0393	Breast combined	E545K	G914R	
MB-0399	Breast combined	H1047R	L10_P17del	
MB-0463	Breast combined	E545K	E726K	
MB-0475	Breast combined	H1047R	E81K	
MB-0554	Breast combined	H1047R	H1048R	D1029H
MB-0571	Breast combined	N345K	N1044K	
MB-0598	Breast combined	V105del	K148N	
MB-0623	Breast combined	H1047R	T727K	
MB-0632	Breast combined	H1047R	E80K	
MB-0904	Breast combined	E542K	T727K	
MB-0906	Breast combined	H1047R	G118D	
MB-2617	Breast combined	H1047R	P471L	
MB-2944	Breast combined	Q546R	E453K	
MB-2971	Breast combined	E542K	Y1021H	
MB-3254	Breast combined	H1047R	E453K	
MB-3295	Breast combined	H1047R	E365K	
MB-3344	Breast combined	H1047R	E453K	
MB-3824	Breast combined	H1047L	P449T	
MB-4343	Breast combined	H1047R	H1048R	
MB-4362	Breast combined	E542K	E970K	
MB-4607	Breast combined	N345K	F83C	
MB-4739	Breast combined	E545K	P104R	
MB-4746	Breast combined	E542K	M1043I	
MB-4749	Breast combined	Y1021H	V105del	
MB-4791	Breast combined	M1043I	E970K	
MB-4800	Breast combined	L113Sfs*32	K111Dfs*16	
MB-4801	Breast combined	H450_P458del	H1065Y	Q1064H
MB-4843	Breast combined	H1047R	E453Q	E726K
MB-4869	Breast combined	H1047R	P471L	R108H
MB-4959	Breast combined	Q546P	*1069Wext*4	
MB-4961	Breast combined	H1047R	E726K	
MB-4967	Breast combined	H1047R	E81K	
MB-4969	Breast combined	E545K	E726K	
MB-5072	Breast combined	H1047R	E542A	
MB-5088	Breast combined	H1047L	C420R	
MB-5119	Breast combined	E726K	N1044K	
MB-5134	Breast combined	H1047Y	N345K	
MB-5169	Breast combined	E542K	E726K	
MB-5179	Breast combined	H1047R	I459T	
MB-5182	Breast combined	H1047R	I354F	
MB-5196	Breast combined	E545K	E542K	
MB-5270	Breast combined	N345K	N114S	
MB-5275	Breast combined	E545K	D1017H	
MB-5288	Breast combined	E545K	M1043I	
MB-5401	Breast combined	G118D	T957P	
MB-5425	Breast combined	H1047R	R108H	
MB-5446	Breast combined	R88Q	C420R	
MB-5470	Breast combined	H1047R	G106R	
MB-5482	Breast combined	H1047R	E365K	
MB-5486	Breast combined	Q546P	P539R	
MB-5511	Breast combined	H1047R	E81A	
MB-5582	Breast combined	H1047R	P104L	
MB-5599	Breast combined	H1047R	P104R	
MB-5623	Breast combined	E545K	E726K	
MB-5656	Breast combined	E545K	E542K	H1047R
MB-6006	Breast combined	H1047R	E726K	
MB-6007	Breast combined	H1047R	E726K	
MB-6018	Breast combined	H1047R	R88Q	
MB-6019	Breast combined	H1047R	Y1021C	E110del
MB-6029	Breast combined	H1047R	I69N	
MB-6030	Breast combined	H1047R	R93W	
MB-6047	Breast combined	C420R	E970K	
MB-6164	Breast combined	H1047R	H1048R	

MB-6194	Breast combined	H1047R	K111N		
MB-6207	Breast combined	E542K	T1025S		
MB-7005	Breast combined	H1047Y	G118D		
MB-7042	Breast combined	E545K	M1004I		
MB-7061	Breast combined	H1047R	G1007R		
MB-7195	Breast combined	H1047R	G106R		
MB-7200	Breast combined	H1047R	R108H		
MB-7230	Breast combined	N345K	T727K		
MB-7244	Breast combined	H1047R	H1048R		
MBC-MBCProject_27uAugT4-Tumor-SM-DL45T	Breast combined	E542K	T1025A		
MBC-MBCProject_57iLiJll-Tumor-SM-CGLIV	Breast combined	H1047L	E81K		
TCGA-3C-AALK-01	Breast combined	E542K	M1004I		
TCGA-A1-A0SI-01	Breast combined	H1047R	E726K		
TCGA-A2-A0CP-01	Breast combined	H1047R	E726K		
TCGA-A2-A0EV-01	Breast combined	H1047R	E469delinsDK		
TCGA-A2-A0T7-01	Breast combined	E542K	M1043I		
TCGA-A8-A075-01	Breast combined	E545K	E453K		
TCGA-A8-A095-01	Breast combined	H1047L	E726K		
TCGA-AC-A23H-01	Breast combined	D603H	L989V		
TCGA-AN-A0XO-01	Breast combined	E453K	E542K		
TCGA-AO-A0JC-01	Breast combined	R108H	E545K		
TCGA-AO-A0JF-01	Breast combined	E545K	E453K		
TCGA-AO-A12A-01	Breast combined	E545G	E542K		
TCGA-AO-A1KR-01	Breast combined	H1047R	M1004I		
TCGA-B6-A0RO-01	Breast combined	H1047R	P539R		
TCGA-BH-A0B6-01	Breast combined	E453K	E81K		
TCGA-BH-A0BT-01	Breast combined	H1047R	P366R		
TCGA-BH-A0DV-01	Breast combined	E545K	E726K	E726G	
TCGA-BH-A0W7-01	Breast combined	H1047R	E726K		
TCGA-BH-A18F-01	Breast combined	H1047R	Q546K		
TCGA-BH-A202-01	Breast combined	H1047R	E365V		
TCGA-C8-A131-01	Breast combined	H1047R	R108H		
TCGA-C8-A278-01	Breast combined	H1047L	M1040V		
TCGA-D8-A1JD-01	Breast combined	E545K	E726K	M1004I	
TCGA-D8-A1JF-01	Breast combined	E545K	R398H		
TCGA-D8-A1JG-01	Breast combined	P447_L455del	L456Afs*13		
TCGA-E2-A159-01	Breast combined	E542K	E542G		
TCGA-E2-A1IN-01	Breast combined	E542K	C901F		
TCGA-E9-A1RH-01	Breast combined	E103_P104del	L531V		
TCGA-EW-A1P5-01	Breast combined	P447_L455del	L456Afs*13		
TCGA-EW-A1PE-01	Breast combined	Q546K	T1025A		
TCGA-GM-A2D9-01	Breast combined	H1047R	E453K		
TCGA-GM-A2DH-01	Breast combined	Q546R	G1007R		
TCGA-OL-A5RX-01	Breast combined	D939G	P366R		
BR-M-083	Breast combined	H1047R	E542Q		
MB-0083	Breast combined	N345K	E81K		
MB-0101	Breast combined	H1047L	E726K		
MB-0188	Breast combined	E542K	E726K		
MB-0306	Breast combined	H1047R	E726K		
MB-0578	Breast combined	E545K	M1043V		
MB-2840	Breast combined	N345K	M1043I		
MB-4484	Breast combined	H1047R	P471A		
MB-4697	Breast combined	N345K	E726K		
MB-4743	Breast combined	E545K	M1004I		
MB-4764	Breast combined	E542K	E726K		
MB-4802	Breast combined	E81K	D1017H		
MB-5035	Breast combined	E542K	E726K		
MB-5107	Breast combined	K111E	G320A		
MB-5326	Breast combined	K111E	M1043I		
MB-6021	Breast combined	H1047R	N345K		
MB-7268	Breast combined	E545K	E726K		
TCGA-A2-A0EN-01	Breast combined	H1047R	H1065L		
TCGA-AC-A5XS-01	Breast combined	E545G	E545K	C378F	E545R
TCGA-B6-A0IP-01	Breast combined	R88Q	H1047R	F83L	
TCGA-B6-A0RQ-01	Breast combined	E542G	E545K		
TCGA-E2-A10F-01	Breast combined	H1047R	E726K		
TCGA-E2-A14U-01	Breast combined	E542K	H1047R		
TCGA-E2-A2P5-01	Breast combined	N345K	G914R		
TCGA-EW-A1J5-01	Breast combined	E545K	E726K		
TCGA-JL-A3YX-01	Breast combined	E542K	E726K		
TCGA-LQ-A4E4-01	Breast combined	H1047R	E542G		
MB-0171	Breast combined	E365K	C420R		
MB-0353	Breast combined	H1047R	G118D		
MB-0356	Breast combined	H1047R	H1048R		
MB-0379	Breast combined	E545K	G320A		
MB-0504	Breast combined	H1047R	R108H		
MB-0653	Breast combined	H1047L	E385K		
MB-0897	Breast combined	E542K	E726K		
MB-5412	Breast combined	H1047R	R108H		
MB-6022	Breast combined	E545A	G1050S		
MB-0170	Breast combined	N345K	N1044K		
MB-0295	Breast combined	H1047R	P104L		
MB-0363	Breast combined	E542K	N345K		
MB-0891	Breast combined	H1047R	K111E		
MB-2790	Breast combined	E726K	P449_L452del		
MB-3181	Breast combined	M1043V	E726K		
MB-3228	Breast combined	E545K	D725N		
MB-3439	Breast combined	E542K	D1045N	Q1064H	
MB-3490	Breast combined	H1047R	R88Q		
MB-3871	Breast combined	N345K	S161R		
MB-7006	Breast combined	E545K	E542K	E726K	D725N
MBC_109	Breast combined	E545K	E726K		
MBC_187	Breast combined	H1047R	P366R		
MBC_189	Breast combined	E542K	E726K		
MBC_29	Breast combined	H1047R	Q546K		
MBC_45	Breast combined	E545K	E726K		
MBC_50	Breast combined	E545K	E385K		
MBC_95	Breast combined	E542K	E453K		

MTS-T0035	Breast combined	H1047R	N345I		
MTS-T0065	Breast combined	H1047R	E263Q		
MTS-T0207	Breast combined	H1047L	N1068K		
MTS-T0255	Breast combined	E542K	H1047R		
MTS-T0327	Breast combined	H1047R	R108H		
MTS-T0340	Breast combined	E545A	E726K		
MTS-T0351	Breast combined	N1044K	E1032Q	D1045H	
MTS-T0380	Breast combined	H1047R	P104L		
MTS-T0396	Breast combined	E545K	E726K		
MTS-T1284	Breast combined	E542K	M1043I		
MTS-T1800	Breast combined	E542K	E726K		
MTS-T2408	Breast combined	H1047R	Q958K		
MTS-T2413	Breast combined	E542K	E726K		
PD4120a	Breast combined	H1047R	K111N		
PD4125a	Breast combined	E81K	E80K		
PD4202a	Breast combined	H1047R	P104L		
PD4844a	Breast combined	L113_N114del	M1040T		
P-0004374-T01-IM5	Cancer of Unknown Primary	E542K	D454G		
P-0008153-T01-IM5	Cancer of Unknown Primary	H1047R	R88Q		
P-0010527-T01-IM5	Cervical combined	E545K	E542K		
TCGA-2W-A8YY-01	Cervical combined	R88Q	R693H	Y432C	D589N
TCGA-C5-A1BJ-01	Cervical combined	E545Q	E600K		
TCGA-C5-A1MH-01	Cervical combined	E545K	E726K		
TCGA-C5-A1MK-01	Cervical combined	E545K	E726K		
TCGA-C5-A8XJ-01	Cervical combined	E545K	L866F		
TCGA-EK-A2RN-01	Cervical combined	E545K	E726K		
TCGA-FU-A3HZ-01	Cervical combined	L339I	E542K		
TCGA-VS-A8QA-01	Cervical combined	E726K	E453K		
TCGA-VS-A959-01	Cervical combined	E542K	E453K		
TCGA-IR-A3LF-01	Cervical combined	E542K	G1007R		
TCGA-LP-A7HU-01	Cervical combined	E545K	E542K		
TCGA-AA-3489-01	Colorectal combined	G1049R	D350G		
TCGA-AA-3675-01	Colorectal combined	H1047Y	V344G		
TCGA-AA-3848-01	Colorectal combined	R88Q	D350G		
TCGA-AA-3977-01	Colorectal combined	R88Q	M1043I		
TCGA-AA-3984-01	Colorectal combined	E970K	R357Q		
TCGA-AD-A5EJ-01	Colorectal combined	H1047R	E542G		
TCGA-AM-5821-01	Colorectal combined	H1047R	A224S		
TCGA-AY-A69D-01	Colorectal combined	C420R	E722K		
TCGA-AZ-4315-01	Colorectal combined	R88Q	H1048R	E81*	
TCGA-CA-5255-01	Colorectal combined	E545A	H1047R		
TCGA-CA-6718-01	Colorectal combined	R88Q	H1047Q	M732I	
TCGA-DM-A0X9-01	Colorectal combined	E545K	E970K		
TCGA-DM-A28A-01	Colorectal combined	H1047Y	V344G		
TCGA-F4-6569-01	Colorectal combined	H1047Y	R357Q		
TCGA-F4-6807-01	Colorectal combined	M1043I	R108H		
TCGA-NH-A50T-01	Colorectal combined	E542K	P104R		
TCGA-QG-A5YX-01	Colorectal combined	H1047R	E542G		
	587220 Colorectal combined	H1047R	K111N		
	587224 Colorectal combined	H1047R	K111E		
	587260 Colorectal combined	R88Q	E545A		
	587356 Colorectal combined	T1052K	H419N		
P-0000788-T01-IM3	Colorectal combined	E542K	M1010I		
P-0001215-T01-IM3	Colorectal combined	E365K	I816N	R992*	
P-0001289-T01-IM3	Colorectal combined	H1047R	V344G		
P-0001732-T01-IM3	Colorectal combined	E542K	M1043I		
P-0001940-T01-IM3	Colorectal combined	H1047R	G118D		
P-0002413-T01-IM3	Colorectal combined	Q546K	E726K		
P-0003513-T01-IM5	Colorectal combined	E365K	H1047Q		
P-0003720-T01-IM5	Colorectal combined	H1047R	R93Q		
P-0004566-T01-IM5	Colorectal combined	E545K	H1047R		
P-0004865-T01-IM5	Colorectal combined	E542K	K111N		
P-0004928-T01-IM5	Colorectal combined	E545K	E542K		
P-0006170-T01-IM5	Colorectal combined	E545G	Q75H		
P-0006581-T01-IM5	Colorectal combined	E545K	L540F		
P-0006612-T01-IM5	Colorectal combined	M1043I	R693C		
P-0007147-T01-IM5	Colorectal combined	R88Q	H1047R		
P-0007272-T01-IM5	Colorectal combined	R38C	R357L		
P-0007836-T01-IM5	Colorectal combined	E110del	R93Q	E418D	
P-0008721-T01-IM5	Colorectal combined	H1047R	A289T		
P-0010125-T01-IM5	Colorectal combined	G364R	V125E		
P-0010167-T01-IM5	Colorectal combined	H1047R	V851A		
P-0011071-T01-IM5	Colorectal combined	E542K	R108S		
P-0011357-T01-IM5	Colorectal combined	K111N	M1004I	R357*	
P-0013010-T01-IM5	Colorectal combined	H1047R	C420R		
P-0013020-T01-IM5	Colorectal combined	H1047R	Q546R		
coadread_dfci_2016_1240	Colorectal combined	E542K	E726K		
coadread_dfci_2016_1762	Colorectal combined	Q546R	*1069Wext*4		
coadread_dfci_2016_2271	Colorectal combined	E542K	F83S		
coadread_dfci_2016_250	Colorectal combined	G1007R	R93W		
coadread_dfci_2016_2641	Colorectal combined	H1047R	R38S		
coadread_dfci_2016_2664	Colorectal combined	E542K	E982K		
coadread_dfci_2016_2936	Colorectal combined	E545K	C604R		
coadread_dfci_2016_3010	Colorectal combined	K111E	V344E		
coadread_dfci_2016_3022	Colorectal combined	E545K	R88Q		
coadread_dfci_2016_3237	Colorectal combined	H1047R	R93W		
coadread_dfci_2016_328	Colorectal combined	G1007R	L1006H		
coadread_dfci_2016_3298	Colorectal combined	R88Q	C604R		
coadread_dfci_2016_3535	Colorectal combined	R88Q	H1047R		
coadread_dfci_2016_3611	Colorectal combined	R88Q	R818C		
coadread_dfci_2016_4508	Colorectal combined	E542K	G106V		
coadread_dfci_2016_578	Colorectal combined	R88Q	K111N		
coadread_dfci_2016_60	Colorectal combined	E542K	C378R		
TCGA-AA-3821-01	Colorectal combined	H1047L	M1043I		
TCGA-AA-3837-01	Colorectal combined	R88Q	N345K		
TCGA-AA-3852-01	Colorectal combined	E81K	G106R	E545Q	
TCGA-AA-A00N-01	Colorectal combined	R357Q	Y1021C	V344A	
TCGA-CA-6717-01	Colorectal combined	R88Q	E970K	S1015Y	

TCGA-CM-6162-01	Colorectal combined	R88Q	R108H			
P-0009189-T01-IM5	Cutaneous Melanoma	S67F	L402F			
P-0009752-T01-IM5	Cutaneous Melanoma	H14Y	S326F			
TCGA-DA-A1IB-06	Cutaneous Melanoma	E674D	Q682K			
P-0001198-T01-IM3	Cutaneous Squamous Cell Carcinoma	E542K	C24S	S66F	W780*	
TCGA-IC-A6RE-01	Esophageal Adenocarcinoma	E545K	K111N			
TCGA-XP-A8T7-01	Esophageal Squamous Cell Carcinoma	E726K	M441I			
PGM4	Esophagogastric Adenocarcinoma	E545K	I13S			
P-0004531-T01-IM5	Glioma combined	E545G	C420R			
TCGA-DU-A5TT-01	Glioma combined	K111E	Q546E			
TCGA-S9-A6TW-01	Glioma combined	E110del	N345Y			
P18_Rec	Glioma combined	E542K	L540V			
P-0000500-T01-IM3	Glioma combined	E545K	E542K			
P-0002633-T01-IM3	Glioma combined	Q546R	R88Q			
P-0002695-T01-IM3	Glioma combined	E545K	E116K			
P-0008649-T01-IM5	Glioma combined	H1047R	L436_P449dup			
TCGA-06-0210-02	Glioma combined	E545K	R38H			
TCGA-06-0879-01	Glioma combined	L455_G460delinsF	E453_G460delinsDDF	E453D		
TCGA-06-5416-01	Glioma combined	R88Q	E81K	S292I		
TCGA-12-5301-01	Glioma combined	R88Q	R108H			
TCGA-19-5954-01	Glioma combined	K111R	R4*			
TCGA-HT-7481-01	Glioma combined	E453del	G118D	M1043V		
OSCJM-PT01-166-T	Head and Neck Carcinoma	K111E	T1052A			
TCGA-BA-A8YP-01	Head and Neck Carcinoma	E418K	C420R			
TCGA-CR-6471-01	Head and Neck Carcinoma	R88Q	M1043V			
TCGA-CR-7404-01	Head and Neck Carcinoma	E545K	E542K			
TCGA-CV-7568-01	Head and Neck Carcinoma	P104L	Y606C			
P-0001105-T01-IM3	High-Grade Serous Ovarian Cancer	R108H	C378F			
P-0002286-T01-IM3	Intrahepatic Cholangiocarcinoma	E545K	C420R			
LO3793	Lung combined	R88Q	E418K			
LUAD-S01473-Tumor	Lung combined	E545K	E453Q			
P-0005985-T01-IM5	Lung combined	PIK3CA-intragenic	E545K			
P-0009431-T01-IM5	Lung combined	E81K	R93W			
TCGA-73-7499-01	Lung combined	M123_P124delinsIA	M123I	P124A	MP123IA	
P-0011388-T01-IM5	Lung combined	D1029H	D1045N	E982Q		
TCGA-18-5595-01	Lung combined	E545K	E726K			
TCGA-21-1078-01	Lung combined	E542K	D538N			
TCGA-33-A4WN-01	Lung combined	E542K	P539S	F667L		
TCGA-60-2721-01	Lung combined	E542K	G1049R			
A14	Lung combined	E529G	G1049S			
MB-REC-31	Medulloblastoma	H1047L	Q958K			
PIP14-47205-T1	Mixed Cancer Types	N345K	I391M			
TCGA-VS-A9UT-01	Mucinous Carcinoma	E418K	G106R			
TCGA-VS-A9UZ-01	Mucinous Carcinoma	E545K	E453Q			
P-0002411-T01-IM3	Nasopharyngeal Carcinoma	E545K	D538Y			
P-0000650-T01-IM3	Non-Seminomatous Germ Cell Tumor	K724del	E542K			
P-0005212-T01-IM5	Oropharynx Squamous Cell Carcinoma	E542K	E78K			
P-0009761-T01-IM5	Oropharynx Squamous Cell Carcinoma	E545K	E579K			
TCGA-5P-A9K3-01	Papillary Renal Cell Carcinoma	E542K	R38C			
P-0003178-T01-IM5	Poorly Differentiated Thyroid Cancer	E542K	H1047R			
TCGA-EJ-A65D-01	Prostate Adenocarcinoma	*1069fs*	R88Q			
TCGA-HC-7081-01	Prostate Adenocarcinoma	E542A	N345I			
TCGA-XK-AAIW-01	Prostate Adenocarcinoma	R108C	L569I			
TCGA-AG-A015-01	Rectal Adenocarcinoma	Q546K	D350G			
TCGA-AH-6903-01	Rectal Adenocarcinoma	H1047R	E726K			
TCGA-EI-6917-01	Rectal Adenocarcinoma	R88Q	E116K			
TCGA-F5-6814-01	Rectal Adenocarcinoma	K337N	E469A			
P-0000957-T01-IM3	Salivary Duct Carcinoma	*1069F	M1004I			
TCGA-HU-8608-01	Stomach combined	E365K	N345K			
TCGA-VQ-A91K-01	Stomach combined	G1049R	E453K			
TCGA-VQ-A91W-01	Stomach combined	E542K	G364R			
TCGA-VQ-A8P2-01	Stomach combined	R88Q	D350N			
P-0009918-T01-IM5	Stomach combined	H1047R	V344M	K111N		
TCGA-BR-4371-01	Stomach combined	E545K	H1047R			
TCGA-BR-6452-01	Stomach combined	R412Q	H1047R	E547K	K179E	V243A
TCGA-BR-6706-01	Stomach combined	E545K	E453K			
TCGA-BR-8284-01	Stomach combined	E542K	Q546K			
TCGA-BR-8366-01	Stomach combined	G118D	Y182H			
TCGA-BR-8591-01	Stomach combined	R88Q	C378R			
TCGA-BR-8676-01	Stomach combined	E542K	E453K			
TCGA-CG-5721-01	Stomach combined	K111E	K948E			
TCGA-F1-6177-01	Stomach combined	R93Q	Q546H			
TCGA-BR-8686-01	Stomach combined	E542K	R88Q			
TCGA-D7-5577-01	Stomach combined	R88Q	M1043I			
TCGA-HU-A4GQ-01	Stomach combined	R93W	Y1021H			
TCGA-VQ-A8PF-01	Stomach combined	R88Q	G106V			
DS-uttcc-042-P	Upper Tract Urothelial Carcinoma	H1047L	D1029Y			
DS-uttcc-060-P	Upper Tract Urothelial Carcinoma	F261V	Q958H	R349*		
P-0004330-T01-IM5	Upper Tract Urothelial Carcinoma	R93Q	R310C			
P-0004688-T01-IM5	Upper Tract Urothelial Carcinoma	R108H	G1007D	T322I		
P-0010803-T01-IM5	Upper Tract Urothelial Carcinoma	H1047Y	E542V			
MM04T	Uterine combined	R88Q	R357Q			
MM18T	Uterine combined	R818C	R916C	R992*		
P-0002357-T01-IM3	Uterine combined	H1047Y	D1029H			
TCGA-N7-A4Y8-01	Uterine combined	E545K	H1047R			
TCGA-ND-A4WC-01	Uterine combined	R88Q	R108H			
P-0006269-T01-IM5	Uterine combined	H1047Y	V344M			
P-0000404-T01-IM3	Uterine combined	K111E	P449R			
P-0000448-T01-IM3	Uterine combined	V344M	T1025A			
P-0003767-T01-IM5	Uterine combined	H1047R	E453del			
P-0004136-T01-IM5	Uterine combined	E542K	I1058L			
P-0004255-T01-IM5	Uterine combined	H1047R	R88Q			
P-0006201-T01-IM5	Uterine combined	R93W	E365K			
P-0009316-T01-IM5	Uterine combined	E545K	H1047Y			
P-0010967-T01-IM5	Uterine combined	R88Q	E81K			
P-0011569-T01-IM5	Uterine combined	R88Q	Y1021C	R93Q	L779M	
P-0011570-T01-IM5	Uterine combined	D549N	F83S	L339I		
P-0012113-T01-IM5	Uterine combined	R88Q	T1025A	Q958R		

P-0012152-T01-IM5	Uterine combined	E545G	P97H				
P-0012358-T01-IM5	Uterine combined	R88Q	L997I	R115Q	R537Q		
P-0012397-T01-IM5	Uterine combined	R88Q	Y1021C	R852Q			
TCGA-4E-A92E-01	Uterine combined	E542K	M1043I				
TCGA-A5-A0GB-01	Uterine combined	R108H	G359R				
TCGA-A5-A0GP-01	Uterine combined	R88Q	G118D				
TCGA-A5-A0RA-01	Uterine combined	W11_P18del	R115L				
TCGA-A5-A0VP-01	Uterine combined	R88Q	E542V				
TCGA-A5-A2K5-01	Uterine combined	R88Q	M1043I				
TCGA-AJ-A3BH-01	Uterine combined	R108H	D1045A				
TCGA-AJ-A3EK-01	Uterine combined	R88Q	R93W				
TCGA-AJ-A3EL-01	Uterine combined	R88Q	I816S				
TCGA-AJ-A8CW-01	Uterine combined	R88Q	H1047R				
TCGA-AP-A054-01	Uterine combined	M1043I	L866W				
TCGA-AP-A056-01	Uterine combined	R88Q	Y1021C				
TCGA-AP-A0LD-01	Uterine combined	R38H	R108H				
TCGA-AP-A0LM-01	Uterine combined	R818C	D350N	N170S	L279I	D454Y	
TCGA-AP-A0LS-01	Uterine combined	H1047Y	P449S				
TCGA-AP-A1DK-01	Uterine combined	R88Q	M811I				
TCGA-AP-A1DV-01	Uterine combined	E545G	T1025A				
TCGA-AP-A1E0-01	Uterine combined	R88Q	M1043I	F667L			
TCGA-AP-A1E1-01	Uterine combined	Q546K	Y1021C				
TCGA-AX-A05Z-01	Uterine combined	T1025A	S576Y	L997I			
TCGA-AX-A060-01	Uterine combined	C604R	V344A				
TCGA-AX-A06J-01	Uterine combined	C378F	G118D				
TCGA-AX-A0J0-01	Uterine combined	R38C	T1025S				
TCGA-AX-A1C5-01	Uterine combined	H1047Y	V344M				
TCGA-AX-A1CE-01	Uterine combined	R88Q	D350G	R818H	L929M	P953S	A1020T
TCGA-AX-A2HC-01	Uterine combined	R88Q	R832*	X555_splice			
TCGA-AX-A2HD-01	Uterine combined	E418K	R93Q	E600K			
TCGA-AX-A2HG-01	Uterine combined	E542K	R310C				
TCGA-AX-A2IN-01	Uterine combined	N345T	R38C				
TCGA-B5-A0JU-01	Uterine combined	E545A	H1047Y				
TCGA-B5-A0JY-01	Uterine combined	G12D	P449L	E522A			
TCGA-B5-A0K2-01	Uterine combined	R93W	C378R				
TCGA-B5-A11I-01	Uterine combined	R93Q	M1004I				
TCGA-B5-A11R-01	Uterine combined	E39K	N1044K				
TCGA-B5-A11S-01	Uterine combined	M1043V	G1007R				
TCGA-B5-A11X-01	Uterine combined	G118D	E39K				
TCGA-B5-A11Y-01	Uterine combined	V344M	H1047Q	R93Q			
TCGA-B5-A3FA-01	Uterine combined	R88Q	Y1021H	R401Q			
TCGA-B5-A3FC-01	Uterine combined	Y1021C	R108C				
TCGA-BG-A0M0-01	Uterine combined	P471L	E365K				
TCGA-BG-A0MQ-01	Uterine combined	Y1021C	R93Q				
TCGA-BG-A0VX-01	Uterine combined	R88Q	Q546P				
TCGA-BG-A0VZ-01	Uterine combined	K111N	N1044K				
TCGA-BG-A187-01	Uterine combined	C420R	R93Q				
TCGA-BK-A0C9-01	Uterine combined	E453Q	E542Q				
TCGA-BK-A56F-01	Uterine combined	FNDC3B-PIK3CA	H1047R	P539R			
TCGA-BS-A0TC-01	Uterine combined	R108H	R38C				
TCGA-BS-A0UF-01	Uterine combined	R401Q	Q643H	F1016C			
TCGA-BS-A0UJ-01	Uterine combined	Q546P	W479*				
TCGA-BS-A0UV-01	Uterine combined	R88Q	R1023*				
TCGA-BS-A0V6-01	Uterine combined	K111E	D939G				
TCGA-BS-A0V7-01	Uterine combined	H1047L	N345K				
TCGA-D1-A103-01	Uterine combined	E39K	R617W				
TCGA-D1-A16R-01	Uterine combined	R88Q	C901F				
TCGA-D1-A16Y-01	Uterine combined	R88Q	E81K				
TCGA-D1-A17F-01	Uterine combined	G118D	D725N				
TCGA-D1-A17T-01	Uterine combined	R88Q	C901F				
TCGA-D1-A1O5-01	Uterine combined	Q546P	E542A				
TCGA-D1-A1O7-01	Uterine combined	R88Q	M1004V				
TCGA-DF-A2KN-01	Uterine combined	C378F	R617Q	R992*			
TCGA-DF-A2KU-01	Uterine combined	R88Q	E365K	Y392H			
TCGA-DF-A2KV-01	Uterine combined	T1025A	R93W				
TCGA-E6-A1LX-01	Uterine combined	R88Q	C378Y	L339I	P266T	F930V	
TCGA-EO-A22R-01	Uterine combined	R88Q	G106V	R19I			
TCGA-EO-A22U-01	Uterine combined	E365K	R93W	I351T			
TCGA-EO-A22X-01	Uterine combined	R88Q	R357Q	M282V	L1006R		
TCGA-EO-A3AV-01	Uterine combined	E81K	M1004R				
TCGA-EO-A3B0-01	Uterine combined	D350N	R38C	R770Q			
TCGA-EO-A3KX-01	Uterine combined	R108H	N1044I				
TCGA-EY-A1GL-01	Uterine combined	E726K	K111N				
TCGA-EY-A1GU-01	Uterine combined	R38H	G118D				
TCGA-EY-A1H0-01	Uterine combined	R38C	E542Q	M282V			
TCGA-EY-A2OM-01	Uterine combined	R88Q	R108H				
TCGA-FI-A2D5-01	Uterine combined	R88Q	M1004I	T322A			
TCGA-PG-A916-01	Uterine combined	G118D	N345I				
P-0001821-T01-IM3	Uterine combined	R88Q	Q546H				
P-0004017-T01-IM5	Uterine combined	H1047L	E453K				
TCGA-DI-A1BU-01	Uterine combined	E110del	G106D	Y165H	I406V		
TCGA-E6-A2P8-01	Uterine combined	R88Q	A1066V				
TCGA-EO-A3AZ-01	Uterine combined	E453del	R108H	E545Q	Q958R		
TCGA-QF-A5YS-01	Uterine combined	R88Q	T1025A	M1055I			
P-0002945-T01-IM3	Uterine combined	H1047Y	E726K				
TCGA-A5-A0G2-01	Uterine combined	L569I	R852Q	G903E			
TCGA-A5-A0R6-01	Uterine combined	M1043V	C378Y				
TCGA-E6-A1LZ-01	Uterine combined	E545K	R992P	E453Q			

Table S2: List of multiple *PIK3CA* mutant tumours (n=451) (MSK-IMPACT)

Sample ID	Cancer Type	*PIK3CA* Mutation
P-0006682-T02-IM6	Anal Cancer	E545K,R108H
P-0018953-T01-IM6	Anal Cancer	M1043I,K111N
P-0020781-T01-IM6	Anal Cancer	E545K,R93W
P-0031461-T01-IM6	Anal Cancer	E545K,E726K
P-0000043-T02-IM3	Bladder Cancer	E545K,V356A
P-0002659-T01-IM3	Bladder Cancer	E545K,Q682H
P-0009101-T01-IM5	Bladder Cancer	E545K,E542K
P-0000423-T01-IM3	Bladder Cancer	E545K,E453Q
P-0003433-T01-IM5	Bladder Cancer	E542K,E453K
P-0004330-T01-IM5	Bladder Cancer	R93Q,R310C
P-0004424-T01-IM5	Bladder Cancer	H1047R,E542K
P-0004688-T01-IM5	Bladder Cancer	R108H,T322I,G1007D
P-0010803-T01-IM5	Bladder Cancer	H1047Y,E542V
P-0010921-T01-IM5	Bladder Cancer	E542K,H1065Y,E453Q
P-0014909-T01-IM6	Bladder Cancer	E542K,E726K
P-0015886-T01-IM6	Bladder Cancer	E726K,E503K
P-0017472-T01-IM6	Bladder Cancer	Q75E,A1066V
P-0019005-T01-IM6	Bladder Cancer	E545K,E542K
P-0024039-T01-IM6	Bladder Cancer	E545K,E542K
P-0031416-T01-IM6	Bladder Cancer	N345K,E978K
P-0031860-T01-IM6	Bladder Cancer	E545K,D133Y
P-0032134-T01-IM6	Bladder Cancer	E545K,R88Q,E453Q,E418K
P-0000138-T01-IM3	Breast Cancer	E542K,E453K
P-0000155-T01-IM3	Breast Cancer	H1047R,D350N
P-0000167-T01-IM3	Breast Cancer	K111E,E418K
P-0000167-T02-IM3	Breast Cancer	E542K,K111E
P-0000234-T01-IM3	Breast Cancer	E542K,M1043I
P-0000397-T01-IM3	Breast Cancer	E542K,E453K
P-0000607-T01-IM3	Breast Cancer	H1047L,E545Q
P-0001114-T02-IM3	Breast Cancer	E545K,E453Q,E978Q
P-0001351-T01-IM3	Breast Cancer	E545K,E726K
P-0001902-T01-IM3	Breast Cancer	E542K,E545D
P-0001990-T01-IM3	Breast Cancer	N345K,H1047Y
P-0002124-T01-IM3	Breast Cancer	H1047R,E365K
P-0002562-T01-IM3	Breast Cancer	E545K,E453Q
P-0002667-T01-IM3	Breast Cancer	H1047R,N107I
P-0002841-T01-IM3	Breast Cancer	H1047R,K111N
P-0002922-T01-IM3	Breast Cancer	H1047R,E545Q
P-0003224-T01-IM5	Breast Cancer	H1047R,G106V
P-0003233-T03-IM6	Breast Cancer	E542K,E453K
P-0003882-T03-IM6	Breast Cancer	N345K,E726K
P-0003987-T01-IM5	Breast Cancer	E545K,H1047R
P-0004187-T01-IM5	Breast Cancer	H1047R,E970K
P-0004264-T01-IM5	Breast Cancer	H1047R,E726K

P-0004433-T01-IM5	Breast Cancer	E545K,L252F
P-0005032-T01-IM5	Breast Cancer	L455Wfs*6,L452Qfs*5
P-0005037-T01-IM5	Breast Cancer	N345K,R93Q
P-0005154-T01-IM5	Breast Cancer	H1047R,E542K
P-0005220-T01-IM5	Breast Cancer	H1047R,C407F
P-0005242-T01-IM5	Breast Cancer	E545K,E726K
P-0005818-T01-IM5	Breast Cancer	H1047R,G118D
P-0006161-T03-IM5	Breast Cancer	E542K,E453K
P-0006166-T01-IM5	Breast Cancer	E542K,E726K
P-0006335-T01-IM5	Breast Cancer	E545K,T1025A
P-0006660-T01-IM5	Breast Cancer	R88Q,Q546H
P-0006723-T01-IM5	Breast Cancer	H1047R,E81K
P-0006780-T01-IM5	Breast Cancer	V344M,E726K
P-0006787-T01-IM5	Breast Cancer	H1047R,E726K
P-0007396-T01-IM5	Breast Cancer	N345K,E970K
P-0009364-T02-IM6	Breast Cancer	E545K,H1047R
P-0010043-T01-IM5	Breast Cancer	H1047R,P539R
P-0010703-T01-IM5	Breast Cancer	H1047L,E726K
P-0010917-T01-IM5	Breast Cancer	E542K,E726K
P-0011305-T01-IM5	Breast Cancer	E545K,E726K
P-0011420-T01-IM5	Breast Cancer	E545K,A1066V
P-0012667-T01-IM5	Breast Cancer	D390N,E385K
P-0013491-T01-IM5	Breast Cancer	G118D,E542Q
P-0013771-T01-IM5	Breast Cancer	H1047R,E726K
P-0013895-T01-IM5	Breast Cancer	E542K,E726K
P-0014091-T01-IM5	Breast Cancer	E81K,H1047L
P-0014136-T01-IM5	Breast Cancer	E542K,N457K
P-0014362-T01-IM6	Breast Cancer	H1047R,N370K
P-0014656-T01-IM6	Breast Cancer	E542K,K240Q
P-0015097-T01-IM6	Breast Cancer	H1047R,E453K
P-0015379-T01-IM6	Breast Cancer	H419_P421delinsQ,M1043_N1044delinsVK
P-0015499-T01-IM6	Breast Cancer	H1047R,E418K
P-0015944-T01-IM6	Breast Cancer	C420R,E726K
P-0015964-T01-IM6	Breast Cancer	E545K,M1004I
P-0016473-T01-IM6	Breast Cancer	E545K,L239R
P-0016686-T01-IM6	Breast Cancer	H1047R,P539R
P-0017015-T01-IM6	Breast Cancer	N345K,E726K
P-0017042-T01-IM6	Breast Cancer	E545K,M1043I
P-0017422-T01-IM6	Breast Cancer	E542K,A1066L
P-0018661-T01-IM6	Breast Cancer	E453K,G451K
P-0019024-T01-IM6	Breast Cancer	E545K,L10_P18del
P-0019040-T01-IM6	Breast Cancer	H1047R,R93Q,E418K
P-0019103-T01-IM6	Breast Cancer	H1047R,L456R
P-0019118-T01-IM6	Breast Cancer	E542K,E453K
P-0019425-T01-IM6	Breast Cancer	H1047R,C257Y
P-0019458-T01-IM6	Breast Cancer	H1047R,E726K
P-0020188-T01-IM6	Breast Cancer	E542K,E726K

P-0020301-T01-IM6	Breast Cancer	E453K,H419_P421delinsQ
P-0021148-T01-IM6	Breast Cancer	H1047R,V344M
P-0021480-T01-IM6	Breast Cancer	H1047R,E81K
P-0021571-T01-IM6	Breast Cancer	H1047R,R88Q
P-0021751-T01-IM6	Breast Cancer	Q546R,E453K
P-0021895-T01-IM6	Breast Cancer	H1047R,E726K
P-0022762-T01-IM6	Breast Cancer	H1047R,G451V
P-0023508-T01-IM6	Breast Cancer	E545K,K228N
P-0023835-T01-IM6	Breast Cancer	H1047R,E722K
P-0024230-T01-IM6	Breast Cancer	K111E,E545V
P-0024231-T01-IM6	Breast Cancer	Q546R,E453_L455del
P-0024285-T01-IM6	Breast Cancer	E545K,E726K
P-0024507-T01-IM6	Breast Cancer	E545K,H1047R
P-0025307-T01-IM6	Breast Cancer	E110del,E453K
P-0025489-T01-IM6	Breast Cancer	E542K,E726K
P-0025528-T01-IM6	Breast Cancer	H1047R,Q546H
P-0026513-T01-IM6	Breast Cancer	E542K,G118D
P-0026885-T01-IM6	Breast Cancer	H1047R,M1004I,E722K
P-0027710-T01-IM6	Breast Cancer	E110del,P539R
P-0028309-T01-IM6	Breast Cancer	H1047R,E39Q
P-0028907-T01-IM6	Breast Cancer	N345K,E726K
P-0028960-T01-IM6	Breast Cancer	G118D,E982D
P-0029802-T01-IM6	Breast Cancer	E545K,E542K
P-0030451-T01-IM6	Breast Cancer	H1047R,R88Q
P-0031280-T01-IM6	Breast Cancer	E545K,V344M
P-0031695-T01-IM6	Breast Cancer	E542K,M1043I
P-0031839-T01-IM6	Breast Cancer	E545K,M1004I
P-0000107-T01-IM3	Breast Cancer	Y1021H,D1017E,I1019V
P-0000207-T01-IM3	Breast Cancer	N345K,K111E
P-0000356-T01-IM3	Breast Cancer	H1047R,E453K
P-0000381-T01-IM3	Breast Cancer	H1047R,E726K
P-0000592-T01-IM3	Breast Cancer	E545K,M1043I
P-0001043-T01-IM3	Breast Cancer	H1047R,R93L
P-0001631-T01-IM3	Breast Cancer	E545K,M1043L
P-0002657-T01-IM3	Breast Cancer	G118D,G364R
P-0002756-T02-IM5	Breast Cancer	E545K,E453Q
P-0004194-T01-IM5	Breast Cancer	E545K,D725G
P-0004196-T01-IM5	Breast Cancer	H1047R,Q958K
P-0004913-T01-IM5	Breast Cancer	H1047R,E542A
P-0005120-T01-IM5	Breast Cancer	E542K,E726K
P-0005314-T01-IM5	Breast Cancer	E542K,E726K
P-0005611-T01-IM5	Breast Cancer	E39K,M1043I
P-0005968-T01-IM5	Breast Cancer	H1047R,R88Q
P-0008679-T01-IM5	Breast Cancer	H1047R,N345I
P-0008694-T01-IM5	Breast Cancer	E542K,E453K
P-0008845-T01-IM5	Breast Cancer	G118D,K111E
P-0009745-T02-IM6	Breast Cancer	C420R,E726K

P-0010002-T01-IM5	Breast Cancer	G1049R,Q546P
P-0011355-T01-IM5	Breast Cancer	H1047R,E81K
P-0012635-T02-IM6	Breast Cancer	H1047R,P539R
P-0012911-T01-IM5	Breast Cancer	C420R,R108H
P-0014278-T01-IM6	Breast Cancer	E542K,E726K
P-0014479-T01-IM6	Breast Cancer	E545K,E542Q
P-0014480-T01-IM6	Breast Cancer	E542K,E726K
P-0014515-T01-IM6	Breast Cancer	Q546R,M1004I
P-0014622-T01-IM6	Breast Cancer	H1047R,P104L
P-0014737-T01-IM6	Breast Cancer	H1047L,P539R
P-0014860-T01-IM6	Breast Cancer	H1047L,E545D
P-0014940-T01-IM6	Breast Cancer	E542K,E726K
P-0014943-T01-IM6	Breast Cancer	H1047R,E542G
P-0015005-T01-IM6	Breast Cancer	E545K,Q546R
P-0015633-T01-IM6	Breast Cancer	H1047L,I112F
P-0015640-T01-IM6	Breast Cancer	N1044K,D350N
P-0016041-T02-IM6	Breast Cancer	R88Q,H1047L
P-0016773-T01-IM6	Breast Cancer	G106V,Q546H
P-0016786-T01-IM6	Breast Cancer	E545K,M1043I
P-0016802-T01-IM6	Breast Cancer	H1047R,G118D
P-0016840-T01-IM6	Breast Cancer	H1047R,V344M
P-0017581-T01-IM5	Breast Cancer	E545G,T1025A
P-0017818-T01-IM6	Breast Cancer	E545K,H1048R
P-0018891-T01-IM6	Breast Cancer	H1047R,N107Y
P-0019133-T01-IM6	Breast Cancer	G1049R,P539R
P-0019191-T01-IM6	Breast Cancer	H1047R,E542K
P-0019808-T01-IM6	Breast Cancer	H1047R,R108H
P-0019935-T01-IM6	Breast Cancer	H1047R,E970K
P-0020020-T01-IM6	Breast Cancer	D549N,*1fs*
P-0020043-T01-IM6	Breast Cancer	D725N,H450_P458del
P-0020049-T01-IM6	Breast Cancer	E545K,H1047R
P-0020551-T02-IM6	Breast Cancer	E545K,E726K
P-0020645-T01-IM6	Breast Cancer	H1047R,M1043V
P-0021040-T01-IM6	Breast Cancer	H1047R,M1055L
P-0021087-T01-IM6	Breast Cancer	E542K,T544S
P-0021129-T01-IM6	Breast Cancer	H1047R,E726K
P-0021135-T02-IM6	Breast Cancer	H1047R,E542Q
P-0021201-T01-IM6	Breast Cancer	N345I,M1040T,L1036S
P-0021218-T01-IM6	Breast Cancer	H1047R,E418K
P-0021660-T01-IM6	Breast Cancer	E545K,E542K
P-0022021-T01-IM6	Breast Cancer	E545K,N1044K,D549H
P-0022048-T01-IM6	Breast Cancer	N345K,M1043_N1044delinsIH
P-0022088-T01-IM6	Breast Cancer	E545K,H1047R
P-0022158-T01-IM6	Breast Cancer	P471L,H1047C
P-0022167-T01-IM6	Breast Cancer	G1049R,R93Q,P539R
P-0022565-T01-IM6	Breast Cancer	H1047R,C378F
P-0022750-T01-IM6	Breast Cancer	H1047R,E542K

P-0023131-T01-IM6	Breast Cancer	H1047R,C420R
P-0023919-T02-IM6	Breast Cancer	H1047R,C378Y
P-0024141-T01-IM6	Breast Cancer	E542K,E726K
P-0024364-T01-IM6	Breast Cancer	H1047R,P449A
P-0024420-T01-IM6	Breast Cancer	E545K,D939G,D549N
P-0024647-T01-IM6	Breast Cancer	H1047R,R88Q
P-0025190-T01-IM6	Breast Cancer	E542K,E726K
P-0026012-T01-IM6	Breast Cancer	E545K,H1047L
P-0026070-T01-IM6	Breast Cancer	E545K,G903A
P-0026484-T01-IM6	Breast Cancer	I31M,I112T
P-0026829-T01-IM6	Breast Cancer	E542K,R93W
P-0026957-T01-IM6	Breast Cancer	H1047R,D350G
P-0028922-T01-IM6	Breast Cancer	G1049R,P104T
P-0029706-T01-IM6	Breast Cancer	H1047R,C378Y
P-0029966-T01-IM6	Breast Cancer	E545K,N1044K
P-0030165-T01-IM6	Breast Cancer	N345K,E418K
P-0030169-T01-IM6	Breast Cancer	R108H,H1047Q
P-0030392-T01-IM6	Breast Cancer	E545K,E453K
P-0030977-T01-IM6	Breast Cancer	H1047R,R108C
P-0031023-T01-IM6	Breast Cancer	H1047R,R88Q
P-0031133-T01-IM6	Breast Cancer	H1047R,S323F
P-0032388-T01-IM6	Breast Cancer	E542K,E418K
P-0004374-T01-IM5	Cancer of Unknown Primary	E542K,D454G
P-0008153-T01-IM5	Cancer of Unknown Primary	H1047R,R88Q
P-0022966-T01-IM6	Cancer of Unknown Primary	M1043I,I932M
P-0023748-T01-IM6	Cancer of Unknown Primary	E545K,H1047R
P-0026350-T01-IM6	Cancer of Unknown Primary	R108_E109del,X353_splice
P-0028427-T01-IM6	Cancer of Unknown Primary	R357Q,K111N,R537Q,L62I,V146A
P-0010527-T01-IM5	Cervical Cancer	E545K,E542K
P-0013774-T01-IM5	Cervical Cancer	E545K,E81K
P-0015136-T01-IM6	Cervical Cancer	C420R,N370K
P-0029938-T01-IM6	Cervical Cancer	E545K,E453K
P-0030876-T01-IM6	Cervical Cancer	E545K,E726K
P-0033211-T01-IM6	Cervical Cancer	K111N,Q546L
P-0001215-T01-IM3	Colorectal Cancer	E365K,R992*,I816N
P-0001732-T01-IM3	Colorectal Cancer	E542K,M1043I
P-0011071-T01-IM5	Colorectal Cancer	E542K,R108S
P-0019593-T01-IM6	Colorectal Cancer	E542K,E453K
P-0020473-T01-IM6	Colorectal Cancer	R88Q,I816S
P-0020493-T01-IM6	Colorectal Cancer	H1047R,R93W
P-0022090-T01-IM6	Colorectal Cancer	H1047R,Y343F
P-0023461-T01-IM6	Colorectal Cancer	E545K,G106V
P-0026678-T01-IM6	Colorectal Cancer	R38C,Y1021C
P-0000788-T01-IM3	Colorectal Cancer	E542K,M1010I
P-0001289-T01-IM3	Colorectal Cancer	H1047R,V344G
P-0001940-T01-IM3	Colorectal Cancer	H1047R,G118D
P-0002413-T01-IM3	Colorectal Cancer	Q546K,E726K

P-0003513-T01-IM5	Colorectal Cancer	E365K,H1047Q
P-0003720-T01-IM5	Colorectal Cancer	H1047R,R93Q
P-0004566-T01-IM5	Colorectal Cancer	E545K,H1047R
P-0004865-T01-IM5	Colorectal Cancer	E542K,K111N
P-0004928-T01-IM5	Colorectal Cancer	E545K,E542K
P-0005270-T02-IM6	Colorectal Cancer	H1065Y,E39D
P-0006170-T01-IM5	Colorectal Cancer	E545G,Q75H
P-0006581-T01-IM5	Colorectal Cancer	E545K,L540F
P-0006612-T01-IM5	Colorectal Cancer	M1043I,R693C
P-0007147-T01-IM5	Colorectal Cancer	H1047R,R88Q
P-0007272-T01-IM5	Colorectal Cancer	R38C,R357L
P-0007836-T01-IM5	Colorectal Cancer	E110del,R93Q,E418D
P-0008721-T01-IM5	Colorectal Cancer	H1047R,A289T
P-0010125-T01-IM5	Colorectal Cancer	G364R,V125E
P-0010167-T01-IM5	Colorectal Cancer	H1047R,V851A
P-0011357-T01-IM5	Colorectal Cancer	M1004I,K111N,R357*
P-0013010-T01-IM5	Colorectal Cancer	H1047R,C420R
P-0013020-T01-IM5	Colorectal Cancer	H1047R,Q546R
P-0016066-T01-IM6	Colorectal Cancer	H1047R,K111E
P-0016314-T01-IM6	Colorectal Cancer	H1047R,C420R
P-0017583-T01-IM5	Colorectal Cancer	Y1021C,H1047Q
P-0017995-T01-IM6	Colorectal Cancer	Y1021H,R93W
P-0018437-T01-IM6	Colorectal Cancer	C420R,H1047Y
P-0019464-T01-IM6	Colorectal Cancer	N345K,H1047Y
P-0020144-T01-IM6	Colorectal Cancer	R38C,Y1021H
P-0020383-T01-IM6	Colorectal Cancer	R108H,N345I
P-0020689-T01-IM6	Colorectal Cancer	R88Q,R108H
P-0022477-T01-IM6	Colorectal Cancer	H1047R,K111N
P-0023187-T01-IM6	Colorectal Cancer	D350N,K111N
P-0023271-T01-IM6	Colorectal Cancer	R88Q,L339F,L144M
P-0025047-T01-IM6	Colorectal Cancer	H1047R,K111E
P-0025073-T01-IM6	Colorectal Cancer	E545K,H1047R
P-0025348-T01-IM6	Colorectal Cancer	H1047R,P449S
P-0025695-T01-IM6	Colorectal Cancer	E545K,E545G
P-0025715-T01-IM6	Colorectal Cancer	H1047R,G914R
P-0025792-T01-IM6	Colorectal Cancer	E542K,L540_S541dup
P-0026962-T01-IM6	Colorectal Cancer	E542K,H1048R,V491Dfs*2
P-0027476-T01-IM6	Colorectal Cancer	H1047R,R88Q,P539R
P-0027608-T01-IM6	Colorectal Cancer	E542K,R93Q
P-0030265-T01-IM6	Colorectal Cancer	R93Q,T1025I
P-0030988-T01-IM6	Colorectal Cancer	H1047R,R412*
P-0032698-T01-IM6	Colorectal Cancer	H1047R,R1023Q
P-0033100-T01-IM6	Colorectal Cancer	H1047R,R88Q,P266H
P-0033196-T01-IM6	Colorectal Cancer	E545K,C420R
P-0000404-T01-IM3	Endometrial Cancer	K111E,P449R
P-0000448-T01-IM3	Endometrial Cancer	V344M,T1025A
P-0003767-T01-IM5	Endometrial Cancer	H1047R,E453del

P-0004136-T01-IM5	Endometrial Cancer	E542K,I1058L
P-0006269-T01-IM5	Endometrial Cancer	V344M,H1047Y
P-0012152-T01-IM5	Endometrial Cancer	E545G,P97H
P-0012358-T01-IM5	Endometrial Cancer	R88Q,R115Q,R537Q,L997I
P-0014720-T01-IM6	Endometrial Cancer	G118D,E110del
P-0018542-T01-IM6	Endometrial Cancer	G118D,T957I
P-0019471-T01-IM6	Endometrial Cancer	P104L,M1043I
P-0024756-T01-IM6	Endometrial Cancer	H1047R,R108H
P-0025003-T01-IM6	Endometrial Cancer	R88Q,E453G
P-0025812-T01-IM6	Endometrial Cancer	M1043V,P539R
P-0026297-T01-IM6	Endometrial Cancer	R88Q,D350G,R230*
P-0027698-T01-IM6	Endometrial Cancer	H1047R,Y1021H
P-0028924-T01-IM6	Endometrial Cancer	V344M,M1043I
P-0029337-T01-IM6	Endometrial Cancer	V346E,D743V
P-0029683-T01-IM6	Endometrial Cancer	H1047Q,F477S
P-0031387-T01-IM6	Endometrial Cancer	V344M,N1044S,E418K
P-0031615-T01-IM6	Endometrial Cancer	H1047R,M1043I
P-0002357-T01-IM3	Endometrial Cancer	H1047Y,D1029H
P-0002945-T01-IM3	Endometrial Cancer	H1047Y,E726K
P-0004017-T01-IM5	Endometrial Cancer	H1047L,E453K
P-0004255-T01-IM5	Endometrial Cancer	H1047R,R88Q
P-0006201-T01-IM5	Endometrial Cancer	E365K,R93W
P-0009316-T01-IM5	Endometrial Cancer	E545K,H1047Y
P-0010967-T01-IM5	Endometrial Cancer	E81K,R88Q
P-0011569-T01-IM5	Endometrial Cancer	R88Q,Y1021C,R93Q,L779M
P-0011570-T01-IM5	Endometrial Cancer	L339I,D549N,F83S
P-0012113-T01-IM5	Endometrial Cancer	R88Q,T1025A,Q958R
P-0012397-T01-IM5	Endometrial Cancer	R88Q,Y1021C,R852Q
P-0012445-T01-IM5	Endometrial Cancer	Y1021C,R992*
P-0012670-T01-IM5	Endometrial Cancer	R88Q,Y1021C
P-0012726-T01-IM5	Endometrial Cancer	R88Q,G106V
P-0012755-T01-IM5	Endometrial Cancer	C420R,R108H
P-0012819-T01-IM5	Endometrial Cancer	R38C,L712I
P-0012881-T01-IM5	Endometrial Cancer	I816S,R19I
P-0013452-T01-IM5	Endometrial Cancer	R93W,C378R
P-0013512-T01-IM5	Endometrial Cancer	R88Q,G118D,G106D
P-0014388-T01-IM6	Endometrial Cancer	R88Q,R93W
P-0014461-T01-IM6	Endometrial Cancer	W11R,L1036S
P-0014495-T01-IM6	Endometrial Cancer	R88Q,Q546R
P-0014528-T01-IM6	Endometrial Cancer	R88Q,Y1021C
P-0014780-T01-IM6	Endometrial Cancer	H1047R,R88Q,V344A,R852Q
P-0015626-T01-IM6	Endometrial Cancer	R88Q,R357Q
P-0015869-T01-IM6	Endometrial Cancer	R357Q,K111N,D883G
P-0015885-T01-IM6	Endometrial Cancer	C420R,Y1021C
P-0015986-T01-IM6	Endometrial Cancer	G118D,H1048R
P-0016099-T01-IM6	Endometrial Cancer	E365K,F1002V
P-0016203-T01-IM6	Endometrial Cancer	V344M,R88Q

P-0016247-T01-IM6	Endometrial Cancer	H1047R,N345D
P-0016537-T01-IM6	Endometrial Cancer	E545K,H1047L
P-0016556-T01-IM6	Endometrial Cancer	C901F,R88Q
P-0016904-T01-IM6	Endometrial Cancer	R88Q,N345K,R93W
P-0016907-T01-IM6	Endometrial Cancer	P366R,H1047Y
P-0017302-T01-IM6	Endometrial Cancer	Y1021H,K111E
P-0017424-T01-IM6	Endometrial Cancer	E545K,R88Q
P-0017681-T01-IM6	Endometrial Cancer	R88Q,R108H,V344A
P-0017896-T01-IM6	Endometrial Cancer	E545K,E542K
P-0018005-T01-IM6	Endometrial Cancer	E545K,R274T,L285F
P-0018009-T01-IM6	Endometrial Cancer	E81K,E453K
P-0018459-T01-IM6	Endometrial Cancer	H1047L,V101del
P-0018616-T01-IM6	Endometrial Cancer	R108C,D743N
P-0018778-T01-IM6	Endometrial Cancer	R115P,P539R
P-0018781-T01-IM6	Endometrial Cancer	R88Q,P449S
P-0018790-T01-IM6	Endometrial Cancer	H1047R,R108H
P-0019107-T01-IM6	Endometrial Cancer	K111N,D350N
P-0019658-T01-IM6	Endometrial Cancer	R88Q,R357Q
P-0019659-T01-IM6	Endometrial Cancer	R88Q,R108S
P-0019741-T01-IM6	Endometrial Cancer	R88Q,H1047Y
P-0019871-T01-IM6	Endometrial Cancer	R88Q,F83I,P458L
P-0019986-T01-IM6	Endometrial Cancer	R88Q,R108C
P-0020227-T01-IM6	Endometrial Cancer	R38H,R38C,E600K
P-0020295-T01-IM6	Endometrial Cancer	E81K,T1025A
P-0020509-T01-IM6	Endometrial Cancer	R38H,R108H
P-0020556-T01-IM6	Endometrial Cancer	E545K,R93Q
P-0020757-T01-IM6	Endometrial Cancer	K111E,P539R
P-0021579-T01-IM6	Endometrial Cancer	N1044K,N345H
P-0021665-T01-IM6	Endometrial Cancer	R38H,E453K
P-0021777-T01-IM6	Endometrial Cancer	R38C,R108H
P-0022813-T01-IM6	Endometrial Cancer	K111E,H450_I459delinsL
P-0023250-T01-IM6	Endometrial Cancer	H1047R,F83C
P-0023555-T01-IM6	Endometrial Cancer	H1047R,D350G,E453K
P-0023857-T01-IM6	Endometrial Cancer	H1047R,R88Q
P-0023969-T01-IM6	Endometrial Cancer	R88Q,K111E
P-0025632-T01-IM6	Endometrial Cancer	R88Q,R108H
P-0025648-T01-IM6	Endometrial Cancer	R88Q,R357Q
P-0025662-T01-IM6	Endometrial Cancer	N345T,E542G
P-0026278-T01-IM6	Endometrial Cancer	R88Q,Y1021C,G364R
P-0026297-T02-IM6	Endometrial Cancer	R88Q,D350G,R401Q,R230*
P-0026714-T01-IM6	Endometrial Cancer	G12D,L422W
P-0027431-T01-IM6	Endometrial Cancer	C420R,M1040K
P-0027652-T01-IM6	Endometrial Cancer	E542A,F744L
P-0028610-T01-IM6	Endometrial Cancer	E726K,P104L
P-0028776-T01-IM6	Endometrial Cancer	H1047R,R951C,L267M,E784D
P-0028970-T01-IM6	Endometrial Cancer	R38H,C378R
P-0029162-T01-IM6	Endometrial Cancer	C378R,R4Q

P-0029274-T01-IM6	Endometrial Cancer	E542K,N107I
P-0029666-T01-IM6	Endometrial Cancer	P366R,E726A
P-0029690-T01-IM6	Endometrial Cancer	R38C,T1025A,L339I,K111N
P-0029778-T01-IM6	Endometrial Cancer	E81K,M1004I
P-0030372-T01-IM6	Endometrial Cancer	R357Q,R992*,G1009E
P-0031042-T01-IM6	Endometrial Cancer	E110del,R93Q
P-0031185-T02-IM6	Endometrial Cancer	E542K,R88Q
P-0031195-T01-IM6	Endometrial Cancer	Q546R,D350G
P-0031271-T01-IM6	Endometrial Cancer	H1047R,V344M
P-0031332-T02-IM6	Endometrial Cancer	H1047Y,R93W
P-0031501-T01-IM6	Endometrial Cancer	V344M,R88Q,H1047Y
P-0032113-T01-IM6	Endometrial Cancer	R88Q,Q981H
P-0032496-T01-IM6	Endometrial Cancer	R88Q,R108H,R357Q
P-0032589-T01-IM6	Endometrial Cancer	R88Q,Y1021C,E365K,T544N
P-0032606-T01-IM6	Endometrial Cancer	C420R,I1058L
P-0032818-T01-IM6	Endometrial Cancer	R88Q,P449S,R115Q
P-0033016-T01-IM6	Endometrial Cancer	T1025A,K111N
P-0024054-T01-IM6	Esophagogastric Cancer	E545K,M1004I
P-0009918-T01-IM5	Esophagogastric Cancer	H1047R,V344M,K111N
P-0031190-T01-IM6	Esophagogastric Cancer	X765_splice,X806_splice,X889_splice,X928_splice
P-0000650-T01-IM3	Germ Cell Tumor	E542K,K724del
P-0019519-T01-IM6	Glioma	E542A,E722K
P-0000500-T01-IM3	Glioma	E545K,E542K
P-0002633-T01-IM3	Glioma	R88Q,Q546R
P-0002695-T01-IM3	Glioma	E545K,E116K
P-0004531-T01-IM5	Glioma	C420R,E545G
P-0008649-T01-IM5	Glioma	H1047R,L436_P449dup
P-0011521-T01-IM5	Glioma	E542K,G106V
P-0013293-T02-IM6	Glioma	E545K,D300N
P-0017482-T01-IM6	Glioma	V71I,V448dup
P-0017675-T01-IM5	Glioma	V125L,D133N,X382_splice
P-0018691-T01-IM6	Glioma	G914R,N345D
P-0023123-T01-IM6	Glioma	R93W,P2L,G411S
P-0023566-T01-IM6	Glioma	E545K,R93W
P-0027147-T01-IM6	Glioma	K111E,P539R
P-0029104-T01-IM6	Glioma	P200S,P57L
P-0031276-T01-IM6	Glioma	E542K,I543F
P-0032337-T01-IM6	Glioma	Q546K,M1043V
P-0005212-T01-IM5	Head and Neck Cancer	E542K,E78K
P-0009761-T01-IM5	Head and Neck Cancer	E545K,E579K
P-0029015-T01-IM6	Head and Neck Cancer	E545K,E542K
P-0002411-T01-IM3	Head and Neck Cancer	E545K,D538Y
P-0024866-T01-IM6	Head and Neck Cancer	E545K,E542K,D549N
P-0032593-T01-IM6	Head and Neck Cancer	N1044K,E453del
P-0002286-T01-IM3	Hepatobiliary Cancer	E545K,C420R
P-0023198-T01-IM6	Hepatobiliary Cancer	E545K,E81K
P-0028463-T01-IM6	Hepatobiliary Cancer	E545K,D549V

P-0009189-T01-IM5	Melanoma	S67F,L402F
P-0009752-T01-IM5	Melanoma	H14Y,S326F
P-0021394-T01-IM6	Melanoma	E545K,C420R
P-0009431-T01-IM5	Non-Small Cell Lung Cancer	E81K,R93W
P-0021735-T01-IM6	Non-Small Cell Lung Cancer	H1047R,G118V
P-0022891-T03-IM6	Non-Small Cell Lung Cancer	H1047R,E726K
P-0023265-T01-IM6	Non-Small Cell Lung Cancer	E545K,E542K
P-0032172-T01-IM6	Non-Small Cell Lung Cancer	E542K,M318V
P-0003551-T02-IM6	Non-Small Cell Lung Cancer	E545K,E542K
P-0011388-T01-IM5	Non-Small Cell Lung Cancer	D1029H,D1045N,E982Q
P-0012580-T01-IM5	Non-Small Cell Lung Cancer	E726K,H1065L
P-0018244-T01-IM6	Non-Small Cell Lung Cancer	E542K,P471A
P-0024921-T01-IM6	Non-Small Cell Lung Cancer	P217A,N444I
P-0027048-T01-IM6	Non-Small Cell Lung Cancer	H450_I459del,G460S
P-0028051-T01-IM6	Non-Small Cell Lung Cancer	A77V,A415Cfs*2
P-0032292-T01-IM6	Non-Small Cell Lung Cancer	E542K,E453K
P-0032614-T01-IM6	Non-Small Cell Lung Cancer	E545K,E542K
P-0033200-T01-IM6	Non-Small Cell Lung Cancer	E542K,D214Y
P-0029643-T01-IM6	Ovarian Cancer	V344M,R115L
P-0001105-T01-IM3	Ovarian Cancer	R108H,C378F
P-0031332-T01-IM6	Ovarian Cancer	H1047Y,E545D
P-0026409-T01-IM6	Prostate Cancer	E542K,I1058L
P-0025880-T01-IM6	Prostate Cancer	E545K,H1047L
P-0000957-T01-IM3	Salivary Gland Cancer	M1004I,*1069Ffs*5
P-0001198-T01-IM3	Skin Cancer, Non-Melanoma	E542K,C24S,S66F,W780*
P-0018328-T01-IM6	Skin Cancer, Non-Melanoma	H1047R,E726K
P-0018382-T01-IM6	Small Bowel Cancer	R88Q,Q546R
P-0032985-T01-IM6	Small Bowel Cancer	K111E,N107H
P-0031236-T01-IM6	Soft Tissue Sarcoma	H1047R,E365K
P-0003178-T01-IM5	Thyroid Cancer	H1047R,E542K
P-0032729-T02-IM6	Thyroid Cancer	N345K,H1047Y

Table S3: Double *PIK3CA* mutant breast tumours phased as *cis* or *trans* mutants, by NGS (MSK-IMPACT)

Sample ID	Cancer Type	*PIK3CA* Mutation (gDNA)	*Cis* or *trans*
P-0012667-T01-IM5	Breast Cancer	E385K + D390N	*Cis*
P-0001902-T01-IM3	Breast Cancer	E542K + E545D	*Cis*
P-0014479-T01-IM6	Breast Cancer	E542Q + E545K	*Cis*
P-0029802-T01-IM6	Breast Cancer	E542K + E545K	*Cis*
P-0022021-T01-IM6	Breast Cancer	E545K + D549H	*Cis*
P-0024420-T01-IM6	Breast Cancer	E545K + D549N	*Cis*
P-0026885-T01-IM6	Breast Cancer	M1004I + H1047R	*Cis*
P-0000107-T01-IM3	Breast Cancer	D1017E + I1019V + Y1021H	*Cis*
P-0021201-T01-IM6	Breast Cancer	L1036S + M1040T	*Cis*
P-0021040-T01-IM6	Breast Cancer	H1047R + M1055L	*Cis*
P-0020645-T01-IM6	Breast Cancer	M1043V + H1047R	*Trans*

Table S4: Double *PIK3CA* mutant breast tumours phased as *cis* mutants, by RNA-seq (TCGA)

Sample ID	Cancer Type	*PIK3CA* mutations (RNA, in cis)	Number of reads calling both mutations	Number of reads spanning both loci
TCGA-AO-A1KR-01A-12D-A142-09	Breast Cancer	1004 + 1047	11	12
TCGA-A2-A0EN-01A-13D-A099-09	Breast Cancer	1047 + 1065	4	10

References and Notes

1. M. H. Bailey, C. Tokheim, E. Porta-Pardo, S. Sengupta, D. Bertrand, A. Weerasinghe, A. Colaprico, M. C. Wendl, J. Kim, B. Reardon, P. Kwok-Shing Ng, K. J. Jeong, S. Cao, Z. Wang, J. Gao, Q. Gao, F. Wang, E. M. Liu, L. Mularoni, C. Rubio-Perez, N. Nagarajan, I. Cortés-Ciriano, D. C. Zhou, W.-W. Liang, J. M. Hess, V. D. Yellapantula, D. Tamborero, A. Gonzalez-Perez, C. Suphavilai, J. Y. Ko, E. Khurana, P. J. Park, E. M. Van Allen, H. Liang, M. S. Lawrence, A. Godzik, N. Lopez-Bigas, J. Stuart, D. Wheeler, G. Getz, K. Chen, A. J. Lazar, G. B. Mills, R. Karchin, L. Ding; MC3 Working Group; Cancer Genome Atlas Research Network, Comprehensive Characterization of Cancer Driver Genes and Mutations. *Cell* **174**, 1034–1035 (2018). doi:10.1016/j.cell.2018.07.034 Medline

2. M. Whitman, C. P. Downes, M. Keeler, T. Keller, L. Cantley, Type I phosphatidylinositol kinase makes a novel inositol phospholipid, phosphatidylinositol-3-phosphate. *Nature* **332**, 644–646 (1988). doi:10.1038/332644a0 Medline

3. D. A. Fruman, H. Chiu, B. D. Hopkins, S. Bagrodia, L. C. Cantley, R. T. Abraham, The PI3K Pathway in Human Disease. *Cell* **170**, 605–635 (2017). doi:10.1016/j.cell.2017.07.029 Medline

4. Y. Samuels, Z. Wang, A. Bardelli, N. Silliman, J. Ptak, S. Szabo, H. Yan, A. Gazdar, S. M. Powell, G. J. Riggins, J. K. Willson, S. Markowitz, K. W. Kinzler, B. Vogelstein, V. E. Velculescu, High frequency of mutations of the PIK3CA gene in human cancers. *Science* **304**, 554 (2004). doi:10.1126/science.1096502 Medline

5. Y. Samuels, L. A. Diaz Jr., O. Schmidt-Kittler, J. M. Cummins, L. Delong, I. Cheong, C. Rago, D. L. Huso, C. Lengauer, K. W. Kinzler, B. Vogelstein, V. E. Velculescu, Mutant PIK3CA promotes cell growth and invasion of human cancer cells. *Cancer Cell* **7**, 561–573 (2005). doi:10.1016/j.ccr.2005.05.014 Medline

6. S. Kang, A. G. Bader, P. K. Vogt, Phosphatidylinositol 3-kinase mutations identified in human cancer are oncogenic. *Proc. Natl. Acad. Sci. U.S.A.* **102**, 802–807 (2005). doi:10.1073/pnas.0408864102 Medline

7. S. J. Isakoff, J. A. Engelman, H. Y. Irie, J. Luo, S. M. Brachmann, R. V. Pearline, L. C. Cantley, J. S. Brugge, Breast cancer-associated PIK3CA mutations are oncogenic in mammary epithelial cells. *Cancer Res.* **65**, 10992–11000 (2005). doi:10.1158/0008-5472.CAN-05-2612 Medline

8. J. J. Zhao, O. V. Gjoerup, R. R. Subramanian, Y. Cheng, W. Chen, T. M. Roberts, W. C. Hahn, Human mammary epithelial cell transformation through the activation of phosphatidylinositol 3-kinase. *Cancer Cell* **3**, 483–495 (2003). doi:10.1016/S1535-6108(03)00088-6 Medline

9. P. Razavi, M. T. Chang, G. Xu, C. Bandlamudi, D. S. Ross, N. Vasan, Y. Cai, C. M. Bielski, M. T. A. Donoghue, P. Jonsson, A. Penson, R. Shen, F. Pareja, R. Kundra, S. Middha, M. L. Cheng, A. Zehir, C. Kandoth, R. Patel, K. Huberman, L. M. Smyth, K. Jhaveri, S. Modi, T. A. Traina, C. Dang, W. Zhang, B. Weigelt, B. T. Li, M. Ladanyi, D. M. Hyman, N. Schultz, M. E. Robson, C. Hudis, E. Brogi, A. Viale, L. Norton, M. N. Dickler, M. F. Berger, C. A. Iacobuzio-Donahue, S. Chandarlapaty, M. Scaltriti, J. S. Reis-Filho, D. B.

Solit, B. S. Taylor, J. Baselga, The Genomic Landscape of Endocrine-Resistant Advanced Breast Cancers. *Cancer Cell* **34**, 427–438.e6 (2018). doi:10.1016/j.ccell.2018.08.008 Medline

10. J. Baselga, S.-A. Im, H. Iwata, J. Cortés, M. De Laurentiis, Z. Jiang, C. L. Arteaga, W. Jonat, M. Clemons, Y. Ito, A. Awada, S. Chia, A. Jagiełło-Gruszfeld, B. Pistilli, L.-M. Tseng, S. Hurvitz, N. Masuda, M. Takahashi, P. Vuylsteke, S. Hachemi, B. Dharan, E. Di Tomaso, P. Urban, C. Massacesi, M. Campone, Buparlisib plus fulvestrant versus placebo plus fulvestrant in postmenopausal, hormone receptor-positive, HER2-negative, advanced breast cancer (BELLE-2): A randomised, double-blind, placebo-controlled, phase 3 trial. *Lancet Oncol.* **18**, 904–916 (2017). doi:10.1016/S1470-2045(17)30376-5 Medline

11. A. Di Leo, S. Johnston, K. S. Lee, E. Ciruelos, P. E. Lønning, W. Janni, R. O'Regan, M.-A. Mouret-Reynier, D. Kalev, D. Egle, T. Csőszi, R. Bordonaro, T. Decker, V. C. G. Tjan-Heijnen, S. Blau, A. Schirone, D. Weber, M. El-Hashimy, B. Dharan, D. Sellami, T. Bachelot, Buparlisib plus fulvestrant in postmenopausal women with hormone-receptor-positive, HER2-negative, advanced breast cancer progressing on or after mTOR inhibition (BELLE-3): A randomised, double-blind, placebo-controlled, phase 3 trial. *Lancet Oncol.* **19**, 87–100 (2018). doi:10.1016/S1470-2045(17)30688-5 Medline

12. J. Baselga, S. F. Dent, J. Cortés, Y.-H. Im, V. Diéras, N. Harbeck, I. E. Krop, S. Verma, T. R. Wilson, H. Jin, L. Wang, F. Schimmoller, J. Y. Hsu, J. He, M. DeLaurentiis, P. Drullinsky, W. Jacot, Phase III study of taselisib (GDC-0032) + fulvestrant (FULV) v FULV in patients (pts) with estrogen receptor (ER)-positive, PIK3CA-mutant (MUT), locally advanced or metastatic breast cancer (MBC): Primary analysis from SANDPIPER. *J. Clin. Oncol.* **36** (suppl.), LBA1006 (2018). doi:10.1200/JCO.2018.36.18_suppl.LBA1006

13. C. Saura, D. Hlauschek, M. Oliveira, D. Zardavas, A. Jallitsch-Halper, L. de la Peña, P. Nuciforo, A. Ballestrero, P. Dubsky, J. M. Lombard, P. Vuylsteke, C. A. Castaneda, M. Colleoni, G. Santos Borges, E. Ciruelos, M. Fornier, K. Boer, A. Bardia, T. R. Wilson, T. J. Stout, J. Y. Hsu, Y. Shi, M. Piccart, M. Gnant, J. Baselga, E. de Azambuja, Neoadjuvant letrozole plus taselisib versus letrozole plus placebo in postmenopausal women with oestrogen receptor-positive, HER2-negative, early-stage breast cancer (LORELEI): a multicentre, randomised, double-blind, placebo-controlled, phase 2 trial. *Lancet Oncol.* **20**, 1226–1238 (2019). doi:10.1016/S1470-2045(19)30334-1

14. D. Juric, J. Rodon, J. Tabernero, F. Janku, H. A. Burris, J. H. M. Schellens, M. R. Middleton, J. Berlin, M. Schuler, M. Gil-Martin, H. S. Rugo, R. Seggewiss-Bernhardt, A. Huang, D. Bootle, D. Demanse, L. Blumenstein, C. Coughlin, C. Quadt, J. Baselga, Phosphatidylinositol 3-Kinase α-Selective Inhibition With Alpelisib (BYL719) in PIK3CA-Altered Solid Tumors: Results From the First-in-Human Study. *J. Clin. Oncol.* **36**, 1291–1299 (2018). doi:10.1200/JCO.2017.72.7107 Medline

15. I. A. Mayer, V. G. Abramson, L. Formisano, J. M. Balko, M. V. Estrada, M. E. Sanders, D. Juric, D. Solit, M. F. Berger, H. H. Won, Y. Li, L. C. Cantley, E. Winer, C. L. Arteaga, A Phase Ib Study of Alpelisib (BYL719), a PI3Kα-Specific Inhibitor, with Letrozole in ER+/HER2- Metastatic Breast Cancer. *Clin. Cancer Res.* **23**, 26–34 (2017). doi:10.1158/1078-0432.CCR-16-0134 Medline

16. D. Juric, F. Janku, J. Rodón, H. A. Burris, I. A. Mayer, M. Schuler, R. Seggewiss-Bernhardt, M. Gil-Martin, M. R. Middleton, J. Baselga, D. Bootle, D. Demanse, L. Blumenstein, K. Schumacher, A. Huang, C. Quadt, H. S. Rugo, Alpelisib Plus Fulvestrant in PIK3CA-Altered and PIK3CA-Wild-Type Estrogen Receptor-Positive Advanced Breast Cancer: A Phase 1b Clinical Trial. *JAMA Oncol.* **5**, e184475 (2019). doi:10.1001/jamaoncol.2018.4475 Medline

17. F. André, E. Ciruelos, G. Rubovszky, M. Campone, S. Loibl, H. S. Rugo, H. Iwata, P. Conte, I. A. Mayer, B. Kaufman, T. Yamashita, Y.-S. Lu, K. Inoue, M. Takahashi, Z. Pápai, A.-S. Longin, D. Mills, C. Wilke, S. Hirawat, D. Juric; SOLAR-1 Study Group, Alpelisib for *PIK3CA*-Mutated, Hormone Receptor-Positive Advanced Breast Cancer. *N. Engl. J. Med.* **380**, 1929–1940 (2019). doi:10.1056/NEJMoa1813904 Medline

18. D. Juric, P. Castel, M. Griffith, O. L. Griffith, H. H. Won, H. Ellis, S. H. Ebbesen, B. J. Ainscough, A. Ramu, G. Iyer, R. H. Shah, T. Huynh, M. Mino-Kenudson, D. Sgroi, S. Isakoff, A. Thabet, L. Elamine, D. B. Solit, S. W. Lowe, C. Quadt, M. Peters, A. Derti, R. Schegel, A. Huang, E. R. Mardis, M. F. Berger, J. Baselga, M. Scaltriti, Convergent loss of PTEN leads to clinical resistance to a PI(3)Kα inhibitor. *Nature* **518**, 240–244 (2015). doi:10.1038/nature13948 Medline

19. D. T. Cheng, T. N. Mitchell, A. Zehir, R. H. Shah, R. Benayed, A. Syed, R. Chandramohan, Z. Y. Liu, H. H. Won, S. N. Scott, A. R. Brannon, C. O'Reilly, J. Sadowska, J. Casanova, A. Yannes, J. F. Hechtman, J. Yao, W. Song, D. S. Ross, A. Oultache, S. Dogan, L. Borsu, M. Hameed, K. Nafa, M. E. Arcila, M. Ladanyi, M. F. Berger, Memorial Sloan Kettering-Integrated Mutation Profiling of Actionable Cancer Targets (MSK-IMPACT): A Hybridization Capture-Based Next-Generation Sequencing Clinical Assay for Solid Tumor Molecular Oncology. *J. Mol. Diagn.* **17**, 251–264 (2015). doi:10.1016/j.jmoldx.2014.12.006 Medline

20. E. Cerami, J. Gao, U. Dogrusoz, B. E. Gross, S. O. Sumer, B. A. Aksoy, A. Jacobsen, C. J. Byrne, M. L. Heuer, E. Larsson, Y. Antipin, B. Reva, A. P. Goldberg, C. Sander, N. Schultz, The cBio cancer genomics portal: An open platform for exploring multidimensional cancer genomics data. *Cancer Discov.* **2**, 401–404 (2012). doi:10.1158/2159-8290.CD-12-0095 Medline

21. J. Gao, B. A. Aksoy, U. Dogrusoz, G. Dresdner, B. Gross, S. O. Sumer, Y. Sun, A. Jacobsen, R. Sinha, E. Larsson, E. Cerami, C. Sander, N. Schultz, Integrative analysis of complex cancer genomics and clinical profiles using the cBioPortal. *Sci. Signal.* **6**, pl1 (2013). doi:10.1126/scisignal.2004088 Medline

22. C. Curtis, S. P. Shah, S.-F. Chin, G. Turashvili, O. M. Rueda, M. J. Dunning, D. Speed, A. G. Lynch, S. Samarajiwa, Y. Yuan, S. Gräf, G. Ha, G. Haffari, A. Bashashati, R. Russell, S. McKinney, A. Langerød, A. Green, E. Provenzano, G. Wishart, S. Pinder, P. Watson, F. Markowetz, L. Murphy, I. Ellis, A. Purushotham, A.-L. Børresen-Dale, J. D. Brenton, S. Tavaré, C. Caldas, S. Aparicio; METABRIC Group, The genomic and transcriptomic architecture of 2,000 breast tumours reveals novel subgroups. *Nature* **486**, 346–352 (2012). doi:10.1038/nature10983 Medline

23. Cancer Genome Atlas Network, Comprehensive molecular portraits of human breast tumours. *Nature* **490**, 61–70 (2012). doi:10.1038/nature11412 Medline

24. S. Banerji, K. Cibulskis, C. Rangel-Escareno, K. K. Brown, S. L. Carter, A. M. Frederick, M. S. Lawrence, A. Y. Sivachenko, C. Sougnez, L. Zou, M. L. Cortes, J. C. Fernandez-Lopez, S. Peng, K. G. Ardlie, D. Auclair, V. Bautista-Piña, F. Duke, J. Francis, J. Jung, A. Maffuz-Aziz, R. C. Onofrio, M. Parkin, N. H. Pho, V. Quintanar-Jurado, A. H. Ramos, R. Rebollar-Vega, S. Rodriguez-Cuevas, S. L. Romero-Cordoba, S. E. Schumacher, N. Stransky, K. M. Thompson, L. Uribe-Figueroa, J. Baselga, R. Beroukhim, K. Polyak, D. C. Sgroi, A. L. Richardson, G. Jimenez-Sanchez, E. S. Lander, S. B. Gabriel, L. A. Garraway, T. R. Golub, J. Melendez-Zajgla, A. Toker, G. Getz, A. Hidalgo-Miranda, M. Meyerson, Sequence analysis of mutations and translocations across breast cancer subtypes. *Nature* **486**, 405–409 (2012). doi:10.1038/nature11154 Medline

25. P. J. Stephens, P. S. Tarpey, H. Davies, P. Van Loo, C. Greenman, D. C. Wedge, S. Nik-Zainal, S. Martin, I. Varela, G. R. Bignell, L. R. Yates, E. Papaemmanuil, D. Beare, A. Butler, A. Cheverton, J. Gamble, J. Hinton, M. Jia, A. Jayakumar, D. Jones, C. Latimer, K. W. Lau, S. McLaren, D. J. McBride, A. Menzies, L. Mudie, K. Raine, R. Rad, M. S. Chapman, J. Teague, D. Easton, A. Langerød, M. T. M. Lee, C.-Y. Shen, B. T. K. Tee, B. W. Huimin, A. Broeks, A. C. Vargas, G. Turashvili, J. Martens, A. Fatima, P. Miron, S.-F. Chin, G. Thomas, S. Boyault, O. Mariani, S. R. Lakhani, M. van de Vijver, L. van 't Veer, J. Foekens, C. Desmedt, C. Sotiriou, A. Tutt, C. Caldas, J. S. Reis-Filho, S. A. J. R. Aparicio, A. V. Salomon, A.-L. Børresen-Dale, A. L. Richardson, P. J. Campbell, P. A. Futreal, M. R. Stratton; Oslo Breast Cancer Consortium (OSBREAC), The landscape of cancer genes and mutational processes in breast cancer. *Nature* **486**, 400–404 (2012). doi:10.1038/nature11017 Medline

26. N. Wagle, C. Painter, E. Anastasio, M. Dunphy, M. McGillicuddy, R. Stoddard, E. Jain, D. Kim, S. Di Lascio, B. N. Tompson, S. Balch, B. Thomas, P. Kumari, S. Johnson, J. Holloway, O. Cohen, E. H. Knelson, K. Larkin, S. Pollock, A. Wong, S. Bahl, S. Maiwald, A. Zimmer, E. O. Baker, J. H. Lapan, S. Sutherland, S. Sassone, V. Adalsteinsson, E. S. Lander, T. R. Golub, Abstract 5371: The Metastatic Breast Cancer Project: Partnering with patients to accelerate progress in cancer research. *Cancer Res.* **78**, 5371 (2018). doi:10.1158/1538-7445.AM2018-5371

27. R. Shen, V. E. Seshan, FACETS: Allele-specific copy number and clonal heterogeneity analysis tool for high-throughput DNA sequencing. *Nucleic Acids Res.* **44**, e131 (2016). doi:10.1093/nar/gkw520 Medline

28. J. Eid, A. Fehr, J. Gray, K. Luong, J. Lyle, G. Otto, P. Peluso, D. Rank, P. Baybayan, B. Bettman, A. Bibillo, K. Bjornson, B. Chaudhuri, F. Christians, R. Cicero, S. Clark, R. Dalal, A. Dewinter, J. Dixon, M. Foquet, A. Gaertner, P. Hardenbol, C. Heiner, K. Hester, D. Holden, G. Kearns, X. Kong, R. Kuse, Y. Lacroix, S. Lin, P. Lundquist, C. Ma, P. Marks, M. Maxham, D. Murphy, I. Park, T. Pham, M. Phillips, J. Roy, R. Sebra, G. Shen, J. Sorenson, A. Tomaney, K. Travers, M. Trulson, J. Vieceli, J. Wegener, D. Wu, A. Yang, D. Zaccarin, P. Zhao, F. Zhong, J. Korlach, S. Turner, Real-time DNA sequencing from single polymerase molecules. *Science* **323**, 133–138 (2009). doi:10.1126/science.1162986 Medline

29. Y. Zhang, P. Kwok-Shing Ng, M. Kucherlapati, F. Chen, Y. Liu, Y. H. Tsang, G. de Velasco, K. J. Jeong, R. Akbani, A. Hadjipanayis, A. Pantazi, C. A. Bristow, E. Lee, H.

S. Mahadeshwar, J. Tang, J. Zhang, L. Yang, S. Seth, S. Lee, X. Ren, X. Song, H. Sun, J. Seidman, L. J. Luquette, R. Xi, L. Chin, A. Protopopov, T. F. Westbrook, C. S. Shelley, T. K. Choueiri, M. Ittmann, C. Van Waes, J. N. Weinstein, H. Liang, E. P. Henske, A. K. Godwin, P. J. Park, R. Kucherlapati, K. L. Scott, G. B. Mills, D. J. Kwiatkowski, C. J. Creighton, A Pan-Cancer Proteogenomic Atlas of PI3K/AKT/mTOR Pathway Alterations. *Cancer Cell* **31**, 820–832.e3 (2017). doi:10.1016/j.ccell.2017.04.013 Medline

30. L. Zhao, P. K. Vogt, Helical domain and kinase domain mutations in p110α of phosphatidylinositol 3-kinase induce gain of function by different mechanisms. *Proc. Natl. Acad. Sci. U.S.A.* **105**, 2652–2657 (2008). doi:10.1073/pnas.0712169105 Medline

31. T. Ikenoue, F. Kanai, Y. Hikiba, T. Obata, Y. Tanaka, J. Imamura, M. Ohta, A. Jazag, B. Guleng, K. Tateishi, Y. Asaoka, M. Matsumura, T. Kawabe, M. Omata, Functional analysis of PIK3CA gene mutations in human colorectal cancer. *Cancer Res.* **65**, 4562–4567 (2005). doi:10.1158/0008-5472.CAN-04-4114 Medline

32. J. A. Beaver, J. P. Gustin, K. H. Yi, A. Rajpurohit, M. Thomas, S. F. Gilbert, D. M. Rosen, B. Ho Park, J. Lauring, PIK3CA and AKT1 mutations have distinct effects on sensitivity to targeted pathway inhibitors in an isogenic luminal breast cancer model system. *Clin. Cancer Res.* **19**, 5413–5422 (2013). doi:10.1158/1078-0432.CCR-13-0884 Medline

33. I. M. Berenjeno, R. Piñeiro, S. D. Castillo, W. Pearce, N. McGranahan, S. M. Dewhurst, V. Meniel, N. J. Birkbak, E. Lau, L. Sansregret, D. Morelli, N. Kanu, S. Srinivas, M. Graupera, V. E. R. Parker, K. G. Montgomery, L. S. Moniz, C. L. Scudamore, W. A. Phillips, R. K. Semple, A. Clarke, C. Swanton, B. Vanhaesebroeck, Oncogenic PIK3CA induces centrosome amplification and tolerance to genome doubling. *Nat. Commun.* **8**, 1773 (2017). doi:10.1038/s41467-017-02002-4 Medline

34. K. M. Kinross, K. G. Montgomery, M. Kleinschmidt, P. Waring, I. Ivetac, A. Tikoo, M. Saad, L. Hare, V. Roh, T. Mantamadiotis, K. E. Sheppard, G. L. Ryland, I. G. Campbell, K. L. Gorringe, J. G. Christensen, C. Cullinane, R. J. Hicks, R. B. Pearson, R. W. Johnstone, G. A. McArthur, W. A. Phillips, An activating Pik3ca mutation coupled with Pten loss is sufficient to initiate ovarian tumorigenesis in mice. *J. Clin. Invest.* **122**, 553–557 (2012). doi:10.1172/JCI59309 Medline

35. C. H. Huang, D. Mandelker, O. Schmidt-Kittler, Y. Samuels, V. E. Velculescu, K. W. Kinzler, B. Vogelstein, S. B. Gabelli, L. M. Amzel, The structure of a human p110alpha/p85alpha complex elucidates the effects of oncogenic PI3Kalpha mutations. *Science* **318**, 1744–1748 (2007). doi:10.1126/science.1150799 Medline

36. J. Yu, Y. Zhang, J. McIlroy, T. Rordorf-Nikolic, G. A. Orr, J. M. Backer, Regulation of the p85/p110 phosphatidylinositol 3′-kinase: Stabilization and inhibition of the p110alpha catalytic subunit by the p85 regulatory subunit. *Mol. Cell. Biol.* **18**, 1379–1387 (1998). doi:10.1128/MCB.18.3.1379 Medline

37. J. E. Burke, O. Perisic, G. R. Masson, O. Vadas, R. L. Williams, Oncogenic mutations mimic and enhance dynamic events in the natural activation of phosphoinositide 3-kinase p110α (PIK3CA). *Proc. Natl. Acad. Sci. U.S.A.* **109**, 15259–15264 (2012). doi:10.1073/pnas.1205508109 Medline

38. D. Mandelker, S. B. Gabelli, O. Schmidt-Kittler, J. Zhu, I. Cheong, C.-H. Huang, K. W. Kinzler, B. Vogelstein, L. M. Amzel, A frequent kinase domain mutation that changes

the interaction between PI3Kα and the membrane. *Proc. Natl. Acad. Sci. U.S.A.* **106**, 16996–17001 (2009). doi:10.1073/pnas.0908444106 Medline

39. M. S. Miller, O. Schmidt-Kittler, D. M. Bolduc, E. T. Brower, D. Chaves-Moreira, M. Allaire, K. W. Kinzler, I. G. Jennings, P. E. Thompson, P. A. Cole, L. M. Amzel, B. Vogelstein, S. B. Gabelli, Structural basis of nSH2 regulation and lipid binding in PI3Kα. *Oncotarget* **5**, 5198–5208 (2014). doi:10.18632/oncotarget.2263 Medline

40. S. Maheshwari, M. S. Miller, R. O'Meally, R. N. Cole, L. M. Amzel, S. B. Gabelli, Kinetic and structural analyses reveal residues in phosphoinositide 3-kinase α that are critical for catalysis and substrate recognition. *J. Biol. Chem.* **292**, 13541–13550 (2017). doi:10.1074/jbc.M116.772426 Medline

41. S. Croessmann, J. H. Sheehan, K. M. Lee, G. Sliwoski, J. He, R. Nagy, D. Riddle, I. A. Mayer, J. M. Balko, R. Lanman, V. A. Miller, L. C. Cantley, J. Meiler, C. L. Arteaga, *PIK3CA* C2 Domain Deletions Hyperactivate Phosphoinositide 3-kinase (PI3K), Generate Oncogene Dependence, and Are Exquisitely Sensitive to PI3K**α** Inhibitors. *Clin. Cancer Res.* **24**, 1426–1435 (2018). doi:10.1158/1078-0432.CCR-17-2141 Medline

42. W. C. Hon, A. Berndt, R. L. Williams, Regulation of lipid binding underlies the activation mechanism of class IA PI3-kinases. *Oncogene* **31**, 3655–3666 (2012). doi:10.1038/onc.2011.532 Medline

43. B. J. Druker, S. Tamura, E. Buchdunger, S. Ohno, G. M. Segal, S. Fanning, J. Zimmermann, N. B. Lydon, Effects of a selective inhibitor of the Abl tyrosine kinase on the growth of Bcr-Abl positive cells. *Nat. Med.* **2**, 561–566 (1996). doi:10.1038/nm0596-561 Medline

44. S. V. Sharma, J. Settleman, Oncogene addiction: Setting the stage for molecularly targeted cancer therapy. *Genes Dev.* **21**, 3214–3231 (2007). doi:10.1101/gad.1609907 Medline

45. K. Edgar, E. Hanan, S. Staben, S. Schmidt, R. Hong, K. Song, A. Young, P. Hamilton, A. Arrazate, C. de la Cruz, M. Belvin, M. Nannini, L. S. Friedman, D. Sampath, Abstract 156: Preclinical characterization of GDC-0077, a specific PI3K alpha inhibitor in early clinical development. *Cancer Res.* **77**, 156 (2017). doi:10.1158/1538-7445.AM2017-156

46. M. Fallahi-Sichani, S. Honarnejad, L. M. Heiser, J. W. Gray, P. K. Sorger, Metrics other than potency reveal systematic variation in responses to cancer drugs. *Nat. Chem. Biol.* **9**, 708–714 (2013). doi:10.1038/nchembio.1337 Medline

47. V. M. Singh, R. C. Salunga, V. J. Huang, Y. Tran, M. Erlander, P. Plumlee, M. R. Peterson, Analysis of the effect of various decalcification agents on the quantity and quality of nucleic acid (DNA and RNA) recovered from bone biopsies. *Ann. Diagn. Pathol.* **17**, 322–326 (2013). doi:10.1016/j.anndiagpath.2013.02.001 Medline

48. J. Baselga, M. Campone, M. Piccart, H. A. Burris 3rd, H. S. Rugo, T. Sahmoud, S. Noguchi, M. Gnant, K. I. Pritchard, F. Lebrun, J. T. Beck, Y. Ito, D. Yardley, I. Deleu, A. Perez, T. Bachelot, L. Vittori, Z. Xu, P. Mukhopadhyay, D. Lebwohl, G. N. Hortobagyi, Everolimus in postmenopausal hormone-receptor-positive advanced breast cancer. *N. Engl. J. Med.* **366**, 520–529 (2012). doi:10.1056/NEJMoa1109653 Medline

49. N. C. Turner, J. Ro, F. André, S. Loi, S. Verma, H. Iwata, N. Harbeck, S. Loibl, C. Huang Bartlett, K. Zhang, C. Giorgetti, S. Randolph, M. Koehler, M. Cristofanilli; PALOMA3

Study Group, Palbociclib in Hormone-Receptor-Positive Advanced Breast Cancer. *N. Engl. J. Med.* **373**, 209–219 (2015). doi:10.1056/NEJMoa1505270 Medline

50. E. A. Eisenhauer, P. Therasse, J. Bogaerts, L. H. Schwartz, D. Sargent, R. Ford, J. Dancey, S. Arbuck, S. Gwyther, M. Mooney, L. Rubinstein, L. Shankar, L. Dodd, R. Kaplan, D. Lacombe, J. Verweij, New response evaluation criteria in solid tumours: Revised RECIST guideline (version 1.1). *Eur. J. Cancer* **45**, 228–247 (2009). doi:10.1016/j.ejca.2008.10.026 Medline

51. C. Kandoth, M. D. McLellan, F. Vandin, K. Ye, B. Niu, C. Lu, M. Xie, Q. Zhang, J. F. McMichael, M. A. Wyczalkowski, M. D. M. Leiserson, C. A. Miller, J. S. Welch, M. J. Walter, M. C. Wendl, T. J. Ley, R. K. Wilson, B. J. Raphael, L. Ding, Mutational landscape and significance across 12 major cancer types. *Nature* **502**, 333–339 (2013). doi:10.1038/nature12634 Medline

52. I. B. Weinstein, A. K. Joe, Mechanisms of disease: Oncogene addiction—a rationale for molecular targeting in cancer therapy. *Nat. Clin. Pract. Oncol.* **3**, 448–457 (2006). doi:10.1038/ncponc0558 Medline

53. P. Zhou, W. Jiang, Y. J. Zhang, S. M. Kahn, I. Schieren, R. M. Santella, I. B. Weinstein, Antisense to cyclin D1 inhibits growth and reverses the transformed phenotype of human esophageal cancer cells. *Oncogene* **11**, 571–580 (1995). Medline

54. D. J. Slamon, B. Leyland-Jones, S. Shak, H. Fuchs, V. Paton, A. Bajamonde, T. Fleming, W. Eiermann, J. Wolter, M. Pegram, J. Baselga, L. Norton, Use of chemotherapy plus a monoclonal antibody against HER2 for metastatic breast cancer that overexpresses HER2. *N. Engl. J. Med.* **344**, 783–792 (2001). doi:10.1056/NEJM200103153441101 Medline

55. B. J. Druker, M. Talpaz, D. J. Resta, B. Peng, E. Buchdunger, J. M. Ford, N. B. Lydon, H. Kantarjian, R. Capdeville, S. Ohno-Jones, C. L. Sawyers, Efficacy and safety of a specific inhibitor of the BCR-ABL tyrosine kinase in chronic myeloid leukemia. *N. Engl. J. Med.* **344**, 1031–1037 (2001). doi:10.1056/NEJM200104053441401 Medline

56. T. J. Lynch, D. W. Bell, R. Sordella, S. Gurubhagavatula, R. A. Okimoto, B. W. Brannigan, P. L. Harris, S. M. Haserlat, J. G. Supko, F. G. Haluska, D. N. Louis, D. C. Christiani, J. Settleman, D. A. Haber, Activating mutations in the epidermal growth factor receptor underlying responsiveness of non-small-cell lung cancer to gefitinib. *N. Engl. J. Med.* **350**, 2129–2139 (2004). doi:10.1056/NEJMoa040938 Medline

57. C. O. Ndubaku, T. P. Heffron, S. T. Staben, M. Baumgardner, N. Blaquiere, E. Bradley, R. Bull, S. Do, J. Dotson, D. Dudley, K. A. Edgar, L. S. Friedman, R. Goldsmith, R. A. Heald, A. Kolesnikov, L. Lee, C. Lewis, M. Nannini, J. Nonomiya, J. Pang, S. Price, W. W. Prior, L. Salphati, S. Sideris, J. J. Wallin, L. Wang, B. Wei, D. Sampath, A. G. Olivero, Discovery of 2-{3-[2-(1-isopropyl-3-methyl-1H-1,2-4-triazol-5-yl)-5,6-dihydrobenzo[f]imidazo[1, 2-d][1,4]oxazepin-9-yl]-1H-pyrazol-1-yl}-2-methylpropanamide (GDC-0032): A beta-sparing phosphoinositide 3-kinase inhibitor with high unbound exposure and robust in vivo antitumor activity. *J. Med. Chem.* **56**, 4597–4610 (2013). doi:10.1021/jm4003632 Medline

58. L. H. Saal, K. Holm, M. Maurer, L. Memeo, T. Su, X. Wang, J. S. Yu, P.-O. Malmström, M. Mansukhani, J. Enoksson, H. Hibshoosh, A. Borg, R. Parsons, PIK3CA mutations

correlate with hormone receptors, node metastasis, and ERBB2, and are mutually exclusive with PTEN loss in human breast carcinoma. *Cancer Res.* **65**, 2554–2559 (2005). doi:10.1158/0008-5472-CAN-04-3913 Medline

59. T. L. Yuan, L. C. Cantley, PI3K pathway alterations in cancer: Variations on a theme. *Oncogene* **27**, 5497–5510 (2008). doi:10.1038/onc.2008.245 Medline

60. K. Jhaveri, D. Juric, C. Saura, A. Cervantes, A. Melnyk, M. R. Patel, M. Oliveira, V. Gambardella, V. Ribrag, C. X. Ma, R. Aljumaily, P. L. Bedard, J. C. Sachdev, J. Bond, S. Jones, T. R. Wilson, M. C. Wei, J. Baselga, Abstract CT046: A phase I basket study of the PI3K inhibitor taselisib (GDC-0032) in *PIK3CA*-mutated locally advanced or metastatic solid tumors. *Cancer Res.* **78**, CT046 (2018). doi:10.1158/1538-7445.AM2018-CT046

61. A. Zehir, R. Benayed, R. H. Shah, A. Syed, S. Middha, H. R. Kim, P. Srinivasan, J. Gao, D. Chakravarty, S. M. Devlin, M. D. Hellmann, D. A. Barron, A. M. Schram, M. Hameed, S. Dogan, D. S. Ross, J. F. Hechtman, D. F. DeLair, J. Yao, D. L. Mandelker, D. T. Cheng, R. Chandramohan, A. S. Mohanty, R. N. Ptashkin, G. Jayakumaran, M. Prasad, M. H. Syed, A. B. Rema, Z. Y. Liu, K. Nafa, L. Borsu, J. Sadowska, J. Casanova, R. Bacares, I. J. Kiecka, A. Razumova, J. B. Son, L. Stewart, T. Baldi, K. A. Mullaney, H. Al-Ahmadie, E. Vakiani, A. A. Abeshouse, A. V. Penson, P. Jonsson, N. Camacho, M. T. Chang, H. H. Won, B. E. Gross, R. Kundra, Z. J. Heins, H.-W. Chen, S. Phillips, H. Zhang, J. Wang, A. Ochoa, J. Wills, M. Eubank, S. B. Thomas, S. M. Gardos, D. N. Reales, J. Galle, R. Durany, R. Cambria, W. Abida, A. Cercek, D. R. Feldman, M. M. Gounder, A. A. Hakimi, J. J. Harding, G. Iyer, Y. Y. Janjigian, E. J. Jordan, C. M. Kelly, M. A. Lowery, L. G. T. Morris, A. M. Omuro, N. Raj, P. Razavi, A. N. Shoushtari, N. Shukla, T. E. Soumerai, A. M. Varghese, R. Yaeger, J. Coleman, B. Bochner, G. J. Riely, L. B. Saltz, H. I. Scher, P. J. Sabbatini, M. E. Robson, D. S. Klimstra, B. S. Taylor, J. Baselga, N. Schultz, D. M. Hyman, M. E. Arcila, D. B. Solit, M. Ladanyi, M. F. Berger, Mutational landscape of metastatic cancer revealed from prospective clinical sequencing of 10,000 patients. *Nat. Med.* **23**, 703–713 (2017). doi:10.1038/nm.4333 Medline

62. H. Li, B. Handsaker, A. Wysoker, T. Fennell, J. Ruan, N. Homer, G. Marth, G. Abecasis, R. Durbin; 1000 Genome Project Data Processing Subgroup, The Sequence Alignment/Map format and SAMtools. *Bioinformatics* **25**, 2078–2079 (2009). doi:10.1093/bioinformatics/btp352 Medline

63. S. L. Carter, K. Cibulskis, E. Helman, A. McKenna, H. Shen, T. Zack, P. W. Laird, R. C. Onofrio, W. Winckler, B. A. Weir, R. Beroukhim, D. Pellman, D. A. Levine, E. S. Lander, M. Meyerson, G. Getz, Absolute quantification of somatic DNA alterations in human cancer. *Nat. Biotechnol.* **30**, 413–421 (2012). doi:10.1038/nbt.2203 Medline

64. F. Bertucci, C. K. Y. Ng, A. Patsouris, N. Droin, S. Piscuoglio, N. Carbuccia, J. C. Soria, A. T. Dien, Y. Adnani, M. Kamal, S. Garnier, G. Meurice, M. Jimenez, S. Dogan, B. Verret, M. Chaffanet, T. Bachelot, M. Campone, C. Lefeuvre, H. Bonnefoi, F. Dalenc, A. Jacquet, M. R. De Filippo, N. Babbar, D. Birnbaum, T. Filleron, C. Le Tourneau, F. André, Genomic characterization of metastatic breast cancers. *Nature* **569**, 560–564 (2019). doi:10.1038/s41586-019-1056-z Medline

65. C. A. Hudis, W. E. Barlow, J. P. Costantino, R. J. Gray, K. I. Pritchard, J.-A. W. Chapman, J. A. Sparano, S. Hunsberger, R. A. Enos, R. D. Gelber, J. A. Zujewski, Proposal for

standardized definitions for efficacy end points in adjuvant breast cancer trials: The STEEP system. *J. Clin. Oncol.* **25**, 2127–2132 (2007). doi:10.1200/JCO.2006.10.3523 Medline

66. J. D. Kalbfleisch, R. L. Prentice, *The Statistical Analysis of Failure Time Data* (Wiley, ed. 2, 2002).

67. M. Sun, J. R. Hart, P. Hillmann, M. Gymnopoulos, P. K. Vogt, Addition of N-terminal peptide sequences activates the oncogenic and signaling potentials of the catalytic subunit p110α of phosphoinositide-3-kinase. *Cell Cycle* **10**, 3731–3739 (2011). doi:10.4161/cc.10.21.17920 Medline

68. C. A. Schneider, W. S. Rasband, K. W. Eliceiri, NIH Image to ImageJ: 25 years of image analysis. *Nat. Methods* **9**, 671–675 (2012). doi:10.1038/nmeth.2089 Medline

69. The PyMOL Molecular Graphics System, Version 1.8 (Schrodinger, 2015).

70. T. A. Clark, J. H. Chung, M. Kennedy, J. D. Hughes, N. Chennagiri, D. S. Lieber, B. Fendler, L. Young, M. Zhao, M. Coyne, V. Breese, G. Young, A. Donahue, D. Pavlick, A. Tsiros, T. Brennan, S. Zhong, T. Mughal, M. Bailey, J. He, S. Roels, G. M. Frampton, J. M. Spoerke, S. Gendreau, M. Lackner, E. Schleifman, E. Peters, J. S. Ross, S. M. Ali, V. A. Miller, J. P. Gregg, P. J. Stephens, A. Welsh, G. A. Otto, D. Lipson, Analytical Validation of a Hybrid Capture-Based Next-Generation Sequencing Clinical Assay for Genomic Profiling of Cell-Free Circulating Tumor DNA. *J. Mol. Diagn.* **20**, 686–702 (2018). doi:10.1016/j.jmoldx.2018.05.004 Medline

71. N. A. O'Leary, M. W. Wright, J. R. Brister, S. Ciufo, D. Haddad, R. McVeigh, B. Rajput, B. Robbertse, B. Smith-White, D. Ako-Adjei, A. Astashyn, A. Badretdin, Y. Bao, O. Blinkova, V. Brover, V. Chetvernin, J. Choi, E. Cox, O. Ermolaeva, C. M. Farrell, T. Goldfarb, T. Gupta, D. Haft, E. Hatcher, W. Hlavina, V. S. Joardar, V. K. Kodali, W. Li, D. Maglott, P. Masterson, K. M. McGarvey, M. R. Murphy, K. O'Neill, S. Pujar, S. H. Rangwala, D. Rausch, L. D. Riddick, C. Schoch, A. Shkeda, S. S. Storz, H. Sun, F. Thibaud-Nissen, I. Tolstoy, R. E. Tully, A. R. Vatsan, C. Wallin, D. Webb, W. Wu, M. J. Landrum, A. Kimchi, T. Tatusova, M. DiCuccio, P. Kitts, T. D. Murphy, K. D. Pruitt, Reference sequence (RefSeq) database at NCBI: Current status, taxonomic expansion, and functional annotation. *Nucleic Acids Res.* **44**, D733–D745 (2016). doi:10.1093/nar/gkv1189 Medline